PERFORMANCE EVALUATION AND PHYSICAL PROPERTY STUDY OF STRUCTURED PACKING HETP CORRELATIONS

By

ANDREW PETER STARRANTINO

Bachelor of Science in Chemical Engineering

Clarkson University

Potsdam, New York

May, 2020

Submitted to the Faculty of the
Graduate College of the
Oklahoma State University
in partial fulfillment of
the requirements for
the Degree of
MASTER OF SCIENCE
July, 2022

PERFORMANCE EVALUATION AND PHYSICAL

PROPERTY STUDY OF STRUCTURED

PACKING HETP CORRELATIONS

Thesis Approved:

Dr. Clint P. Aichele

Thesis Adviser

Dr. Tony J. Cai

Dr. Jindal K. Shah

ACKNOWLEDGEMENTS

I would like to thank my advisor, Dr. Clint Aichele, for always being able to help with any questions or concerns I had. He has helped me immensely in terms of developing my research and communications skills while at OSU. It has been an honor to be a part of his lab group and I will always be thankful for the opportunity. During my time I've seen him treat his lab group like a family, inviting them to his house, planning get-togethers and playing ping-pong with us, it is truly amazing to see, and it speaks volumes to who he is as a person.

I would like to acknowledge all the help Fractionation Research Inc. has provided to me. I received so much valuable feedback from Dr. Sayeed Mohammad, Dr. Tony Cai and Dr. Ken McCarley about my research, presentations, and papers. I have learned so much about distillation from them and I am thankful for the opportunities to present at FRI TAC meetings.

I would also like to thank Dr. Jindal Shah for serving in my committee. He was an amazing Thermodynamics professor and always filled his lecture with valuable lessons and witty jokes. I am also appreciative of our group's post-doc, Dr. Michael Miranda, he always had valuable research advice and is a great person. In addition to Michael, the rest of our lab group and my fellow classmates I had during core classes were awesome and extremely nice people to be around.

Lastly, I want to thank my family. I am grateful for their unconditional love and support for anything that I have decided to do in my life. I know it has not been easy for them to be so far away from me, but I still feel their immense support no matter where I go.

Name: ANDREW PETER STARRANTINO

Date of Degree: JULY, 2022

Title of Study: PERFORMANCE EVALUATION AND PHYSICAL PROPERTY STUDY OF STRUCTURED PACKING HETP CORRELATIONS

Major Field: CHEMICAL ENGINEERING

Abstract:

Structured packing HETP correlations play a significant role in the design and operation of packed distillation columns. A model derived from inadequate HETP data will not only affect where it may perform poorly but will also impact the relationship between specific physical properties and the model's predicted HETP. This study focused on the impact of physical properties on structured packing HETP correlations in the literature, as well as their HETP prediction capabilities.

The evaluated models included Gualito (1997), Billet & Schultes (1999), Delft (2004, 2014), Aspen (2012) and Song (2017). Multiple hydrocarbon and aqueous systems were analyzed, with pressures ranging from 0.130 – 27.6 bara. The sensitivity testing was meant to highlight the differences in model relationships with physical properties, caused by assumptions, different physical property ranges used for development, etc. As a result of the analysis, the counter-intuitive relationships between HETP and liquid viscosity were observed with the Billet & Schultes and Gualito correlations. For these two correlations, HETP decreased with increased liquid viscosity. In general, all the models showed varying degrees of sensitivity to liquid viscosity, some were more impacted at low pressures, while others at high pressures. In addition to liquid viscosity, the differences in dependency on surface tension were highlighted between all the models. Some correlations demonstrated predicted HETP changes of 15% or more, while other correlations were impacted by less than 3%, with the same variation of surface tension. Overall, the physical property sensitivity results quantified the impact of surface tension and liquid viscosity with multiple types of systems. Monte Carlo methods were also utilized to determine the uncertainty of each model with different physical property inputs.

In addition to the physical property study, a HETP performance evaluation was conducted with various types of packings and test systems. Billet & Schultes correlation generally performed the best, due to regressed packing-specific constants, but other correlations such as Song and Aspen performed nearly as well, and in some cases better. Other aspects of the models such as effective area predictions were discussed in detail and observations were made about model strengths and weaknesses.

TABLE OF CONTENTS

Chapter Page

I. INTRODUCTION 1

1.1 Aspects of the HETP Model 1
1.1.1 Theoretical Plates 2
1.1.2 Definition of HETP 3
1.2 Column Internals 4
1.3 Research Objectives 5

II. LITERATURE REVIEW 7

2.1 Mass Transfer Coefficient Theories 7
2.2 Effective Area Terms 9
2.3 Review of Common HETP Correlations 10
2.3.1 SRP I Correlation 10
2.3.2 SRP II Correlation 12
2.3.3 Revised SRP II Correlation: Gualito et al. 15
2.3.4 Billet & Schultes (1993, 1999) 18
2.3.5 Delft Model (1997, 2004, 2014) 19
2.3.6 Hanley and Chen (Aspen, 2012) 23
2.3.7 Song (2017) 25
2.4 Other Notable Correlations 26
2.5 Previous Work 26

III. PERFORMANCE EVALUATION OF CONVENTIONAL STRUCTURED PACKING HETP MODELS 28

3.1 Abstract 28
3.2 Introduction 29
3.3 Experimental Methods 29
3.3.1 HETP Data Collection Process 29
3.3.2 Evaluating Pre-Loading Prediction Accuracy 31
3.4 Results and Discussion 32
3.4.1 Evaluation of Mellapak 250Y Structured Packings 32

Chapter Page

3.5 Conclusions....45

IV. PERFORMANCE COMPARISON OF HETP CORRELATIONS FOR HIGH-CAPACITY STRUCTURED PACKINGS....46

4.1 Abstract....46
4.2 Introduction....47
4.3 Model Background....48
4.4 Experimental Method....50
4.5 Results and Discussion....51
4.5.1 Comparison of HETP Predictions....51
4.5.2 Comparison of Effective Area Predictions....60
4.6 Conclusions....63

V. THE INFLUENCE OF PHYSICAL PROPERTIES ON STRUCTURED PACKING HETP CORRELATIONS....64

5.1 Abstract....64
5.2 Introduction....65
5.3 Results and Discussion....65
5.3.1 Sensitivity Analysis Sub....65
5.3.2 Monte Carlo Simulation....74
5.4 Conclusions....76

VI. FUTURE WORK AND CONCLUSIONS....77

REFERENCES....79
APPENDICES....86
APPENDIX A....86

LIST OF TABLES

Table Page

2.1 Hydraulic Model Constants in Gualito Correlation 17
3.1 Test Systems Collected for Model Evaluation.....33
3.2 Regressed Billet & Schultes Packing-specific Constants 34
3.3 Summary of MAPD for Test Systems with Mellapak 250Y. 35
4.1 Summary of Model HETP Performance. 59
5.1 Comparison of Uncertainty and Performance Evaluation. 75

LIST OF FIGURES

Figure Page

1.1 Example of Sieve Tray.....4
1.2 Example of Structured Packing 5
3.1 Model HETP Performance Comparison – C6/C7, 1.65 bara with Mellapak 250Y. 37
3.2 Model Fractional Area Comparison – C6/C7, 1.65 bara with Mellapak 250Y. .38
3.3 Model HETP Performance Comparison – O/P-Xylene, 0.13 bara with Mellapak 250Y.....39
3.4 Model Fractional Area Comparison – O/P-xylene, 0.13 bara with Mellapak 250Y. 40
3.5 Model HETP Performance Comparison – iC4/nC4, 11.4 bara with Mellapak 250Y. 41
3.6 Model HETP Performance Comparison – iC4/nC4, 20.7 bara with Mellapak 250Y. 41
3.7 Model Fractional Area Comparison – iC4/nC4, 20.7 bara with Mellapak 250Y. 43
3.8 Model HETP Performance Comparison – MeOH/Water, 1.00 bara with Mellapak 250Y.....44
3.9 Model Fractional Area Comparison – MeOH/Water, 1.00 bara with Mellapak 250Y 44
4.1 Predicted versus measured HETP values as a function of F-factor, for C6/C7 at 0.33 bara with MellapakPlus 252Y.....53
4.2 Predicted versus measured HETP values as a function of F-factor, for C6/C7 at 1.65 bara with MellapakPlus 252Y.....53
4.3 Predicted versus measured HETP values as a function of F-factor, for o/p-xylene at 0.13 bara with MellapakPlus 252Y.....54
4.4 Bias plot across the preloading regime (Predicted Model HETP-Experimental HETP) for all systems with MellapakPlus 252Y.....56
4.5 Bias plot across the preloading regime (Predicted Model HETP-Experimental HETP) for all systems with MellapakPlus 452Y.....57
4.6 Bias plot across the preloading regime (Predicted Model HETP-Experimental HETP) for all systems with MellapakPlus 752Y.....59
4.7 Fractional area of C6/C7 at 0.33 bara with MellapakPlus 252Y.. 61
4.8 Fractional area of C6/C7 at 0.33 bara with MellapakPlus 752Y.. 62
5.1 Effect of liquid viscosity on Gualito Model with Mellapak 250Y... 67

Figure Page

5.2 Effect of liquid viscosity on Billet and Schultes with Mellapak 250Y.....67
5.3 Effect of liquid viscosity on Delft Model with Mellapak 250Y.. 68
5.4 Effect of liquid viscosity on Song with Mellapak 250Y.....69
5.5 Effect of liquid viscosity on Aspen with Mellapak 250Y.....70
5.6 Effect of surface tension on Gualito Model with Mellapak 250Y.....71
5.7 Effect of surface tension on Delft with Mellapak 250Y. 72
5.8 Effect of surface tension on Song with Mellapak 250Y. 73
5.9 Effect of surface tension on Aspen with Mellapak 250Y. 73

NOMENCLATURE

a_e	Effective packing area per unit volume (m^2/m^3)
a_p	Specified packing area per unit volume (m^2/m^3)
A_t	Cross sectional area of column (m^2)
B	Corrugation base length (m)
c	Concentration (mol/m^3)
C_E	Correction factor for surface renewal
C6/C7	Cyclohexane/n-heptane
D_{AB}	Diffusivity (m^2/s)
d_{eq}	Equivalent diameter of channel (m)
D_G	Gas phase diffusivity (m^2/s)
d_{hG}	Hydraulic diameter for gas phase (m)
D_L	Liquid phase diffusivity (m^2/s)
Fr_L	Liquid Froude number
F_v	F-factor ($Pa^{0.5}$)
F_{SE}	Surface enhancement factor
F_t	Correction factor for total holdup
g	Gravity acceleration (m/s^2)
G	Gas molar flow rate (kmol/s)
IC4/NC4	i-Butane/n-Butane
N	Theoretical stage
HETP	Height equivalent to theoretical plate
HTU	Overall height transfer unit
HTU_G	Gas height transfer unit
HTU_L	Liquid height transfer unit
h	Corrugation height (m)
h_L	Operating liquid holdup (m^3 liq/m^3 bed)
h_{pb}	Height of packed bed (m)
k_G	Gas side mass transfer coefficient (m/s)
k_L	Liquid side mass transfer coefficient (m/s)
L	Liquid molar flow rate (kmol/s)
$l_{G,pe}$	Length of gas flow channel in a packing element (m)
m	Equilibrium slope
Re_G	Reynolds number for gas phase
Re_{Ge}	Effective Reynolds number for gas phase
Re_{Grv}	Relative velocity Reynolds number
Re_L	Reynolds number for liquid phase
S	Corrugation side length (m)
Sh	Sherwood number
t	Exposure time (s)
U_{GE}	Effective gas velocity (m/s)
U_{GS}	Superficial gas velocity (m/s)
U_{LE}	Effective liquid gas velocity (m/s)

U_{LS}	Superficial liquid velocity (m/s)
We_L	Weber number for liquid phase
x	Light component mole fraction
Z	Song correlation height of packed bed (m)

Greek Letters

θ	Corrugation angle (degrees)
θ_L	Effective liquid flow angle (degrees)
α_{avg}	Relative volatility, top and bottom average
α_{lk}	Relative volatility of the light key
δ	Liquid film thickness (m)
ε	Packing void fraction
φ	Fraction of the triangular channel occupied by liquid
μ_G	Viscosity of the gas (Pa s)
μ_L	Viscosity of the liquid (Pa s)
λ	Stripping factor
ρ_G	Density of the gas (kg/m^3)
ρ_L	Density of the liquid (kg/m^3)
σ	Surface tension (N/m)
ξ_{GL}	Gas-liquid friction factor
Ω	Fraction of packing surface area occupied by holes

CHAPTER I

INTRODUCTION

Distillation is one of the most important processes in the energy and chemical industries. It is used for natural gas processing, oil refining, air separation and many more chemical processes. Distillation columns can be costly to manufacture and assemble, as well as require significant amounts of energy to successfully separate chemicals to desired purities. As much as 40% of the energy utilized in the chemical process industry is attributed to distillation.[1] Therefore, by avoiding the oversizing of a column can result in significant energy savings. Efficiency correlations are an important tool to the sizing of both types of distillation columns, which are trayed and packed. These two classifications describe the internals of the separation column. Internals are placed in distillation columns to improve mass transfer between the liquid and gas phases. A further distinction for packed columns is either structured or random packing. A later section in this chapter is dedicated to describing column internals more in-depth. The focus of this study is on structured packing HETP correlations.

1.1 ASPECTS OF THE HETP MODEL

Section 1.1 provides fundamental definitions and background information to understand the features that make-up HETP correlations in the literature. It also briefly outlines the importance of HETP and how it relates to the design process of separation columns.

1.1.1 THEORETICAL PLATES

In the design of a packed distillation column, packed bed height equivalent to theoretical plate (HETP) is considered a metric of mass transfer efficiency for packed columns. A high HETP means that separation efficiency is low and vice versa. Packed efficiency models are used to predict HETP, which convert a theoretical plate number into a packed bed height, seen in Equation 1.1.

$$h_{pb} = N \cdot HETP \tag{1.1}$$

The packed bed height, h_{pb}, is the required packing height to achieve the desired purity of the chemical that was the basis for the theoretical stage calculation. A theoretical stage, *N*, represents vapor and liquid leaving a stage in equilibrium, thus both have the same chemical potential and temperature, which is not representative of real-life mass transfer. HETP is the key term that allows theoretical mass transfer to be translated to how an actual column will perform. As HETP increases, packed bed height increases and costs to construct and operate the column do as well. Therefore, the prediction of HETP is very important to the successful design of an efficient column. For binary distillation experiments published in the literature, the number of theoretical stages, *N*, is usually calculated by the Fenske equation.[2] The Fenske equation, seen in Equation 1.2, requires liquid mole fraction of the light component at the top and bottom of the column and relative volatility.

$$N = log[(x/1-x))_{top}/(x/(1-x))_{btm}]/log(\alpha_{avg}) \tag{1.2}$$

In the Fenske equation, α_{avg} is the geometric average of the top and bottom relative volatilities, where relative volatility is the ratio of the light component K-value to the heavy component K-value. There are other variations of the Fenske equation, such as the Winn equation[3] and others but their selection is dependent on the application. Once theoretical stage count is established via

Fenske equation or process modeling software, the only unknown parameter in Equation 1.1 is the HETP value.

1.1.2 DEFINITION OF HETP

For HETP to be estimated, it is related to height of transfer unit (HTU)[4], as seen in Equation 1.3. According to two-film theory,[5] the relationship between overall height transfer unit and individual film transfer units can be substituted and results in Equation 1.4.

$$HETP = \left[\frac{ln\,\lambda}{\lambda - 1}\right] HTU \tag{1.3}$$

$$HETP = \left[\frac{ln\,\lambda}{\lambda - 1}\right] (HTU_G + \lambda HTU_L) \tag{1.4}$$

Two-film theory has been widely established for use in the HETP equation. HTU_G and HTU_L describe the concentration driving force across each respective phase. In Equation 1.3 and Equation 1.4, stripping factor (λ) is an important parameter that relates HTU to HETP. Stripping factor is the ratio of equilibrium line slope to operating line slope, which is below in Equation 1.5.

$$\lambda = \frac{m}{(L/G)} \tag{1.5}$$

Both the equilibrium and operating line slopes in the stripping factor must be straight for Equation 1.3 to be an applicable relationship between HETP and HTU. The operating line slope is represented by, *L/G*, which is a ratio of liquid phase molar flow rate to gas phase molar flow rate. For total reflux experiments, the operating line slope is equal to one. The equilibrium line slope, *m,* is described in Equation 2.6 for binary distillation applications.

$$m = \frac{\alpha}{[1 + (\alpha - 1)x]^2} \tag{1.6}$$

As stated earlier, the relative volatility is the ratio of the light component to heavy component in Equation 1.6. The equilibrium slope varies across the height of the column since it is dependent on composition. With Equation 1.3 and Equation 1.4, this approach allows for analysis to be

broken down into mass transfer coefficients, superficial velocities, and effective area terms. By substituting into the definitions of HTU_G and HTU_L in Equation 1.4, the final equation for HETP, which is used by different models to predict HETP can be seen in Equation 1.7.

$$HETP = \left[\frac{ln\,\lambda}{\lambda - 1}\right]\left(\frac{u_{GS}}{k_G a_e} + \lambda\frac{u_{LS}}{k_L a_e}\right) \tag{1.7}$$

In Equation 1.7, the new substituted parameters are a_e, which is the effective interfacial area, u_{GS} and u_{LS} are the gas and liquid superficial velocities, and k_G and k_L are the gas and liquid mass transfer coefficients, respectively. With this structure, the robustness of an HETP correlation is dependent on the development of the mass transfer coefficients (k_G, k_L) and the effective area (a_e) term. The discussion of individual HETP correlations from the literature will be discussed in Chapter 2.

1.2 COLUMN INTERNALS

As discussed in the beginning of Chapter 1, there are two main internal classifications for separation columns: trays and packings. The purpose of internals is to increase surface area for the contact of liquids and gases to improve separation. Each type makes up approximately half of the internals used in industry.[6] An example of a sieve tray is seen in Figure 1.1; the design allows for liquid holdup on the tray portion and vapor to flow through the sieve holes in order for mass transfer to occur.

Figure 1.1. Example of Sieve Tray (Image taken from Sulzer.com).

Packings can be classified into random and structured types. Random packings are randomly distributed in the inside of a distillation column, hence the name. These packings include Raschig rings, Pall rings, Berl saddles, INTALOX® saddles and more. Furthermore, structured packings can be further broken up into different types such as gauze packings or corrugated metal sheet packings. Structured packings thrive in vacuum distillation settings. While random packings can operate at higher liquid rates compared to structured packings. An example of structured packing can be seen in Figure 1.2, unlike trays, packings give constant surface area for mass transfer to occur across the bed height.

Figure 1.2. Example of Structured Packing (Image taken from Sulzer.com).

Lower nominal areas of structured packing will result in lower separation efficiency. The focus of this study will be on HETP data collected with corrugated metal sheet structured packings, such as Mellapak 250Y.

1.3 RESEARCH OBJECTIVES

The primary goals of this research are to evaluate HETP correlations in terms of HETP prediction accuracy and quantify how impactful certain physical properties are on their calculation of HETP. Important steps/objectives along the way to achieve:

- Review and select newer HETP correlations to compare performance against and older, established HETP correlations that are employed in a lot of process modeling software applications
- Develop MATLAB code for every selected correlation to analyze their HETP prediction performance, as well as eventually pass on the files to a future graduate student.
- Collect an experimental HETP database of corrugated sheet metal structured packing that reflects efficiency performance of industrial distillation columns.
- Quantify uncertainty from physical property inputs in all the selected models.
- Computationally investigate the impact of liquid viscosity and surface tension on overall HETP prediction for each correlation.

CHAPTER II

LITERATURE REVIEW

There have been numerous studies on mass transfer and structured packing performance that have led to the development of HETP correlations in the literature. The chapter intends to highlight significant HETP correlations and the differences between them in terms of their structure. This includes discussing about the assumptions, test systems and packing types that were used to come up with the final HETP correlation. In addition to a review on HETP correlations, a part of this chapter will be dedicated to discussing previous studies on the performance of these HETP correlations.

2.1 MASS TRANSFER COEFFICIENT THEORIES

For many of the older and well-established structured packed mass transfer correlations, there are two widely adopted methods behind the development of the gas and liquid mass transfer coefficients. The first, penetration theory,[7] which assumes liquid molecules move between the bulk phase to the liquid/gas interface.[8] At the liquid/gas interface, gas contacts liquid molecules where mass transfer occurs for a specific amount of time. The mass transfer assumed under penetration theory can be described by unsteady-state conditions. After assuming constant diffusivity and depth to be infinite, taking the appropriate integral of Fick's law, given in Equation 2.1, results in the liquid film coefficient in Equation 2.2.

$$\frac{\partial c}{\partial t} = D_{AB}\frac{\partial^2}{\partial x^2} \tag{2.1}$$

$$k_L = 2\sqrt{\frac{D_{AB}}{\pi t_e}} \tag{2.2}$$

In Equation 2.2, the liquid mass transfer coefficient is expressed in terms of exposure time, t_e, and diffusivity, D_{AB}. In the literature, penetration theory is mostly used as the basis to develop more complex liquid-side mass transfer coefficient terms.

The second widely adopted method for development of mass transfer coefficients is using a wetted-wall column. The notable HETP models in the literature use wetted-wall column experiments to develop gas-side mass transfer coefficient. A wetted-wall column is a vertical tube that allows for gas and liquid mass transfer to be studied. A liquid flow down the wall of the column and forms a liquid film on its surface. Another fluid flows through the column, sometimes counter-current or co-currently with the liquid that flows down the walls of the column.[9] One of the most notable wetted-wall studies is by Gilliland and Sherwood,[10] which included multiple chemical systems with both counter-current and co-current flows. From this study, an experimental correlation for gas-side mass transfer coefficient was developed to relate Sherwood number, Reynolds number and Schmidt number, seen in Equation 2.3.

$$Sh_G = 0.023 Re_G^{0.83} Sc_G^{0.44} \tag{2.3}$$

The equation above is considered accurate with an approximate Reynolds number range of 2,000 to 27,000.[11] Other notable studies WWC studies are McCarter and Stutzman,[12] Schwarz and Hoelscher,[13] and Johnstone and Pigford.[14] Johnstone and Pigford[14] will be mentioned later as it was the basis for the SRP I's gas-side mass transfer coefficient.

Another common method, especially for absorption experiments, is deconstructing mass transfer coefficient terms from volumetric mass transfer coefficient measurements. For example, Onda et al.[15] used $k_L a_e$ measurements to determine k_L term, as they had already studied effective area and determined a term for it. This same method can be used but determining k_L first, via assuming a theory (such as Higbie's penetration theory) to then establish a_e from $k_L a_e$. Modern mass transfer correlations have adapted these two previous theories in some capacity but also have transitioned to constructing terms with dimensional analysis. Hanley and Chen[16] utilized Buckingham Pi theorem to develop liquid, gas mass transfer coefficients and even the effective area term. Despite these new strategies being employed to determine mass transfer coefficients, traditional wetted wall column experiments are still conducted to verify them.

2.2 EFFECTIVE AREA TERMS

Like mass transfer coefficients, effective area terms, a_e, have been developed with a multitude of strategies. As stated in Section 2.1, volumetric mass transfer coefficient measurements can be deconvoluted into effective area and liquid mass transfer coefficients when one of them is known. For the development of effective area terms with this method, Billet & Schultes correlation[17,18] assumed penetration theory to determine the liquid mass transfer coefficient. So, with this approach the effective area has turned into a term that is "fit" to make up for weaknesses of the derived mass transfer coefficient term. In addition to these empirical effective area models, there is some semi-theoretical models that are based on surface flow studies. Generally, though, most models in the literature are heavily regressed based on data. This has resulted in effective interfacial area terms from the literature having poor agreement amongst each other. This is due to multiple reasons, the first being the selected test systems for development and validation. If the physical property ranges are limited in viscosity, surface tension and other important physical property parameters related to effective area, then model's

will be limited in performance and their applications. Limitations to available data or studies as it pertains to packing can also be detrimental to an effective area model. Many of the models discussed in depth later contain correction factors that are based on the wetting of examined packings. Second, the interpretation of the definition of effective interfacial area seems to be up to the model developer. Some deduce that effective interfacial area is only the area represented by wetting on the specified nominal area. Others interpret effective interfacial area as any area in which mass transfer can occur, such as on waves, droplets, etc. Even when the later definition is adopted, rarely does the effective area prediction surpass the specified nominal area of the respective packing. In Section 2.3, specific effective area terms will be discussed more in-depth when specific HETP correlations are introduced.

2.3 REVIEW OF COMMON HETP CORRELATIONS

The purpose of this section is to discuss notable HETP models that will be analyzed in Chapter 3 and Chapter 4. Subsection 2.3.1 and 2.3.2 feature models that will not be analyzed but they are included since they are earlier variations of the model in Section 2.3.3 that will be analyzed. Each model will have their working equations, assumptions and other information related to development highlighted. The last Section 2.4 has a recap of previous work and studies related to HETP models.

2.3.1 SRP I Correlation

The first structured packing HETP model was developed by Bravo et al.[19] which focused on experimental data with gauze-type structured packing. The gas-side mass transfer coefficient is assumed to be accurately described by wetted wall column experiments. As stated earlier, there has been many notable studies with wetted wall columns, this model utilized the work from Johnstone and Pigford[14], as seen in Equation 2.4.

$$Sh_G = 0.0328 Re_G^{0.77} Sc_G^{0.333} \tag{2.4}$$

The constant and exponents in Equation 2.4 were modified based on the experimental data that Bravo et al.[19] had analyzed. The two sources for experimental data were total reflux experiments from Fractionation Research Inc.[20] and BASF.[21] After modification, the Sherwood gas number equation took the final form seen in Equation 2.5.

$$Sh_G = 0.0338 Re_G^{0.80} Sc_G^{0.333} \tag{2.5}$$

The Sherwood gas number can be converted into an expression for gas-side mass transfer coefficient. Since $Sh_G = \frac{k_G d_{eq}}{D_G}$, the gas-side mass transfer coefficient, k_G, is displayed in Equation 2.6.

$$k_G = 0.0338 Re_G^{0.80} Sc_G^{0.333} \left(\frac{D_G}{d_{eq}}\right) \tag{2.6}$$

Where the new terms in Equation 2.6 are the diffusion coefficient for gas, D_G, and the equivalent diameter of channel, d_{eq}. The equivalent diameter of channel is dependent on the type of packing used and its crimp height (h), channel base (B) and channel side (S) dimensions. The equation for equivalent diameter of channel can be seen in Equation 2.7.

$$d_{eq} = Bh[1/(B + 2S) + 1/2S] \tag{2.7}$$

Other important terms that are necessary to calculate the gas-side mass transfer coefficient in Equation 2.6 are the Reynolds number for gas and Schmidt number for gas, which are presented in Equation 2.13 and 2.14, respectively. Before calculating the Reynolds number for gas, the gas and liquid superficial velocity, liquid flow per unit length of perimeter, effective liquid and gas superficial velocities must be calculated, as seen in Equation 2.8, Equation 2.9, Equation 2.10, Equation 2.11, Equation 2.12 respectively.

$$U_{GS} = F_v/\sqrt{\rho_G} \tag{2.8}$$

$$U_{LS} = U_{GS}(\rho_G/\rho_L) \tag{2.9}$$

$$\Gamma = \frac{L}{(P\ A_t)} = \frac{L}{\left(\frac{4S + B}{Bh}\right) A_t} \tag{2.10}$$

$$U_{LE} = (3\Gamma/2\rho_L)(\rho_L^2 g/3\mu_L\Gamma)^{0.333} \quad (2.11)$$

$$U_{GE} = (U_{GS}/\varepsilon)sin(\theta) \quad (2.12)$$

$$Re_G = \frac{d_{eq}\rho_G}{\mu_G}(U_{GE} + U_{LE}) \quad (2.13)$$

$$Sc_G = \frac{\mu_G}{\rho_G D_G} \quad (2.14)$$

In Equation 2.10, liquid flow based on the perimeter requires tower cross sectional area, A_t, packing geometry and the mass velocity of the liquid, L. With the previous equations, it is now possible to calculate the gas-side mass transfer coefficient in Equation 2.6.

The liquid mass transfer coefficient is developed from penetration theory, the initial equation described by Higbie[22] is presented earlier in Equation 2.2. The modified version by Bravo et al.,[15] which is the utilized version in SRP I is as seen in Equation 2.15.

$$k_L = 2\sqrt{\frac{D_L U_{LE}}{(\pi S)}} \quad (2.15)$$

The exposure time seen in Equation 2.2, was replaced by the term S/U_{LE}, which better describes liquid flow across the corrugation side length. Unlike the next models that will be discussed later, SRP I assumes effective interfacial area to be equivalent to the specified packing area. Bravo et al.[15] found that at relatively high liquid rates, the gauze packing showed complete wetting to make this assumption. At this point, effective area, gas-side, and liquid-side mass transfer coefficient equations have been established for SRP I and now Equation 1.7 can be used to predict HETP.

2.3.2 SRP II Correlation

Like the SRP I correlation, SRP II[23,24] had similar model assumptions for development of its mass transfer coefficient equations. This means penetration theory was the basis for the liquid-side mass transfer and wetted wall column experiments for the gas-side mass transfer. One of the largest differences in the SRP II correlation is the development of a hydraulic model. The

hydraulic model is a critical part of the correlation that must be solved first before proceeding to use the mass transfer model. The important output of the hydraulic model that is ultimately a required input in the mass transfer model is the liquid holdup. The pressure drop model was developed from air/water experimental data of liquid holdup across multiple types of structured packings. McNulty and Hsieh[25] studied hydraulic effects with Flexipac while Chen et al.[26,27] conducted studies with Gempack. The first two steps to solving SRP II's hydraulic model is estimating dry pressure drop and correction factor for total holdup, which are respectively seen in Equation 2.19. and Equation 2.20. The dimensionless numbers required throughout SRP II are documented in Equation 2.16-2.20.

$$We_L = \frac{U_{LS}^2 \rho_L S}{\sigma} \tag{2.16}$$

$$Fr_L = \frac{U_{LS}^2}{Sg} \tag{2.17}$$

$$Re_L = \frac{U_{LS} S \rho_L}{\mu_L} \tag{2.18}$$

$$\left(\frac{\Delta P}{\Delta Z}\right)_{dry} = \left(\frac{0.1775 \rho_G}{S\varepsilon^2 (sin\theta)^2} U_{GS}^2 + \frac{88.774 \mu_G}{S^2 \varepsilon (sin\theta)} U_{GS}\right) \tag{2.19}$$

$$F_t = \frac{29.12 (We_L Fr_L)^{0.15} S^{0.359}}{Re_L^{0.2} \varepsilon^{0.6} (1 - 0.93 cos\gamma)(sin\theta)^{0.3}} \tag{2.20}$$

The horizontal corrugation angle, θ, is not to be confused with the contact angle between liquid and solid, γ, which are both seen in the correction factor for liquid holdup. The value for $cos\gamma$ is dependent on packing type and surface tension of the test system, if the surface tension is less than or equal to 0.055 N/m, then $cos\gamma = 0.90$. If surface tension is greater than 0.055 N/m, then $cos\gamma = 5.211 \times 10^{-16.835\sigma}$, where σ is the actual surface tension of the system. Once these values are calculated, liquid-holdup is then solved iteratively. First, liquid hold-up is calculated with Equation 2.28., with $\left(\frac{\Delta P}{\Delta Z}\right)_{new} = \left(\frac{\Delta P}{\Delta Z}\right)_{dry}$, once this value is set, pressure drop at the flood point can be estimated. Rocha et al.[23,24] states that a pressure range of 900-1200 Pa/m was common to witness flooding for the packings and systems studied.

$$h_L = \left[\frac{4F_t}{S}\right]^{2/3} \left\{ \frac{3\mu_L U_{LS}}{\rho_L \varepsilon sin\theta g \left[\left(\frac{\rho_L - \rho_G}{\rho_L}\right)\left(1 - \frac{\left(\frac{\Delta P}{\Delta Z}\right)_{new}}{\left(\frac{\Delta P}{\Delta Z}\right)_{flood}}\right)\right]} \right\}^{1/3} \tag{2.21}$$

$$\left(\frac{\Delta P}{\Delta Z}\right) = \frac{\left(\frac{\Delta P}{\Delta Z}\right)_{dry}}{[1 - (0.614 + 71.35S)h_L]^5} \tag{2.22}$$

With a liquid holdup and pressure drop value calculated, the pressure drop value from Equation 2.22, is compared to $\left(\frac{\Delta P}{\Delta Z}\right)_{new}$. If $\left(\frac{\Delta P}{\Delta Z}\right) \neq \left(\frac{\Delta P}{\Delta Z}\right)_{new}$, then $\left(\frac{\Delta P}{\Delta Z}\right)_{new}$ is set to $\left(\frac{\Delta P}{\Delta Z}\right)$ which is then the new pressure drop value used to recalculate Equation 2.21. Equation 2.22 is also recalculated given that there is a new liquid holdup value, where again, $\left(\frac{\Delta P}{\Delta Z}\right)$ is checked if it is equal to $\left(\frac{\Delta P}{\Delta Z}\right)_{new}$. The process will continue for multiple iterations until the conditions are met, once $\left(\frac{\Delta P}{\Delta Z}\right) \approx \left(\frac{\Delta P}{\Delta Z}\right)_{new}$, the iteration process can be stopped, and the user of SRP II model has the liquid holdup calculation that will be used for the mass transfer model.

As stated earlier, SRP II used the wetting wall column relationship to develop the gas-side mass transfer coefficient term. The exponents are the same as seen in SRP I, but there are slight modifications to the constant value, as well as Reynolds number term, seen in Equation 2.23.

$$k_G = 0.054\left(\frac{D_G}{S}\right)\left(\frac{(U_{GE} + U_{LE})\rho_G S}{\mu_G}\right)^{0.8}\left(\frac{\mu_G}{D_G \rho_G}\right)^{0.33} \tag{2.23}$$

The effective velocities are more complex than the versions seen in SRP I, with the implementation of the liquid holdup parameter in both the liquid and gas effective superficial velocities. The liquid and gas effective velocities are presented in Equation 2.24 and Equation 2.25, respectively.

$$U_{LE} = \frac{U_{LS}}{\epsilon h_L sin\theta} \tag{2.24}$$

$$U_{GE} = \frac{U_{GS}}{\epsilon(1 - h_L)sin\theta} \tag{2.25}$$

The liquid mass transfer coefficient term is also like the version seen in SRP I, seen in Equation 2.26. The difference is the addition of a correction factor for surface renewal, C_E, this is done to account for parts of the packed bed where surface renewal is not rapid.

$$k_L = 2\sqrt{\frac{D_L C_E U_{LE}}{\pi S}} \tag{2.26}$$

Murrieta[28] found that the correction factor for surface renewal typically was around 0.9. This study was conducted with commonly known structured packings and the test system was an air/water system.

Along with the addition of a hydraulic model to SRP II, an effective interfacial area term was established. Shi and Mersmann[29] studied liquid flows and wetted surface area in a packed column with multiple systems which became the basis for development of SRP II's effective interfacial area term, seen in Equation 2.27.

$$\frac{a_e}{a_p} = F_{SE}\frac{29.12(We_L Fr_L)^{0.15}S^{0.359}}{Re_L^{0.2}\varepsilon^{0.6}(1 - 0.93cos\gamma)(sin\theta)^{0.3}} \tag{2.27}$$

In Equation 2.27, the surface enhancement factor, F_{SE}, which accounts for variations in the surface of the packing, such as fluting. This term was created from studies of surface performance under distillation by McGlamery.[30]

2.3.3 Revised SRP II Correlation: Gualito et al.

Based on the SRP II correlation's performance with new high-pressure data published by Fractionation Research Inc., Gualito et al.[31] revised aspects of the SRP II correlation to improve its predictions at those pressures. The new data, published by Fitz et al.,[32] contained the pressure range of 6.9 bara to 27.6 bara, for the test system IC4/NC4. The main change from SRP II to Gualito correlation is the effective area term. There are also minor changes to hydraulic and mass transfer model equations. The Weber number, Froude number and Reynolds number for the

liquid are the same equations as in Section 2.2.2. The new hydraulic model equations are presented in Equation 2.28-2.31.

$$\left(\frac{\Delta P}{\Delta Z}\right)_{dry} = \left(\frac{\rho_G}{\rho_{air,1bar}}\right)^{0.4} \left(\frac{C_1 \rho_G}{S\varepsilon^2 (sin\theta)^2} U_{GS}^2 + \frac{C_2 \mu_G}{S^2 \varepsilon (sin\theta)} U_{GS}\right) \tag{2.28}$$

$$F_t = \frac{(We_L Fr_L)^{0.15} A_1 S^{A_2}}{Re_L^{0.2} \varepsilon^{0.6} (1 - 0.93 cos\gamma)(sin\theta)^{0.3}} \tag{2.29}$$

$$h_L = \left[\frac{4F_t}{S}\right]^{2/3} \left(\frac{3\mu_L U_{LS}}{\rho_L \varepsilon sin\theta g \left[\left(\frac{\rho_L - \rho_G}{\rho_L}\right)\left(1 - \frac{\left(\frac{\Delta P}{\Delta Z}\right)_{new}}{\left(\frac{\Delta P}{\Delta Z}\right)_{flood}}\right)\right]}\right)^{1/3} \tag{2.30}$$

$$\left(\frac{\Delta P}{\Delta Z}\right) = \frac{\left(\frac{\Delta P}{\Delta Z}\right)_{dry}}{[1 - (D_1 + D_2 S) h_L]^5} \tag{2.31}$$

In Equation 2.28, has a new term added with the implementation of $\left(\frac{\rho_G}{\rho_{air,1bar}}\right)^{0.4}$, as well as new constants seen in the Equations 2.28-2.31. The new constants which are: A_1, A_2, B_1, B_2, C_1, C_2, D_1, and D_2, allow for the interchanging of constants based on the packing material being used, these values are presented in Table 2.1. As discussed in SRP II, the value for $cos\gamma$ is dependent on packing type and surface tension of the test system. For SRP II, the reference surface tension is equal to 0.055 N/m, for deciding what equation to use to find the value of $cos\gamma$. For the Gualito correlation, the reference surface tension is equal to 0.045 N/m. If the surface tension is equal to or less than 0.045 N/m, $cos\gamma = 0.90$. If the surface tension was greater than 0.045 N/m, then $cos\gamma = B_1 \times 10^{B_2 \sigma}$.

Table 2.1. Hydraulic Model Constants in Gualito Correlation

Material Type	A_1	A_2	B_1	B_2	C_1	C_2	D_1	D_2	F_{SE}
Sheet Metal	29.12	0.3600	5.210	-16.83	0.1770	88.77	0.6140	71.35	0.3500
Ceramic	11.54	0.3600	1.520	-3.510	0.2440	0.000	0.5320	92.22	0.4600
Polypropylene	21.67	0.1300	10.88	-30.92	0.1340	44.06	0.6330	130.94	0.4600

For calculations used in later chapters, only the constants under the sheet metal material type were utilized. It is interesting to note that in Gualito et al.,[31] the surface enhancement factor is recommended as 0.35, no matter the structured sheet metal packing type, unlike in the original SRP II correlation. After solving Equation 2.28-2.29, $\left(\frac{\Delta P}{\Delta Z}\right)_{new}$ is set to $\left(\frac{\Delta P}{\Delta Z}\right)_{dry}$ but the value for pressure drop at the flooding point now follows a correlation, is not selected based on an estimated range like it is in SRP II. The new recommendation for the estimation of $\left(\frac{\Delta P}{\Delta Z}\right)_{flood}$ is presented by Gualito et al., seen in Equation 2.32.

$$\left(\frac{\Delta P}{\Delta Z}\right)_{flood} = 1500 + 65{,}000 \cdot U_{LS} \tag{2.32}$$

The correlation for pressure drop at the flooding point predicts a much higher pressure drop range than the observed range stated in SRP II's development. Now that pressure drop at flood and "new" pressure drop is calculated, Equation 2.30 and Equation 2.31 can be solved. The same iterative process described in Section 2.2.2. for SRP II hydraulic model is performed in Equations 2.30-2.31 until convergence is met between pressure drop, $\left(\frac{\Delta P}{\Delta Z}\right)$, and the "new" pressure drop, $\left(\frac{\Delta P}{\Delta Z}\right)_{new}$.

Besides the changes seen in the hydraulic model, there is only one variation in the mass transfer model. It is one slight change in the liquid mass transfer coefficient term, seen in Equation 2.33.

$$k_L = 2\sqrt{\frac{D_L U_{Le}}{\pi S}} \tag{2.33}$$

The difference between SRP II's liquid mass transfer coefficient and Gualito correlation is the omission of the C_E term in Equation 2.33. Gualito et al.[31] do not state a reason for removing the correction factor for surface renewal. This could be an error, but its presence is fairly inconsequential on HETP prediction and for further studies involving Gualito correlation, the equaations are used as presented in the publication.

The major update in the Gualito correlation is found in the effective area term. This was inspired by the HETP predictions by SRP II which underpredicted for the high-pressure data published by Fitz et al.[32] A correction factor was inserted into the effective area term, which was a ratio of liquid and gas superficial velocities. This was done to adjust the original effective area term in SRP II which predicted effective area terms being greater than the specified nominal area of the packing being utilized. The new effective area term with the addition of the correction factor is presented below in Equation 2.34.

$$\frac{a_e}{a_p} = \frac{(We_L Fr_L)^{0.15} A_1 S^{A_2} F_{SE}}{Re_L^{0.2} \varepsilon^{0.6} (1 - 0.93 cos\gamma)(sin\theta)^{0.3}} \left[\frac{1.2}{1 + 0.2e^{30(U_{LS}/(2U_{GS}))}}\right] \tag{2.34}$$

The beneficial aspect of the new correction term is that it does not greatly impact low-pressure test system predictions. So, the performance of Gualito and SRP II only diverges for high pressure systems. The same gas side mass transfer coefficient is utilized in this update as the original SRP II, as well as the Reynolds, Weber, Froude, effective superficial velocity equations.

2.3.4 Billet & Schultes (1993, 1999)

Billet & Schultes correlation was developed from a wide range of test systems used in mass transfer studies at Bochum University. The first model, published in 1993 by Billet and Schultes[17] had introduced packing specific constants implemented in the mass transfer coefficient terms. Both mass transfer coefficient terms were uniquely formulated from Higbie's penetration theory, and the mass transfer model can predict HETP for random and structured packing

applications. Many of the other models preceding and succeeding the Billet & Schultes correlation use penetration theory for the liquid mass transfer coefficient and wetted wall column experiments to construct the gas mass transfer coefficient. The equations published in the 1993 version of Billet & Schultes correlation are given below.

$$h_L = \left(\frac{12\mu_L a_p^2 U_{LS}}{\rho_L g}\right)^{1/3} \tag{2.35}$$

$$d_h = 4\frac{\varepsilon}{a_p} \tag{2.36}$$

$$k_L = C_L\left(\frac{g\rho_L}{\mu_L}\right)^{1/6}\sqrt{D_L/d_h}\left(\frac{U_{LS}}{a_p}\right)^{1/3} \tag{2.37}$$

$$k_G = C_V\left(\frac{1}{\sqrt{\varepsilon - h_L}}\right)\sqrt{a_p/d_h}\,D_G\left(\frac{\rho_G U_{GS}}{\mu_G a_p}\right)^{3/4}\left(\frac{\mu_G}{\rho_G D_G}\right)^{1/3} \tag{2.38}$$

$$\frac{a_e}{a_p} = (1.5/\sqrt{a_p d_h})\left(\frac{U_{LS} d_h \rho_L}{\mu_L}\right)^{-0.2}\left(\frac{U_{LS}^2 d_h \rho_L}{\sigma}\right)^{0.75}\left(\frac{U_{LS}^2}{g d_h}\right)^{-0.45} \tag{2.39}$$

The packing-specific constants, C_V and C_L are seen in the liquid and gas mass transfer coefficients, seen respectively in Equation 2.37 and Equation 2.38. The packing specific constants are regressed with experimental HETP data, so each packing type has a unique set of constants. Along with the working equations of the correlation, Billet and Schultes[17,18] published values for packing-specific constants, applicable to the packing types that were used in their mass transfer studies.

In the later publishing in 1999, Billet and Schultes[18] presented a model dependent on the type of flow regime being predicted. There essentially was a different set of working equations for the pre-loading regime, loading point and flooding regime.

2.3.5 Delft Model (1997, 2004, 2014)

Olujić[33] initially developed the Delft Model in 1997, which predicted hydraulic parameters such as liquid film thickness and liquid hold-up. Like previous models, the liquid mass transfer coefficient term was developed from penetration theory and gas mass transfer

coefficient term was developed from wetted wall column experiments. The working equations for solving the gas mass transfer coefficient term in the 1997 version of the Delft Model are listed in Equations 2.40-2.55.

$$i_{G,pe} = \frac{h_{pe}}{sin(\theta)} \tag{2.40}$$

$$\delta = \left(\frac{3\mu_L U_{LS}}{\rho_L\, g\, a_p\, sin(\theta)}\right)^{1/3} \tag{2.41}$$

$$d_{hG} = \frac{\frac{(bh-2\delta s)^2}{bh}}{\left[\left(\frac{bh-2\delta s}{2h}\right)^2 + \left(\frac{(bh-2\delta s)}{bh}\right)^2\right]^{0.5} + \frac{bh-2\delta s}{2h}} \tag{2.42}$$

$$h_L = \delta a_p \tag{2.43}$$

The liquid holdup is then implemented into the effective liquid and gas velocities, in Equations 2.44-2.45. The gas mass transfer coefficient for the Delft model was divided into laminar and turbulent flow regimes. The turbulent Sherwood gas number, seen in Equation 2.49, was developed by Petukhov[34] using mineral oils like transformer oil, and was accurate within 5% over the Reynolds number range of 10^4 to 5×10^6 and Prandtl number range of 0.5 to 2,000. Millsaps and Pohlhausen[35] utilized the momentum-integral equation by Karman[36] to build the laminar Sherwood gas number. The gas side mass transfer coefficient is established in Equation 2.53.

$$U_{Ge} = \frac{U_{GS}}{(\epsilon - h_L)sin(\theta)} \tag{2.44}$$

$$U_{Le} = \frac{U_{LS}}{\epsilon h_L sin(\theta)} \tag{2.45}$$

$$\xi_{GL} = \left\{-2log\left[\frac{\left(\frac{\delta}{d_{hG}}\right)}{3.7} - \frac{5.02}{Re_{Grv}} log\left(\frac{\left(\frac{\delta}{d_{hG}}\right)}{3.7} + \frac{14.5}{Re_{Grv}}\right)\right]\right\}^{-2} \tag{2.46}$$

$$Re_{Grv} = \frac{\rho_G(U_{Ge} + U_{Le})d_{hG}}{\mu_G} \tag{2.47}$$

$$Sc_G = \frac{\mu_G}{\rho_G D_G} \tag{2.48}$$

$$Sh_{G,turb} = \frac{Re_{Grv} Sc_G \frac{\xi_{GL}}{8}}{1 + 12.7\sqrt{\frac{\xi_{GL}}{8}}(Sc_G^{2/3} - 1)}\left[1 + \left(\frac{d_{hG}}{l_{G,pe}}\right)^{2/3}\right] \tag{2.49}$$

$$Sh_{G,lam} = 0.664 Sc_G^{1/3}\sqrt{Re_{Gvr}\frac{d_{hG}}{l_{G,pe}}} \tag{2.50}$$

$$k_{G,turb} = \frac{Sh_{G,turb} D_G}{d_{hG}} \tag{2.51}$$

$$k_{G,lam} = \frac{Sh_{G,lam} D_G}{d_{hG}} \tag{2.52}$$

$$k_G = \sqrt{k_{G,lam}^2 + k_{G,turb}^2} \tag{2.53}$$

The liquid mass transfer coefficient term, seen in Equation 2.54, is quite like SRP II, except for the d_{hG} term, or hydraulic diameter. Both SRP II and Delft adopted Higbie's penetration theory to derive the k_L term, both adopted a correction factor value for surface renewal, this value is 0.9. In the denominator of SRP II, the corrugation side length is present, while for the Delft model it has been switched out for the hydraulic diameter that was defined in Equation 2.42.

$$k_L = 2\sqrt{\frac{D_L U_{Le}}{\pi 0.9 d_{hG}}} \tag{2.54}$$

The effective area model in the 1997 version is empirical in nature, where the constants *A* and *B*, are packing dependent and is a function of liquid load. The effective area model seen below, also has the term, Ω, which is the void fraction of packing. For Mellapak, Flexipac and Montz BSH packings, this value would be set to 0.1 while packings like Montz B1 that are unperforated, would be set to 0.

$$a_e = a_p \frac{(1 - \Omega)}{\left(1 + \frac{A}{U_{LS}^B}\right)} \tag{2.55}$$

The Delft model was updated after suggestions from Fair et al.,[37] which ended up resulting in a new effective area term, effective liquid flow angle and updated turbulent gas phase Sherwood number[38]. The effective liquid flow angle, Equation 2.56, replaces the angle of packing

corrugation in multiple equations of the Delft model, specifically the liquid film thickness and effective liquid velocity, which are presented in Equation 2.57 and 2.58, respectively. The angle of packing corrugation is still utilized in the effective gas velocity, seen in Equation 2.44. The change from packing angle to a calculated effective angle is theoretical modification that liquid will flow at a steeper angle that the packing angle due to gravity.

$$\theta_L = arctan\left[\frac{cos(90-\alpha)}{sin(90-\alpha)cos(arctan(\frac{b}{2h})}\right] \tag{2.56}$$

$$\delta = \left(\frac{3\mu_L U_{LS}}{\rho_L\, g\, a_p\, sin(\theta_L)}\right)^{1/3} \tag{2.57}$$

$$U_{Le} = \frac{U_{LS}}{\epsilon h_L sin(\theta_L)} \tag{2.58}$$

Another significant change is the implementation of the fraction of the triangular flow channel occupied by liquid, or φ. Of the changes in the 2004 modification[38] of Delft, this has the largest impact on predicted HETP. In the first version, φ was equal to one, now there is a calculation for determining it, seen in Equation 2.59, which is based on packing specific dimensions.

$$\varphi = \frac{2s}{b+2s} \tag{2.59}$$

$$Sh_{G,turb} = \frac{Re_{Grv} Sc_G \frac{\xi_{GL}\varphi}{8}}{1+12.7\sqrt{\frac{\xi_{GL}\varphi}{8}}(Sc_G^{2/3}-1)}\left[1+\left(\frac{d_{hG}}{l_{G,pe}}\right)^{2/3}\right] \tag{2.60}$$

The final modification presented in this paper is the update to the effective area model. The new effective area term, in Equation 2.64, was adopted from Onda et al.,[15] who conducted CO_2 absorption experiments with random packings. An additional term was added, (1-Ω), to provide flexibility with different packings that had variability in holes.

$$We_L = \frac{U_{LS}^2 \rho_L}{a_p \sigma} \tag{2.61}$$

$$Fr_L = \frac{U_{LS}^2 a_p}{g} \tag{2.62}$$

$$Re_L = \frac{U_{LS}\rho_L}{a_p \mu_L} \tag{2.63}$$

$$a_e = (1-\Omega)\, a_p \left\{1 - exp\left[-1.45\left(\frac{0.075}{\sigma}\right)^{0.75} Re_L^{0.1} Fr_L^{-0.05} We_L^{0.2}\right]\right\} \tag{2.64}$$

Since the implementation of fraction of the triangular flow channel occupied by liquid, φ, into the turbulent gas phase Sherwood number, Olujić et al.[39] concluded after a study with high-capacity structured packings that this parameter should be equal to one, for those specific packings.

After more experimental data was published and Olujić and Seibert[40] examined the Delft model again, determined that φ should be equal to one, for any structured packings, which is a reversion back to the original turbulent Sherwood gas number. The final modification presented in this study is an updated liquid mass transfer coefficient. The new term incorporates liquid holdup, packing void fraction, corrugation side length and superficial liquid velocity, shown in Equation 2.65.

$$k_L = 2\sqrt{\frac{D_L U_{Ls}}{\pi \varepsilon h_L s}} \tag{2.65}$$

The equations used for further analysis of the Delft Model were the 2004 version with the 2014 updates to k_L and turbulent Sherwood number. This would be the latest form available and provides significant performance improvement with the packings analyzed later, when compared to the equations of the 2004 version.

2.3.6 Hanley and Chen (Aspen, 2012)

Another model capable of predicting HETP for random and structured packing was published by Hanley and Chen[16] for implementation into Aspen Plus software. The goal of this model is to provide an accurate HETP for a wide range of chemical systems in a rate-based column simulator. The model is also set-up to evaluate experimental binary test systems from in the literature, which was done by the original authors when the model's performance was compared to a couple other correlations. The model includes a redefined definition of HETP that includes

superficial molar vapor flux, which is different than the HETP term adopted by the other models. The equations used to calculate Aspen's HETP term are seen in Equation 2.66-2.68.

$$C_y = \langle \frac{ln[m(x)]}{m(x)-1} \rangle \tag{2.66}$$

$$C_x = \langle \frac{m(x)\ ln[m(x)]}{m(x)-1} \rangle \tag{2.67}$$

$$\langle HETP \rangle = \frac{G}{a_e}\left(\frac{C_y}{k_G} + \frac{C_x}{k_L}\right) \tag{2.68}$$

The equilibrium slope, m(x), is defined the same as Equation 1.6, for binary systems. The Aspen model has different sets of mass transfer coefficient and effective area terms, depending on the packing type. The construction of the mass transfer coefficient and effective area terms were done with dimensional analysis. Specifically, Buckingham Pi theorem with the addition of correction factors that were regressed based on a wide range of public efficiency data. For this study, only sheet metal structured packing equations were utilized, as shown in Equation 2.69-2.76.

$$d_e = \frac{4\varepsilon}{a_p} \tag{2.69}$$

$$Re_G = \frac{d_e U_{GS} \rho_G}{\mu_G} \tag{2.70}$$

$$Re_L = \frac{d_e U_{LS} \rho_L}{\mu_L} \tag{2.71}$$

$$We_L = \frac{d_e \rho_L U_{LS}^2}{\sigma} \tag{2.72}$$

$$Fr_L = \frac{U_{LS}^2}{g d_e} \tag{2.73}$$

$$k_L = 0.33 Re_L Sc_L^{1/3}\left(\frac{c_L D_L}{d_e}\right) \tag{2.74}$$

$$k_G = 0.0084 Re_G Sc_G^{1/3}\left(\frac{c_G D_G}{d_e}\right)\left(\frac{cos(\theta)}{cos(\pi/4)}\right)^{-7.15} \tag{2.75}$$

$$\frac{a_e}{a_p} = 0.539 Re_G^{0.145} Re_L^{-0.153} We_L^{0.2} Fr_L^{-0.2}\left(\frac{\rho_G}{\rho_L}\right)^{-0.033}\left(\frac{\mu_G}{\mu_L}\right)^{0.090}\left(\frac{cos(\theta)}{cos(\pi/4)}\right)^{4.078} \tag{2.76}$$

Many of the systems collected model regression and validation were from non-distillation applications such as available absorption/stripping data. One of the main goals of the Aspen

correlation was to be able to perform well with public distillation data and with chemical systems in distillation, absorption, stripping, etc.

2.3.7 Song (2017)

This model was published in a doctoral dissertation by Di Song but is the culmination of multiple graduate students at the University of Texas.[41] Previous work included surface tension and viscosity studies on effective area[42] and the development of mass transfer coefficients[43] with a more limited scope of systems and studies than Song's final version.

This correlation is not like previously discussed correlations, as its development was not specifically meant for distillation applications. All the data used for development and validation was with SRP's air/water column database. Although it does not fit the same category as previous discussed correlations like Gualito, Delft, etc., due to its promising showing of predicting HETP[44], it was included as a model of interest in this study. As stated, the Song model was derived from air/water mass transfer data and studied a wide range of packing types. The liquid mass transfer coefficient was measured via air stripping experiments and the effective area term was developed from CO_2 absorption into NaOH. Many packings were investigated during the data collection phase of this work, this included 39 different structured and random packings for the effective area and k_L terms and 20 packings for the k_G term.

$$k_G = 0.28 U_{GS}^{0.62} \left(\frac{\mu_G}{\rho_G}\right)^{-0.12} D_G^{0.5} a_p^{0.38} (sin2\theta)^{0.65} \tag{2.77}$$

$$k_L = 0.12 U_{LS}^{0.565} \left(\frac{\mu_L}{\rho_L}\right)^{-0.4} D_L^{0.5} g^{1/6} a_p^{-0.065} \left(\frac{Z}{1.8}\right)^{-0.54} \tag{2.78}$$

$$\frac{a_e}{a_p} = 1.16\eta \left[\left(\frac{\rho_L}{\sigma}\right) g^{1/2} U_{LS} a_p^{-3/2}\right]^{0.138} \tag{2.79}$$

Obviously, the Song correlation is developed with experimental data where liquid side mass transfer would dominate, whereas in distillation, efficiency/HETP is more dependent on the gas side mass transfer coefficient. Besides differences in the developmental database, another unique feature is the implementation of packed bed height, *Z*, in the liquid mass transfer coefficient term,

seen in Equation 2.78. If a practitioner were to use this correlation to design a column, it would have to be done iteratively due to the packed bed height parameter.

2.4 OTHER NOTABLE CORRELATIONS

Although this study is limited to a handful of structured packing HETP correlations, specifically Gualito, Billet & Schultes, Delft, Aspen and Song, there has been many other influential correlations. Nawrocki et al.[45] adopted similar equations for k_L and k_G as the SRP I correlation but implemented liquid distribution and wetted area work from Shi and Mersmann.[29] Around the same time, Henriques de Brito et al.[46] modified the k_L term from Higbie's penetration theory with the addition of packing-specific constants for Mellapak 250Y and Mellapak 500Y. Hanley et al.,[47,48] created a mass transfer model that was dependent on a pressure drop model, through the liquid holdup parameter, which is similar to the structure of the SRP II correlation. Brunazzi and Paglianti[49] focused on coming up with a new liquid mass transfer coefficient term using k_La measurements. Shetty and Cerro[50] also only focused on liquid mass transfer coefficient development with conducting studies of liquid flow over micro and macrostructures. Xu et al.[51] produced a correlation that mixed the Billet & Schultes mass transfer coefficients with liquid holdup equations of SRP II, as well as developing a new effective area model. Del Carlo et al.[52] adopted semiempirical terms from previous absorption studies on pressure drop and efficiency to create a model specifically for systems where no experimental data was readily available.

2.5 PREVIOUS WORK

There have been multiple studies that have investigated prediction performance by HETP correlations. Fitz et al.[32] compared the performance of the Gualito and Billet & Schultes correlations across various test systems, including high pressure data. Fair et al.[37] examined SRP II and Delft model performance with SRP experimental data, before suggesting modifications to improve the performance of the models. Olujić[38,39,40,53,54] constantly evaluated the Delft Model, as new experimental data was published to verify its robustness and suggest improvements.

Jammula et al.,[55] investigated several correlations with published HETP data, but only average deviation was reported in table form in a conference presentation. Some of the best analyses of other models were conducted when new models were introduced in the literature. Hanley and Chen[16] reported average HETP value predictions of multiple models with different experimental datasets. Another similar comparative study was with liquid holdup, pressure drop and flood point by Wolf-Zöllner et al.,[56] while this is not a study about HETP prediction performance, many aspects investigated in this study are important parameters of HETP models. Olujić and Seibert[40] compared the liquid mass transfer coefficient model of seven structured packing efficiency correlations. Different observations about performance were tied back to the development of the selected models.

The later portion of this thesis is dedicated to a physical property study on the selected efficiency correlations. The bulk of existing studies related to physical properties and structured packings are physical experiments. Examples of such studies would be varying viscosity or surface tension and measuring its impacts on packed column performance. Multiple studies[57,58,59,60,61] have investigated liquid viscosity on efficiency, liquid phase resistance, etc. A recent impactful study by Bradtmöller and Scholl[61], presented the positive relationship of viscosity and HETP. In some instances, an increase of liquid viscosity by a factor of 6, resulted in an efficiency decrease of 50%. Song[41,59] conducted two different aspects of a liquid viscosity study – the first was a numerical analysis on liquid viscosity relationship with the liquid mass transfer coefficient of many public correlations, the second was deriving a correlation by varying the systems liquid viscosity over a wide range. Surface tension has also been studied in similar ways to that of liquid viscosity. There has been multiple studies[58,60,62,63] of the impact of surface tension gradients on packed column performance. In general, the focus of physical property studies has generally been to quantify certain parameters experimentally and then try to incorporate these relationships into model.

CHAPTER III

PERFORMANCE EVALUATION OF CONVENTIONAL STRUCTURED PACKING HETP MODELS

This chapter contains the full methodology, selection of test data/systems, calculations and analysis for the performance evaluation conducted in *Distillation & Absorption* conference paper presented in Chapter 5.

3.1 ABSTRACT

This study focuses on performance of five HETP correlations in the literature. The correlations evaluated were Gualito, Billet and Schultes, Delft, Aspen and Song. The analysis presented here in Chapter 3, explains the criteria for HETP data collection and the performance evaluation results that were coupled with Monte Carlo simulations in Chapter 5. The systems selected were i-butane/n-butane, cyclohexane/n-heptane, o/p-xylene, and methanol/water, across a pressure range of 0.13 bara to 27.6 bara. This chapter provides additional analysis that was not included in the *Distillation and Absorption* conference paper. Overall, Billet & Schultes had the lowest average deviation in HETP predictions for all systems analyzed, this is due to the benefit of regressed packing-specific constants. Song's performance was second to Billet & Schultes, which is surprising as it was derived from an air/water column databank. In addition to HETP performance, other parameters such as effective area predictions by all the models are presented and analyzed.

3.2 INTRODUCTION

The selected correlations are a mix of well-established models (Billet & Schultes, Delft, and Gualito) and some newer models that feature different developmental methods (Song, and Aspen). The background of these models and their working equations were discussed in Chapter 2. The main justification for the data selected in this chapter were to conduct the physical property study presented in Chapter 5. The data required to perform a physical property sensitivity and Monte Carlo simulation meant that the physical property ranges needed to be as a wide as possible and that the structured packings were of similar nature (in terms of nominal area, corrugation angle, etc.). This same data was selected to evaluate the model's HETP performance capabilities to couple the results with the uncertainty data obtained from Monte Carlo simulation. In addition to evaluating the closeness of their HETP predictions, effective interfacial area calculations of each model are also compared. All the datasets except the methanol/water system from Sulzer, have corresponding compositions and physical property inputs to each experimental HETP datapoint. This was done to increase the preciseness of the physical property sensitivity tests and the HETP evaluation in this chapter. The methanol/water system was still included in analysis because it is a system of value to the industry, and it provided a system with a higher surface tension than the hydrocarbon data.

3.3 EXPERIMENTAL METHODS

This section is dedicated to explaining the general steps for data collection, performance evaluation and comparison. A discussion on criteria for adequate experimental HETP data is included as well as equations utilized for analysis.

3.3.1 HETP DATA COLLECTION PROCESS

The screening of experimental HETP data published in the literature is an important step to properly evaluate the performance of HETP correlations. The objective is to select experimental HETP data that would reflect similar column performance seen in industry. There

are many test facilities capable of measuring HETP in the world, each has their own major differences when it comes to column diameter, taking samples, operation, etc. The first difference, column diameter, can be the distinguishing factor between usable efficiency data or not. Olujić[64] studied the impact of column diameter on HETP and noted differences of performance in smaller columns. It was concluded that smaller columns suffer from increased pressure drop that is not representative of industrial sized columns. As columns get smaller in diameter, they tend to be more dominated by wall effects. Ottenbacher et al.[65] stated that columns 0.4 m and larger in diameter should only be considered for efficiency measurements. This value represents a rough estimate of twice the height of a packing element. Plenty of HETP data has been published with columns smaller than this recommendation and data from these small columns should not be used to develop HETP correlations or test their performance. HETP data included in the study contained column diameters of 0.43 m and larger.

Perhaps one of the obvious requisites for acceptable HETP data are experiments with satisfactory liquid distribution. Obviously, this study is not doing any of the experimental work, so it must rely on published data that seldom discusses liquid distribution. The best way to ensure that this requirement is met is to consider efficiency measurements from trusted and skilled testing facilities. In this study, a majority of collected datasets are from Fractionation Research Inc. and Separations Research Program. FRI is one of the oldest testing facilities, founded in the 1950's, dedicated to conducting distillation experiments for its 70+ member companies. SRP has spent the past couple of decades performing efficiency measurements and being trusted with proprietary packing experiments like FRI. Along with FRI and SRP, efficiency measurements were collected from packing providers such as Sulzer, Koch-Glitsch and other well-known test facilities like Delft.

3.3.2 EVALUATING PRE-LOADING PREDICTION ACCURACY

After efficiency measurements are collected, physical property inputs needed to be decided to compare experimental HETP data with predicted HETP values. Typically, HETP data published in the literature is also presented with physical properties for each of the test systems. This physical property set usually corresponds to a respective composition at the specific F-factor that a composition sample was taken from the experiment. Technically, there should be a unique physical property set for each HETP point, as the liquid composition at the respective sampling location is changing with the F-factor. For the most part, the test systems that are commonly utilized for efficiency measurements do not vary greatly and using one physical property set across all the HETP points for a run can be considered acceptable for HETP prediction purposes. A good example of a commonly used test system where this would be acceptable is O/P-xylene, where the relative volatility varies little in an experiment. This study had access to FRI's Topical Reports, so for HETP data from FRI, each HETP point had a corresponding composition and physical property set. For any non-FRI source, the physical property set, or composition of one HETP point is used for the HETP correlations input.

The quantifying parameter to establish differences in accuracy for the selected HETP correlations is mean absolute percent deviation (MAPD). The equation for MAPD is presented below in Equation 3.1.

$$\text{MAPD} = \frac{1}{n}\sum_{i=1}^{n}\left|\frac{\text{Predicted HETP - Measured HETP}}{\text{Measured HETP}}\right| \times 100 \qquad (3.1)$$

The only HETP points considered in Equation 3.1. are HETP points from the pre-loading regime. Thus, MAPD is an average of all HETP points across the pre-loading regime of a respective test system.

It is important to note that although nominal area, a_p, is discussed as something that is specified and subsequent sections are labeled with nominal areas that are based on the name of

the packing, but there is a calculation method for nominal area. This equation can be seen below in Equation 3.2.

$$a_p = \frac{4s}{bh} \tag{3.2}$$

Typically, the calculated nominal area is very close to the area presented in the name of the packing, for example, Mellapak 250Y, where the "250" is meant to specify the nominal area, using the equation presented above, the actual calculated nominal area is around 260 m^2/m^3. The difference in value does not have a large impact on predicted HETP, with the analyzed correlations, but for the purpose of having highest accuracy possible, the effective area determined from Equation 3.2 was utilized in the studies in Section 3.4.

3.4 RESULTS AND DISCUSSION

3.4.1 EVALUATION OF MELLAPAK 250Y STRUCTURED PACKING

One of the most studied structured packings in the literature is the corrugated sheet metal packings, Mellapak 250Y. It has a nominal packing area around 250 m^2/m^3 and a corrugation angle of 45 degrees. Due to the vast amount of published data with Mellapak 250Y, it is a perfect candidate for a physical property study and thus a performance evaluation. The HETP data collected contains multiple hydrocarbon and aqueous test systems, with pressures ranging between 0.13 bara – 27.6 bara.[32,66] A summary of the collected experimental data, with information such as chemical system, test facility, column diameter, and packing name can be seen in Table 3.1.

Table 3.1. Test Systems Collected for Model Evaluation

Test System	Pressure (bara)	Test Facility	Column Diameter (m)	Packing Name
C6/C7	0.330	FRI	1.20	Mellapak 250Y
C6/C7	1.65	FRI	1.20	Mellapak 250Y
O/P-Xylene	0.130	FRI	1.20	Mellapak 250Y
O/P-Xylene	1.00	FRI	1.20	Mellapak 250Y
IC4/NC4	6.90	FRI	1.20	Mellapak 250Y
IC4/NC4	11.4	FRI	1.20	Mellapak 250Y
IC4/NC4	20.7	FRI	1.20	Mellapak 250Y
IC4/NC4	27.6	FRI	1.20	Mellapak 250Y
MeOH/Water	1.00	Sulzer	1.00	Mellapak 250Y

As stated, Billet & Schultes is dependent on packing specific constants in the liquid and gas mass transfer coefficient terms. Billet & Schultes did not provide constants for Mellapak 250Y, therefore the values need to be regressed with the experimental data gathered. For the performance study conducted on Mellapak 250Y, C_L and C_V, were regressed around the Fractionation Research Inc. experimental HETP datasets in Table 3.1. The same process to that of Fitz et al.[32] was employed in regressing the packing specific constants until the difference between HETP prediction and HETP experimental was minimized. The constants regressed around FRI experimental data were also used for all HETP predictions with Mellapak 250Y, including the system that was from the Sulzer testing facility. The utilized constants for Mellapak 250Y are presented in Table 3.2.

Table 3.2. Regressed Billet & Schultes Packing-specific Constants

Packing Name	C_L value	C_V value
Mellapak 250Y	1.49	0.517

The other model that requires an assumption for a constant is in the Gualito model with surface enhancement factor, F_{SE}. Gualito et al.[31] states for any corrugated sheet metal structured packing, surface enhancement factor should be 0.35. This is also the same value presented by Rocha et al.[23,24] for use with Mellapak 250Y HETP predictions.

As stated in Section 3.3., the physical property inputs for the data sourced from FRI represent physical properties that align to each individual HETP point. The physical properties obtained from FRI represent compositions sampled from near the middle of the packed bed. Ottenbacher et al.[65] recommends using mid-bed properties to be used to calculate HETP in models. For the MeOH/Water system, from Sulzer's testing facility, an average of the top and bottom compositions is used to generate the set of physical properties used in analysis. Other practitioners commonly have used an average of the top and bottom compositions as the basis. For the hydrocarbon systems, the mid-bed composition and average of the top and bottom compositions at the same F-factor is very similar, in many cases the difference is within 5%. Due to the MeOH/Water test data presented by Meier et al.,[66] there is only one physical property set for the HETP data across the pre-loading regime. With physical property inputs established, the working equations outlined in Section 2.2., were utilized to calculate HETP for each correlation. The preloading MAPD (using Equation 3.1) results of the test systems with Mellapak 250Y, are revealed in Table 3.3.

Table 3.3. Summary of MAPD for Test Systems with Mellapak 250Y.

Test Systems	P (bara)	Gualito	Billet & Schultes	Delft	Aspen	Song
C6/C7	0.330	15.1%	20.9%	16.4%	10.9%	11.8%
C6/C7	1.65	8.56%	10.8%	3.33%	17.2%	9.86%
O/P-Xylene	0.130	43.1%	11.7%	18.4%	10.1%	14.9%
O/P-Xylene	1.00	35.0%	10.5%	9.50%	15.8%	19.7%
IC4/NC4	6.90	7.11%	3.18%	17.5%	26.3%	7.48%
IC4/NC4	11.4	16.6%	25.1%	18.4%	17.3%	13.7%
IC4/NC4	20.7	15.2%	15.0%	54.0%	41.7%	34.1%
IC4/NC4	27.6	30.8%	29.1%	76.9%	62.3%	63.0%
MeOH/ Water	1.00	48.3%	6.41%	58.9%	4.01%	4.23%
Total Average	N/A	24.4%	14.7%	30.4%	22.9%	19.9%
Low P, HC System Average	N/A	25.4%	13.5%	11.9%	13.5%	14.1%

For each model and test system there is an MAPD value, the second row from the bottom is an average of all the test systems' MAPD values, for that respective model. The bottom row is an average of all the low pressure, hydrocarbon test systems for that respective model. The averages at the bottom are not a weighted average of all points, rather each system has an equal weight, despite the amount of HETP points in that system. It should be noted that subsequent figures of the results presented in Table 3.3. may show HETP points at flood but these are not factored into the calculation of MAPD.

For the cyclohexane/n-heptane (C6/C7) systems, the "traditional" models of Gualito, Billet & Schultes and Delft had a similar pattern in performance. Under vacuum, the models performed much worse with C6/C7 then the data collected above atmospheric pressure. While they performed worse at lower pressures, the models did not over/underpredict in the same ways for the two pressures. Billet & Schultes underpredicted across the preloading regime for both pressures, Gualito mostly overpredicted across the same range and the Delft model would underpredict at low F-factors and overpredict at higher F-factors. The sensitivity of k_G to pressure of these three models were relatively close, with a range of 2.1-2.4 times greater with the physical property inputs at 0.33 bara than 1.65 bara. This can partly explain why none of them have major differences in HETP behavior between the pressures, experimental HETP is slightly smaller at 1.65 bara than 0.33 bara so without an excessive change with k_G, a model overpredicting at one pressure will probably overpredict at the other. Song also predicts slightly better at 1.65 bara versus 0.33 bara, but overall was the most consistent in terms of performance between the two pressures. Like Delft, it tends to underpredict at lower F-factors and overpredict at higher F-factors, as it is quite dependent on superficial velocity. This is apparent in Figure 3.1, where Song's initial HETP prediction is around 0.33 m and its final preloading regime HETP prediction was around 0.41. This trend is even more apparent in Figure 3.3 with the o/p-xylene system at 0.13 bara. Song is having the strongest upward trend with F-factor, compared to the other models, but it is apparent in Billet & Schultes and Delft. Gualito also appears to have a relationship with F-factor, but in the downward trend across the preloading regime. It has been previously emphasized that each HETP point for the models has its own physical property input, which corresponds to the measured experimental composition. This does not cause the upward or downward trends by the models, but slight fluctuations in composition do show up in the correlations predicted HETP values, in Figure 3.1, there is a small but temporary dip seen with the models in the F-factor range of 2.1-2.3 $Pa^{0.5}$. Generally, these fluctuations are obvious to spot and do not occur frequently, as demonstrated in the figures below.

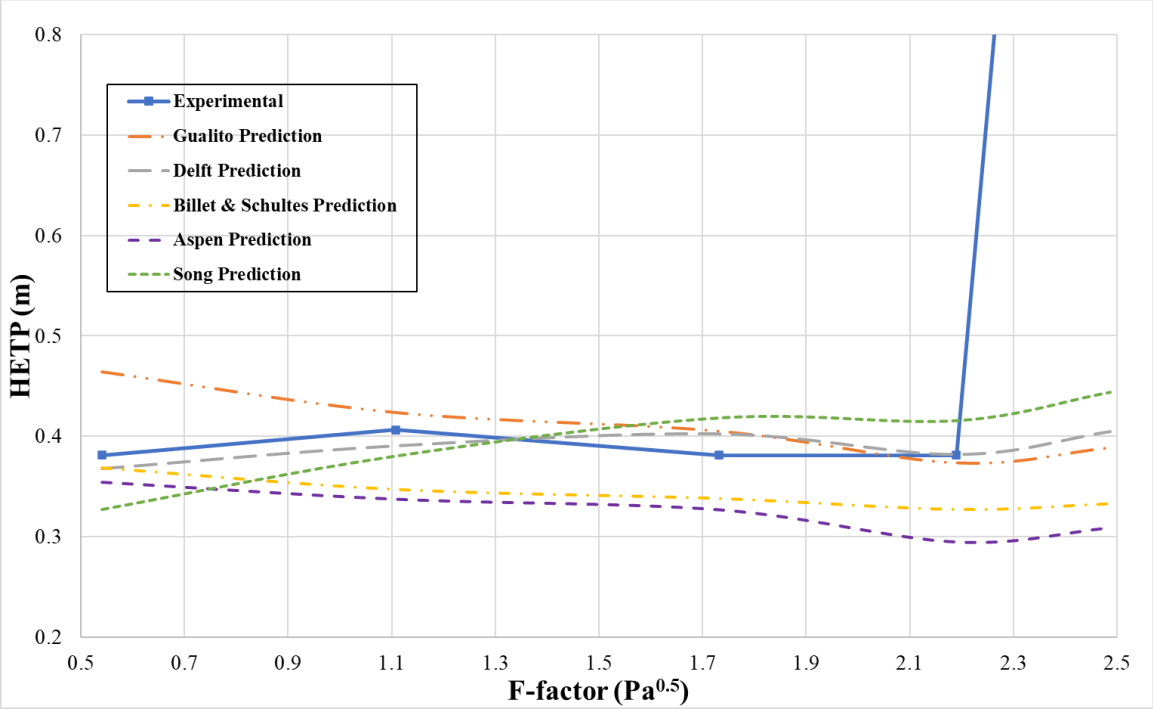

Figure 3.1. Model HETP Performance Comparison – C6/C7, 1.65 bara with Mellapak 250Y.

Aspen was the only model to perform better at 0.33 bara than at 1.65 bara, interestingly, its k_G predictions were the smallest out of the models for both pressures. Despite this, it did not overpredict HETP greater than the other models, in fact, it underpredicted HETP for C6/C7 at both pressures. This is due to Aspen's large effective area prediction, which is the largest of all the models, and can be seen in Figure 3.2. There is not much agreement in predicted effective areas by any of the HETP correlations. In fact, the definition and structure of what effective area should represent is different amongst the models. While most of the models stay less than unity, the Aspen correlation predicts an effective area almost double the nominal area of packing. Hanley and Chen[16] stated that effective area should not be quantified by how much wetting is taking place but rather all interfacial area that is participating in mass transfer. Thus, the Aspen model accounts for waves or droplets that could be on the packing surface and contributing to mass transfer. It should be noted that some of the other correlations have effective area terms which exceed unity at high liquid rates or high pressures, this will be highlighted in later

discussed systems. Three of the models, Song, Gualito and Billet & Schultes show an uptrend of fractional area with increasing F-factor. This would intuitively make sense as higher liquid loads will ultimately mean more of the packing is getting wet and thus more would be taking part in mass transfer. The Aspen and Delft correlations display a constant fractional area that seems to be irrelevant of changing F-factor. This detail will be discussed in more detail after more types of systems are looked at.

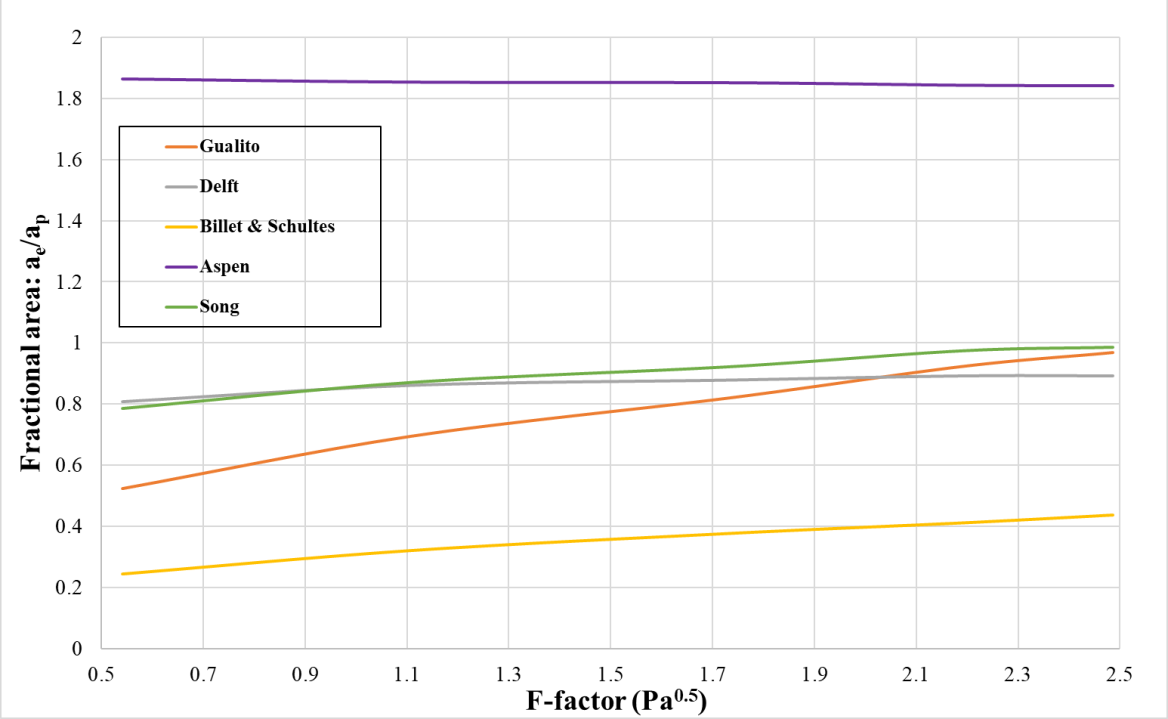

Figure 3.2. Model Fractional Area Comparison – C6/C7, 1.65 bara with Mellapak 250Y.

Like both C6/C7 systems, each model's performance with O/P-xylene at 0.13 bara and 1.00 bara had similar trends. For example, if HETP is underpredicted at 0.13 bara, it also underpredicted at 1.00 bara, which is the case with Billet & Schultes. Billet & Schultes had the lowest average MAPD with the o/p-xylene systems, which can be attributed to regressing packing-specific constants around available experimental data. One thing that should be stated, the practitioner has some flexibility with these constants, as we see in Figure 3.3, Billet & Schultes does not provide a safe estimate of HETP, one could theoretically lower the packing

specific present in the k_G term, to provide higher predictions. Gualito had the worst performance with the o/p-xylene systems and overpredicted across the preloading regime for both analyzed pressures.

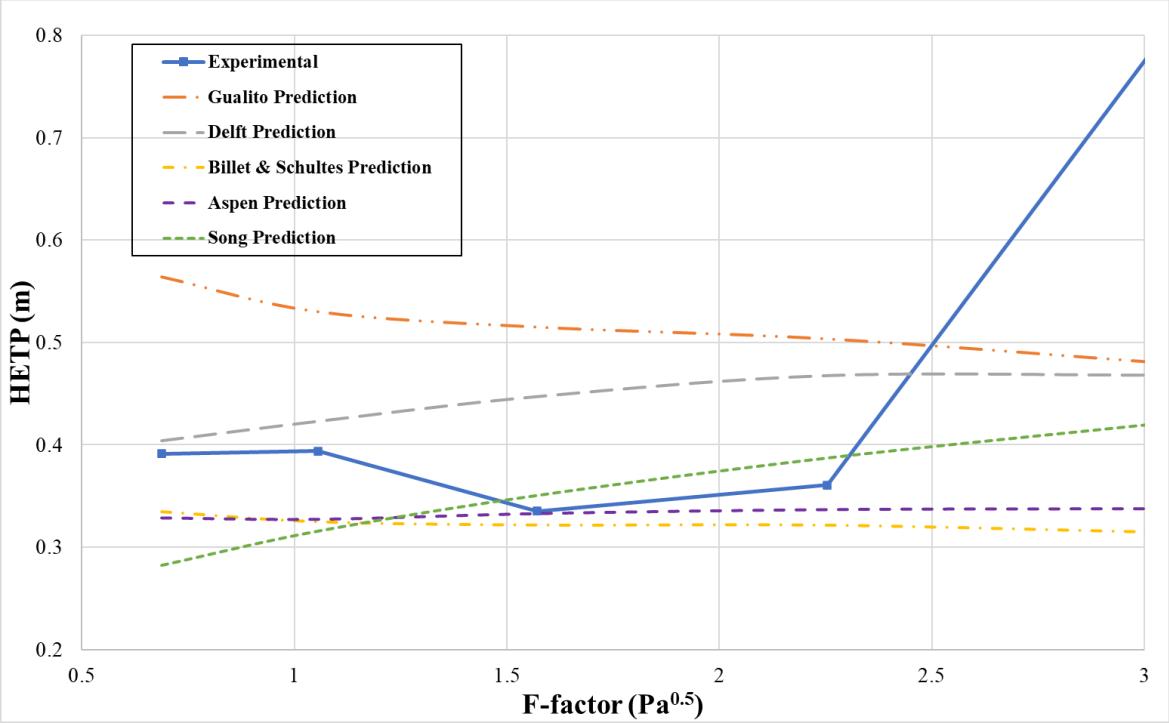

Figure 3.3. Model HETP Performance Comparison – O/P-Xylene, 0.13 bara with Mellapak 250Y.

The corresponding fractional area predictions for o/p-xylene at 0.13 bara can be seen in Figure 3.4. The similar uptrend with fractional area with Song, Gualito and Billet & Schultes is present. There is a more pronounced upward trend with Delft, although it seems to plateau early in terms of F-factor. Another observation is the similarity in fractional areas in Figure 3.2 and Figure 3.4 for Delft and Song. Both models utilize effective area models that were developed with CO_2 absorption data, although the packings studied were much different. Delft adopted a slightly modified version of the work by Onda et al.,[15] which focused heavily on CO_2 absorption with random packings and Song conducted their own studies with both types of packings but an emphasis on structured packing. The packings employed in the study would ultimately impact

regressed correction factors, yet the two effective area models are still pretty close for the C6/C7 and o/p-xylene systems.

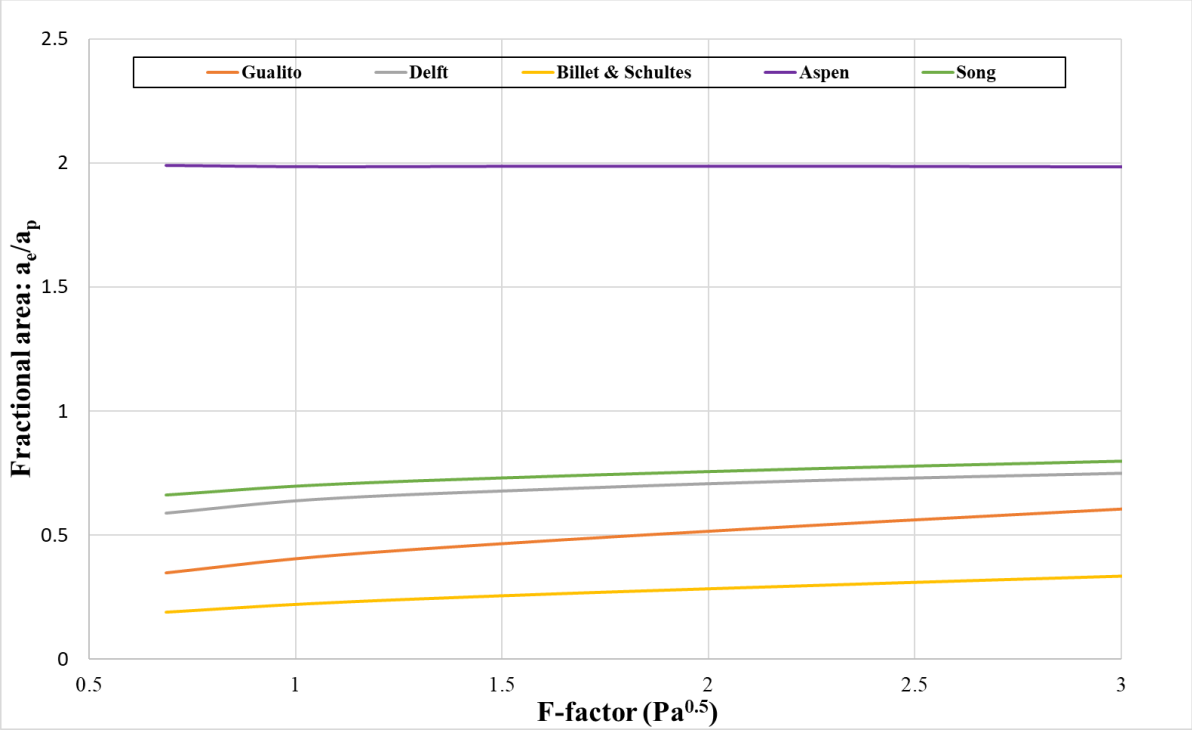

Figure 3.4. Model Fractional Area Comparison – O/P-xylene, 0.13 bara with Mellapak 250Y.

Another important point to highlight, which cannot be inferenced from Table 3.3, is trends seen in the experimental FRI high pressure data. So far, the pre-loading regimes have appeared relatively flat until the flooding point, as demonstrated by Figure 3.1, and Figure 3.3. In the pre-loading regimes for all the systems above 6.9 bara in Table 3.3, there appears to be a "kneecap" or "efficiency hump" at the higher liquid rates. This was hypothesized by multiple studies to be caused by backmixing.[32,67,68] At high liquid loads, there can be significant entrainment, where vapor bubbles are pulled down and efficiency decreases. Cai et al.[68] investigated bed height as a possible factor but ruled it out as the cause behind the increasing in HETP. The study also found that packing with a nominal area of 133 m^2/m^3 did not show a hump at the same high pressures. The severity of the "efficiency hump" increases with pressure, as seen in the difference between Figure 3.5. and Figure 3.6.

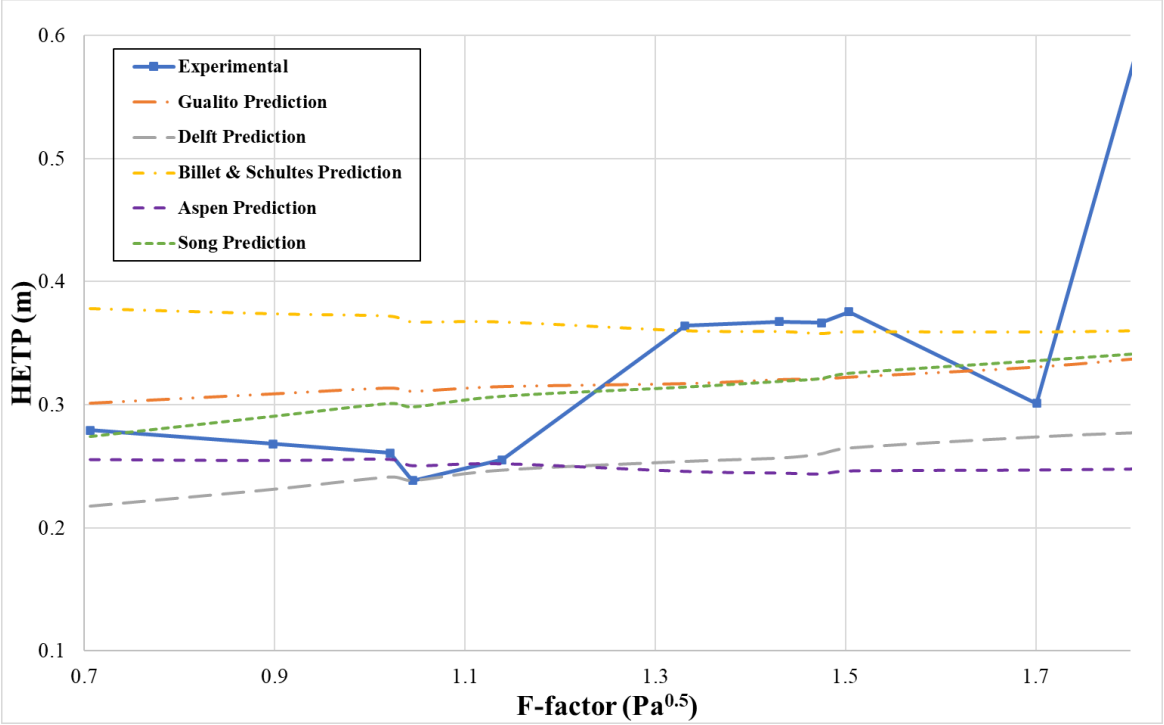

Figure 3.5. Model HETP Performance Comparison – iC4/nC4, 11.4 bara with Mellapak 250Y.

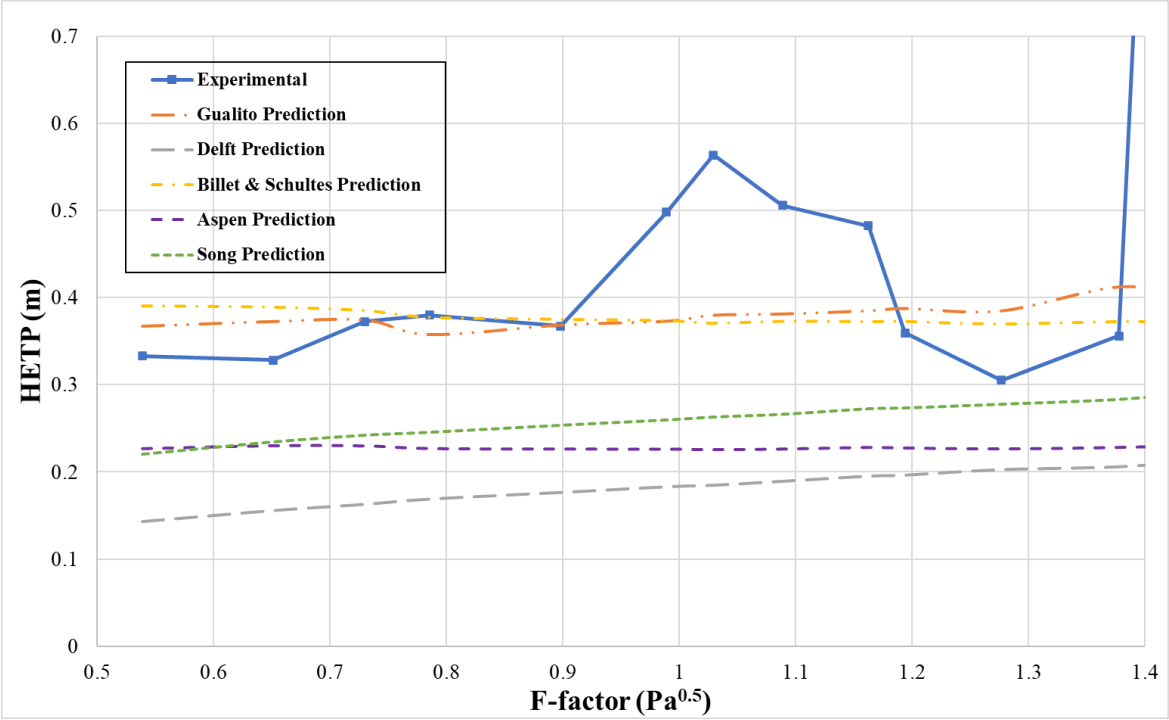

Figure 3.6. Model HETP Performance Comparison – iC4/nC4, 20.7 bara with Mellapak 250Y.

The “efficiency hump” in Figure 3.6, at 20.7 bar, is nearly two times larger than the HETP in the pre-loading regime prior to the occurrence of the hump. In Figure 3.5, at 11.4 bar, the hump is much more modest compared to the HETP at lower liquid rates. None of the models can predict this phenomenon, while some have low MAPD in Figure 3.5, with the presence of a hump, it is due to overpredicting at low liquid rates and the experimental mass transfer efficiency decreasing until the predicted HETP and experimental HETP met at higher F-factors. This is a good example of structured packings not being the ideal internal of choice at high pressures, except for specific applications like glycol dehydration.

The fractional area results for iC4/nC4 at 20.7 bar with Mellapak 250Y are shown in Figure 3.7. The Aspen correlation, seemingly independent of the test mixture, pressure and F-factor has remained near double the nominal area for effective area prediction. Another model that went above unity for effective area prediction is Song. At elevated pressures, it should not be a surprise that some effective area models are significantly different than the predictions at lower pressures. They are not validated there by the developing authors, and they are usually outside of their design limits, especially if the models are functions of liquid load/superficial velocity. It is here where Song and Delft effective area models decouple, when compared to the results of the previous systems. Many effective area studies, especially with structured packing, do not conduct research at the pressures seen with FRI’s high pressure data. As seen earlier with pressures above atmospheric, the Delft model’s effective area values remain steady. In this case, it is the exact same effective area prediction at first HETP point and the last. Billet & Schultes has consistently predicted the small fractional area of the models, irrelevant of the system. Due to its packing specific constants, this has not resulted in it predicting the highest HETP across many of the systems.

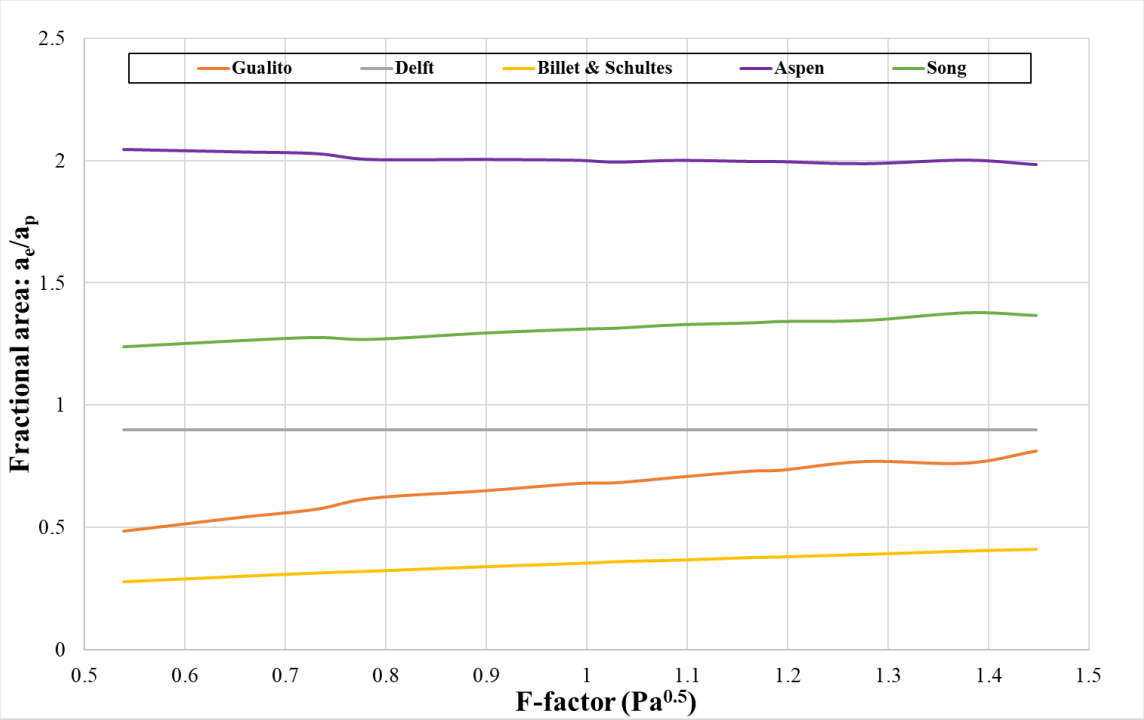

Figure 3.7. Model Fractional Area Comparison – iC4/nC4, 20.7 bara with Mellapak 250Y

The final system that will be discussed for the Mellapak 250Y packings is MeOH/Water at 1.00 bara. While Billet & Schultes correlation has had much of its solid performance attributed by its regressed constants to FRI data, it still performed well with the MeOH/Water system that was not a part of its regression database. Along with Billet & Schultes, Aspen and Song also performed well, with Aspen performing the best at an MAPD of 4.01%. The fractional area results for MeOH/Water at 1.00 bara with Mellapak 250Y can be seen in Figure 3.9. Interestingly, Billet & Schultes has a higher fractional area with MeOH/Water than some of the low-pressure hydrocarbon systems. Even though surface tension is lower with the hydrocarbon systems, wetting should theoretically benefit from this, but that is not the case for Billet & Schultes in this instance.

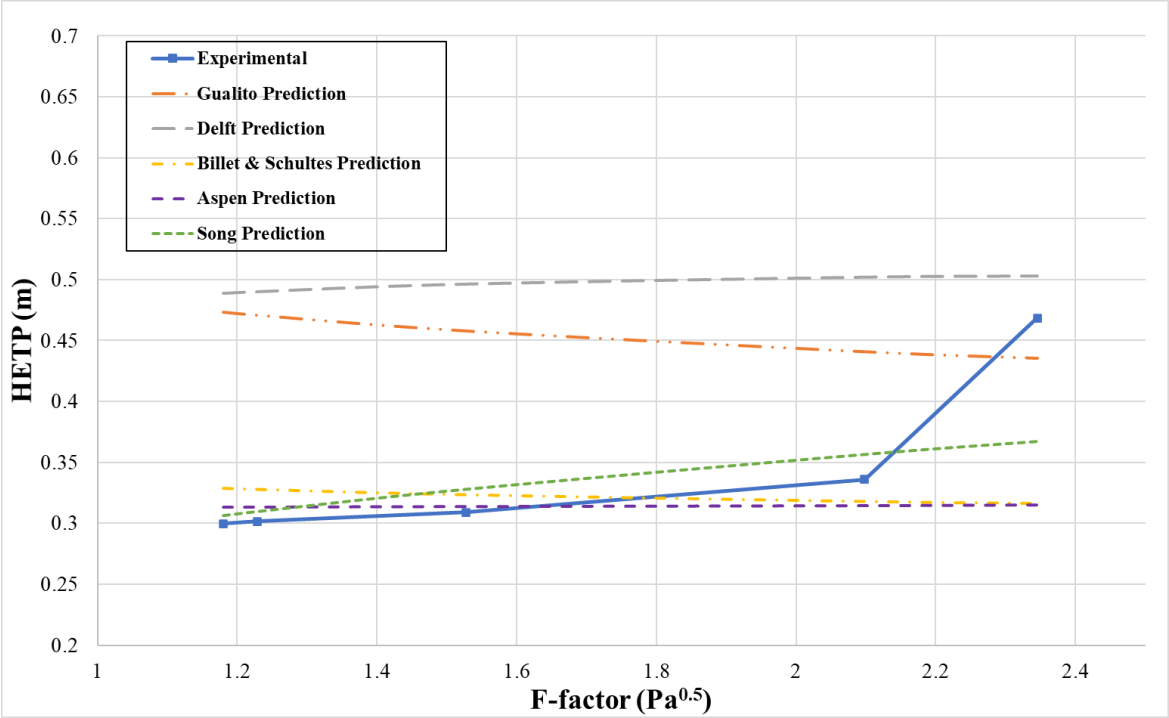

Figure 3.8. Model HETP Performance Comparison – MeOH/Water, 1.00 bara with Mellapak 250Y.

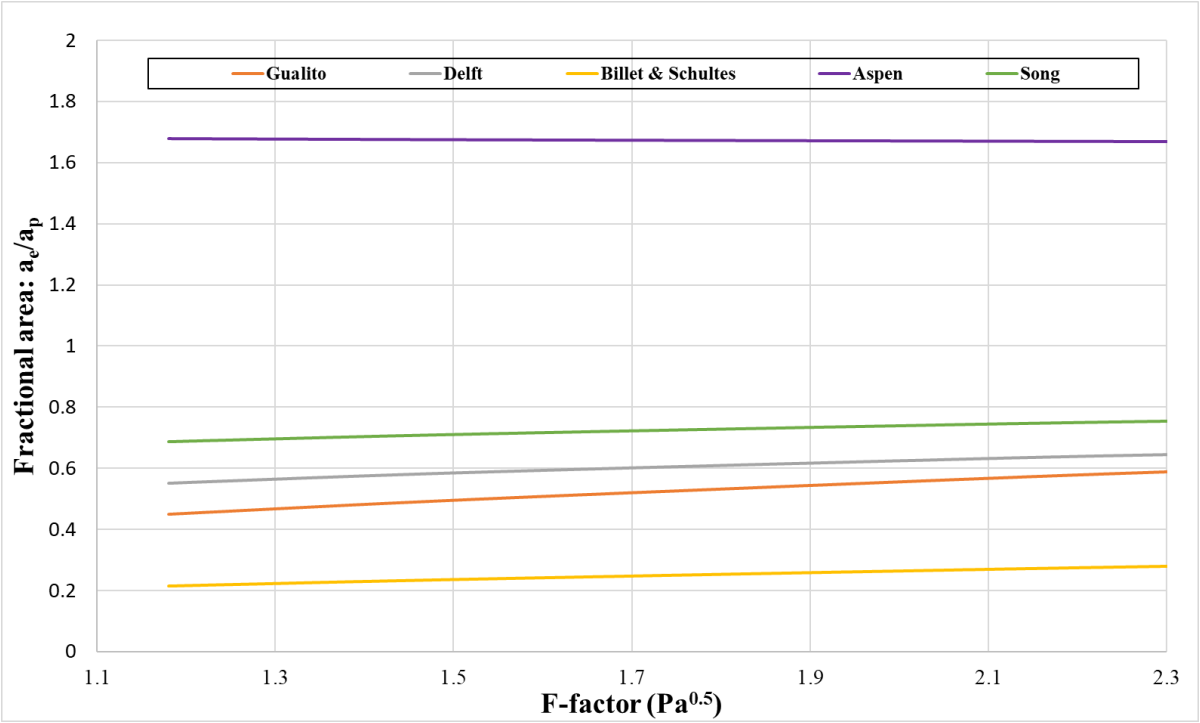

Figure 3.9. Model Fractional Area Comparison – MeOH/Water, 1.00 bara with Mellapak 250Y

3.5 CONCLUSIONS

A performance evaluation conducted with nine different systems with Mellapak 250Y has been conducted. Most of the data was taken from Fractionation Research Inc. experiments except for one dataset from Sulzer. Multiple hydrocarbon systems of low and high pressure and one aqueous system near atmospheric was analyzed. No models could predict the efficiency hump seen at high pressures with structured packings, the correlation performance was worse as the pressure got higher and efficiency hump. For the low-pressure hydrocarbon systems, Billet & Schultes, Delft, Aspen and Song provided adequate HETP predictions. Delft struggled with the methanol/water system while Song, Aspen and Billet & Schultes performed as well as the low-pressure hydrocarbon systems. Gualito overpredicted by more than 30% with both o/p-xylene systems but provided more conservative HETP predictions with cyclohexane/n-heptane. Many observations were also made about performance weakness and parameters causing them. In addition to HETP prediction, effective area and mass transfer coefficient predictions were discussed. There was little agreement between effective area models, besides the Delft and Song's effective area models with hydrocarbon low pressure systems.

CHAPTER IV

PERFORMANCE COMPARISON OF HETP CORRELATIONS FOR HIGH-CAPACITY STRUCTURED PACKINGS

The contents of this chapter are under review for publication in *Chemical Engineering Research and Design.*

4.1 ABSTRACT

The performance of HETP correlations is important to the successful design of packed distillation columns. A performance comparison of five structured packing HETP correlations in the literature was carried out. The correlations evaluated were Gualito, Billet & Schultes, Delft, Aspen, and Song. Experimental HETP data consisted of total reflux data from Fractionation Research Inc., with cyclohexane/n-heptane and o/p-xylene as the test systems of interest. The data was collected over a range of high-capacity structured packings, including MellapakPlus 252Y, 452Y and 752Y. This paper presents the performance of the studied efficiency correlations, as well as discusses major differences in behavior between the models. In addition to HETP performance, effective area predictions by all models are presented and analyzed. Overall, Billet & Schultes and Song correlations provided the lowest error in HETP predictions across all packings, but the other models displayed strength in specific packings or systems.

4.2 INTRODUCTION

Corrugated sheet metal packings have been a popular choice for structured packed columns in industry. Therefore, correlations capable of accurately predicting HETP for these packings is important. While there are many published structured packing HETP correlations in the literature, only a handful of those correlations have been popularized, and even less have been evaluated against each other. There are many studies in the literature that have looked at the performance of notable correlations. For example, Fitz et al.[32] presented new high pressure HETP data from Fractionation Research Inc. and analyzed the Gualito and Billet & Schultes correlations. Fair et al.[37] examined the performance of the SRP II correlation and the Delft model, across multiple test systems and packings. Some valuable performance comparisons have come from papers unveiling new correlations such as Hanley and Chen[16], who proposed a new HETP model and compared its performance to a handful of other correlations. Other studies have looked at specific parameters of HETP models, such as Olujić and Seibert,[40] who investigated the prediction of liquid phase mass transfer resistance for seven published mass transfer models. Wolf-Zöllner et al.[56] investigated 11 structured packing hydraulic models, which for some of these hydraulic models, like SRP II, are important to be accurate because calculated parameters from the pressure drop model, like liquid hold-up, are used in the mass transfer model to predict HETP. Jammula et al.[55] evaluated multiple models, with a majority of the collected HETP data focused on Mellapak 250Y. In many of the previous studies discussed, some of the evaluated HETP correlations have been updated. For example, the Delft Model was updated with a new effective area term after Fair et al.[37] recommended the change. In addition to revised models, more experimental HETP data and new correlations have been published. In addition to updated or new models, new experimental data has since been published that look at systems and packings that were not in existence or accessible in the public domain.

The purpose of this study is to compare the performance of well-established mass transfer correlations, being that of Gualito, Billet & Schultes and the Delft model against the newer correlations of Aspen and Song. In addition to looking at correlation performance in terms of HETP, observations about effective area predictions, model sensitivity and differences are discussed. By looking at multiple packings and systems, the study can validate models and highlight strengths or shortcomings of all models.

4.3 MODEL BACKGROUND

As stated, the correlations analyzed in this study were Gualito, Billet & Schultes, Delft, Aspen, and Song. Gualito is a revision of the SRP II correlation, modified to improve performance with high-pressure test systems. Like SRP II, Gualito utilizes the same liquid and gas mass transfer coefficient terms. Therefore, the model assumes penetration theory to describe the k_L term and previous wetted wall column experiments to develop k_G. The working equations of the Gualito correlation are outlined in Table 7 and Table 8 of Gualito et al.,[31] where the main change of SRP II is found in the effective area term. A correction factor, which included a ratio of liquid to gas superficial velocity was added to the effective area term to better predict HETP with FRI high-pressure data from Fitz et al.[32] Other changes include the reference surface tension that is important for determining the contact angle value and a dry pressure drop equation with an additional term. In general, the Gualito correlation and SRP II have similar HETP predictions with low-pressure hydrocarbon systems. The major difference is Gualito's improved accuracy with high-pressure systems from the literature compared to the original SRP II model. The sheet metal packing constants provided by Gualito et al. were utilized for this study. The Billet & Schultes correlation, although there are multiple publications[17,18] of its working equations, the preloading equations have stayed the same in both versions. In the later paper, additional equations were added to predict HETP at different regimes such as at flooding. The model uniquely formulated both mass transfer coefficient terms from Higbie's penetration theory.[6]

There are additional parameters present then other correlations that used penetration theory, most notably the packing specific constants in both the k_L and k_G terms. The authors conducted many experiments with a wide range of packings but there is a lack of provided modern structured packing constants. Thus, if the packing constants are unknown, they are regressed with experimental HETP data so that the correlation minimizes prediction error.

The third correlation studied, Delft Model,[33] has been analyzed many times as new data was published, and subsequently updated after its initial development. The version applied to this study were the working equations in 2004 publishing by Olujic et al.,[38] with the new update[40] to k_L and φ, where φ is the fraction of the triangular flow channel occupied by liquid.

One of the newer correlations analyzed, referred to as Aspen by the authors, Hanley and Chen,[16] was developed for utilization in Aspen Plus® software. As opposed to the three traditional models, Aspen constructed the basis for the mass transfer coefficient and effective area terms with Buckingham Pi theorem. With this dimensional analysis, important parameters were assumed, and dimensionless groups were subsequently formed. A wide range of experimental HETP data was collected, which included many experiments with newer packings and different systems than what was available to the previously discussed correlations. This data was then used to regress aspects of the correlation and minimize error as well as be used to validate the performance of the Aspen model.

The newest correlation that was a part of this study was that of Song's dissertation work.[41] This correlation did not utilize distillation data in development but rather absorption and stripping experiments from SRP's air/water database. Although these experiments would not reflect the same mass transfer conditions as distillation, the correlation still showed promising results in predicting HETP for distillation data.[44]

4.4 EXPERIMENTAL METHOD

The experimental HETP data was sourced from Fractionation Research Inc., experiments that were published in the literature.[69] The column utilized for these efficiency measurements has a diameter of 1.2 m. The test systems included o/p-xylene at 0.13 bara and cyclohexane/n-heptane at 0.33 bara and 1.65 bara. These systems were run with multiple packings, they include MellapakPlus 252Y, 452Y and 752Y. All of these are high-capacity packings, which generally have a corrugation angle of 45° except at the top and bottom of the packing elements were there are slight bends toward the direction of the vertical axis. The geometrical change of the corrugation angle results in an increase of capacity when compared to the conventional structured packing of the same nominal area. The packings examined ranged from a specified nominal area of 250 to 500 m^2/m^3.

For HETP calculations, preciseness was an important factor, so each HETP point had its own corresponding physical property input based on FRI measurements. The composition was an average of the top and bottom of the column at each respective F-factor, to provide physical property estimates that provided the most accurate HETP predictions. If the top of the column's composition were utilized, the predicted HETP would provide values that were quite higher than the experimental HETP. The opposite would be true if the bottom conditions were used to calculate HETP in the models. To quantify error between predicted versus experimental HETP points, mean absolute percent deviation (MAPD) was calculated and presented in Table 4.1. MAPD is only used to quantify performance in the preloading regime and the results in Table 4.1 are coupled with bias plots in Figure 4.4-4.6 to determine if the MAPD is an over/underprediction. Bias plots only include preloading HETP data and predictions.

As stated, Billet & Schultes correlation requires packing specific constants, when these are unknown, they need to be regressed with the experimental data available to the practitioner. The packing-specific constants are represented in the Billet & Schultes correlation by C_L and C_V, which are the packing-specific constants for the liquid and gas side mass transfer coefficient

terms, respectively. The packing specific constants are found by taking the physical property inputs and regressing the constants until the prediction from the correlation is minimized with the experimental HETP data. For this study, C_L and C_V was 0.858 and 0.604, 1.00 and 0.850, 1.79 and 0.900, for MellapakPlus 252Y, 452Y, 752Y, respectively.

4.5 RESULTS AND DISCUSSION

The results of HETP calculations by all the models examined are presented in Figures 4.1-4.6. In addition to comparing efficiency calculations, the effective area term was also investigated. For both figures, the HETP and effective area are displayed as a function of F-factor ($Pa^{0.5}$). As stated, the calculation process outlined in the previous section was utilized for the presented results. Table 1 includes a summary of model performance and their respective MAPD for each system and respective packing.

4.5.1 COMPARISON OF HETP PREDICTIONS

Many of the models from the literature conducted experiments with structured packings of a nominal area around 250 m^2/m^3. For example, Mellapak 250Y and B1-250.45 are two packings that dominate available HETP data in the literature. Therefore, it is not surprising that many models, especially older ones, use a large amount of this data to construct aspects of the correlation. In addition, new test data with larger nominal area packings and new packings with modified geometry have been publicly released. Some newer models benefit from having this relative new data and thus a larger database to develop and validate their models than some of the well-established, older correlations. With the packings selected for analysis, a wide range of nominal areas and geometric dimensions of the packing can be explored to compare each model's performance with predicting HETP.

The first investigated packing type is the MellapakPlus 252Y, Figure 4.1 and Figure 4.2 show the model's performance with this packing in the cyclohexane/n-heptane test system at 0.33 and 1.65 bara, respectively. For Figure 4.1, the predicted HETP values correspond to the effective

area predictions seen in Figure 4.7. Based on the results presented in the figures for the C6/C7 systems, it is evident that the Song, Billet & Schultes and Delft have a stronger dependency on F-factor than the other models. As F-factor is increasing, HETP predictions are also growing, as physical property changes do not have a wide enough discrepancy across each HETP point in the preloading regime to cause this upward trend. Any small deviations in the smoothness of the curves can be attributed to slight fluctuations in the measured composition for that respective HETP point, but these are extremely small differences.

For Figure 4.1 and 4.2, all the models performed relatively well and had an MAPD within 20% for the preloading regime. The Delft, Gualito and Song provided the safest predictions for the C6/C7 system under vacuum with M252Y. All the models except Aspen predicted mostly safe predictions for the same system at 1.65 bara. The large effective area prediction of the Aspen correlation could be a factor in the smaller HETP predictions. A discussion about effective area predictions is discussed more in-depth in Section 4.2. Song and Aspen model both predict a much smaller k_L in some cases as a factor of ~3 when compared to the other model's liquid mass transfer coefficient value. Even still, there is instances where Song and Aspen may be much smaller than the other models, are also apart by as much as 50-60%. That is not to say that a particular model is incorrect with its prediction of the mass transfer coefficient, as there is no definitive way to measure any of the mass transfer coefficients or effective area terms for distillation applications.

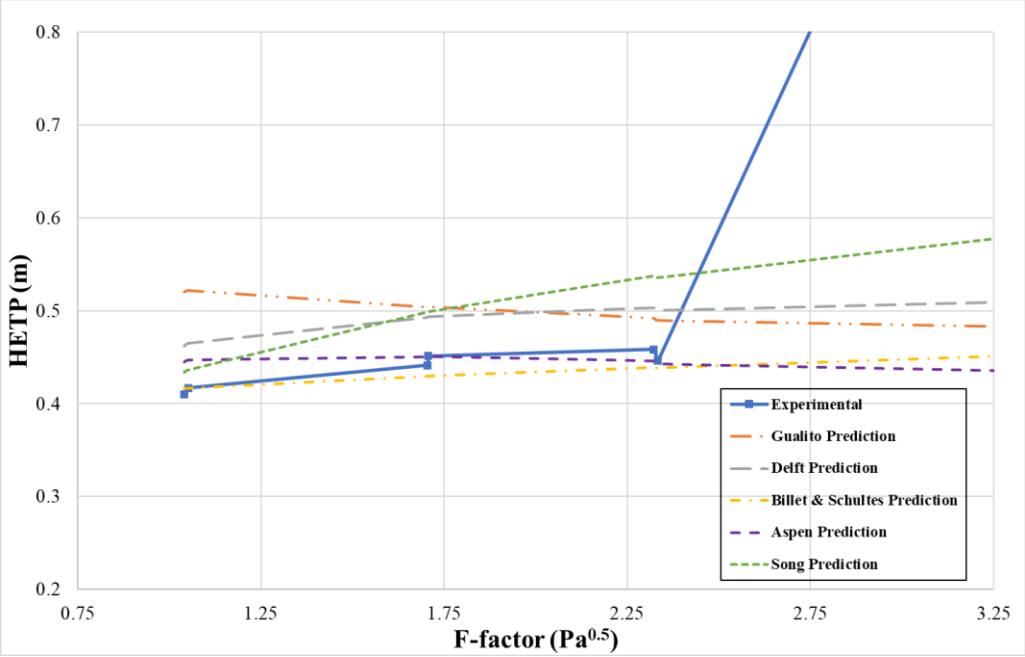

Figure 4.1. Predicted versus measured HETP values as a function of F-factor, for C6/C7 at 0.33 bara with MellapakPlus 252Y.

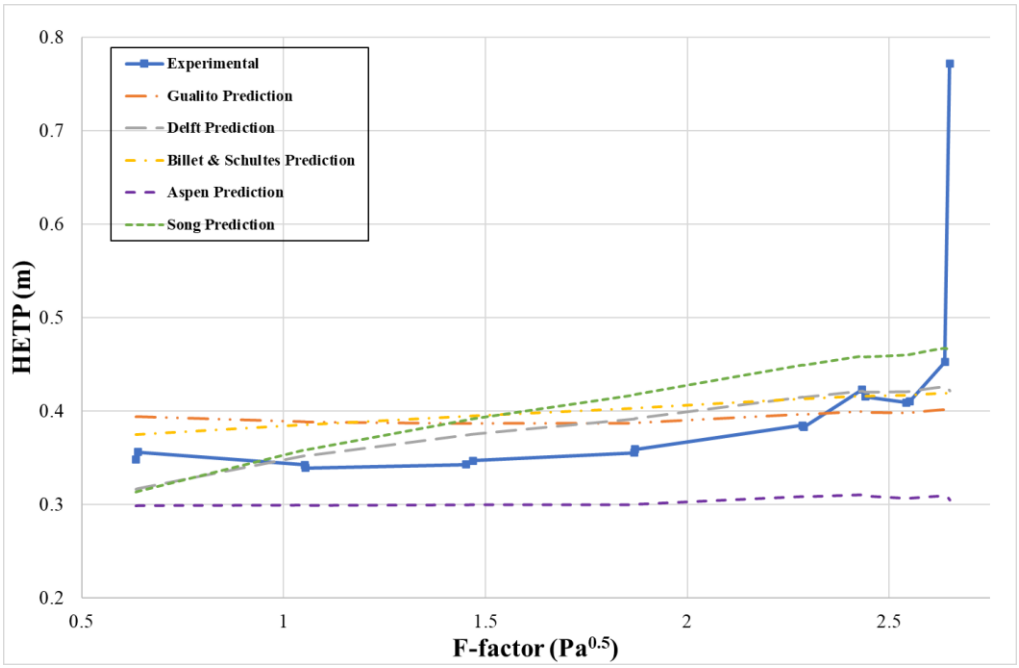

Figure 4.2. Predicted versus measured HETP values as a function of F-factor, for C6/C7 at 1.65 bara with MellapakPlus 252Y.

Figure 4.3 contains the HETP predictions for the o/p-xylene system at 0.33 bara with MellapakPlus 252Y. Some of the models analyzed in this study have had their performance

previously validated with the systems in Figures 4.1-4.3 for Mellapak 250Y (Fitz et al., 1999). The experimental HETP values taken at FRI with Mellapak 250Y and MellapakPlus 252Y are almost exact for the same system. Typically, if a model can predict HETP across the preloading regime well with Mellapak 250Y, then it can predict HETP reasonably well with MellapakPlus 252Y. As stated earlier, some of these models are much more dependent on F-factor than others. Therefore, with these types of models, the first predicted preloading HETP point compared to the last point, can be much different. With the high-capacity packing of MellapakPlus 252Y, it extends the preloading regime to higher F-factors furthering the difference between predicted HETP points at low versus higher F-factors. This is visible in all figures but especially apparent in Figure 4.3 with the Song correlation. The first predicted preloading HETP point is around 0.31 m and the last at 0.46 m, which is more than a 30% difference. Similar trends are seen in some of the other models, but not as pronounced and there seems to be a plateauing of predicting HETP points after the model reaches a certain F-factor.

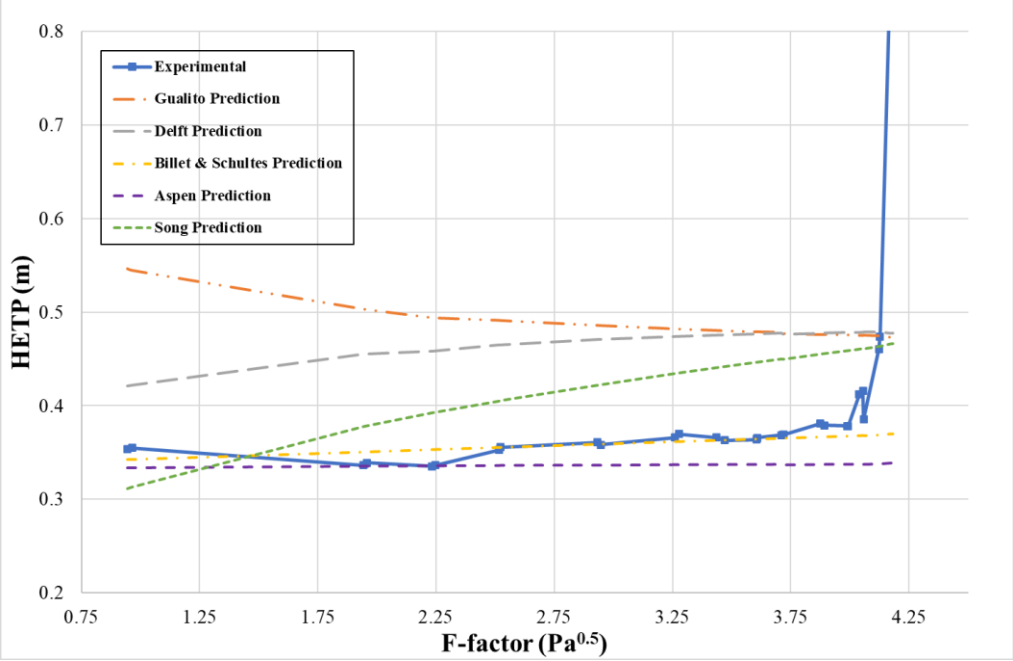

Figure 4.3. Predicted versus measured HETP values as a function of F-factor, for o/p-xylene at 0.13 bara with MellapakPlus 252Y.

Figure 4.4 presents a bias plot of the preloading regime predicted model HETP's subtracted by each respective experimental HETP, for all the systems in Figures 4.1-4.3. The plot summarizes areas of over/underprediction for all the test data taken in the preloading regime with MellapakPlus 252Y, across the complete F-factor range. The Billet & Schultes correlation predicted many points straddling closely to the experimental HETP, this pattern is a result of the regression method for the packing coefficients. As discussed earlier, the MellapakPlus 252Y packing specific constants in both mass transfer coefficient terms is solved by minimizing error. The other models generally had a majority of their predicted HETP values either overpredicting or underpredicting across the three systems. In Table 4.1, each model's MAPD for the systems ran with MellapakPlus 252Y can be seen in the top third of the table. Billet & Schultes benefitted from having regressed constants around the collected experimental data with the lowest overall MAPD for MellapakPlus 252Y. For correlations that did not require packing specific constants, the Aspen correlation performed the best with M252Y. Obviously, the Song correlation was not designed to be used to predict HETP for distillation applications, but its accuracy is surprisingly quite good. Its performance would be even better if it was a weaker function of F-factor or had a plateau section of HETP predictions.

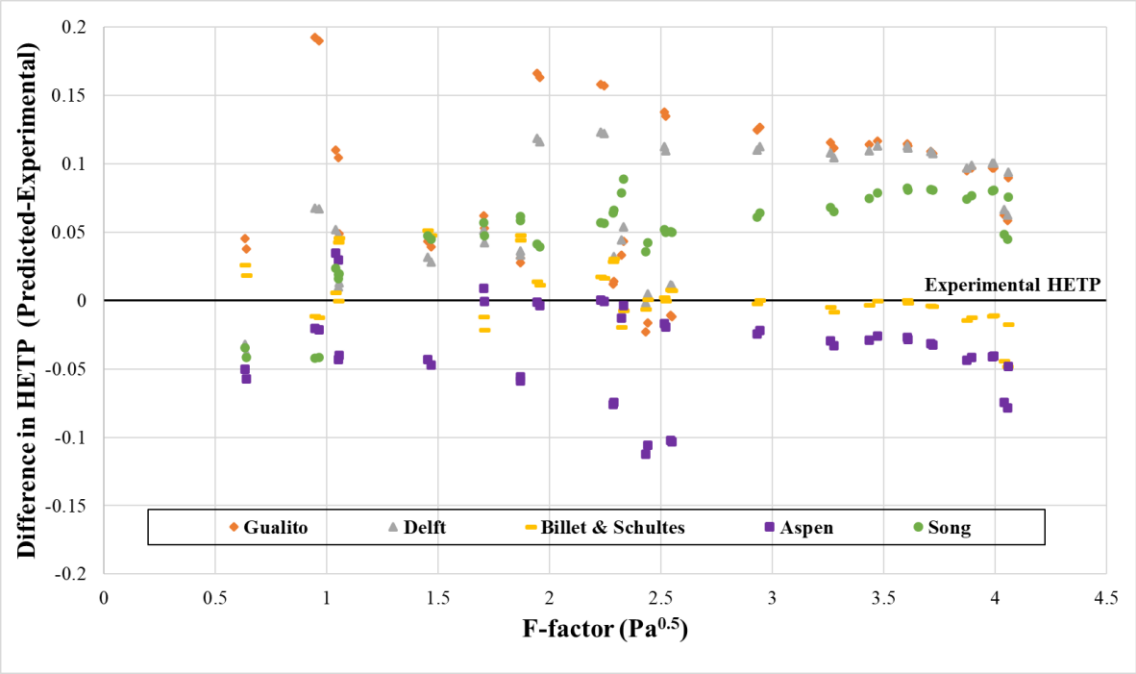

Figure 4.4. Bias plot across the preloading regime (Predicted Model HETP-Experimental HETP) for all systems with MellapakPlus 252Y.

Figure 4.5 is all the same test systems as Figure 4.4, except it is with the MellapakPlus 452Y packing. While the physical properties inputs for calculations were not the exact same for MellapakPlus 252Y as MellapakPlus 452Y, they were still relatively close. FRI adjusts bed height to keep each components composition similar at the mid-bed and below the bed points, despite the different efficiency of packings. HETP values were also measured at different F-factors in each experiment, and this is another contributing factor to slight differences of calculation inputs. But the largest impact on HETP prediction differences between Figure 4.4 and Figure 4.5 is typically due to the geometrical changes of the packing. While the small changes in physical properties do make an impact, the nominal area increase from 250 m^2/m^3 to 350 m^2/m^3, as well as changes with void fraction, corrugation dimensions, etc. have the largest influence. Similarly seen with the M252Y packing, Delft and Gualito both performed poorly with the o/p-xylene system compared to the C6/C7 system. In both instances, the models overpredict across the entirety of the preloading regime for o/p-xylene. It is surprising that the Delft model struggled with o/p-xylene, since much of the validation work with the Delft model was done with the

chlorobenzene/ethylbenzene system which has a similar relative volatility to o/p-xylene. All the models except Billet & Schultes had performance improvements at M452Y versus M252Y, in terms of MAPD.

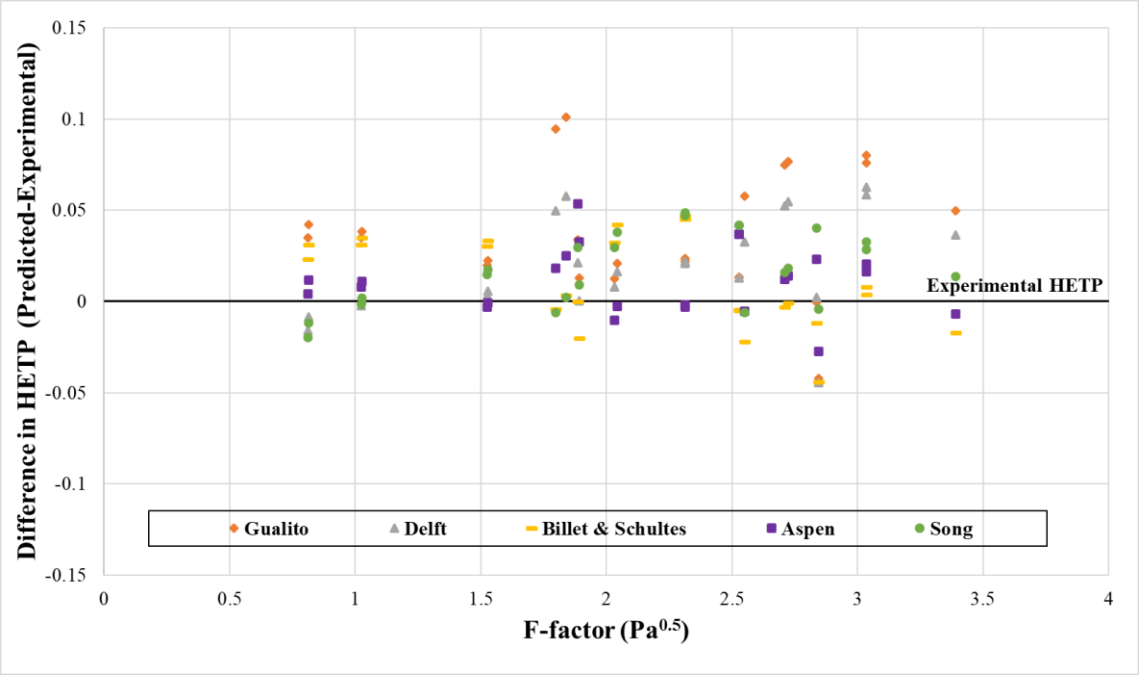

Figure 4.5. Bias plot across the preloading regime (Predicted Model HETP-Experimental HETP) for all systems with MellapakPlus 452Y.

Figure 4.6 displays the final packing analyzed, which is the packing with the highest nominal area, MellapakPlus 752Y. Aspen's HETP predictions had a very sensitive relationship with increasing nominal area, with M252Y, the values went from a general underprediction, to slightly overpredicting at M452Y. The values then considerably overpredicted HETP at M752Y. Its performance was optimized with the systems at M452Y packing in terms of having its lowest MAPD. The changes in geometry of the packings have resulted in an effective area term that is much more sensitive than the other models. The geometry specific parameters that Aspen's effective area is dependent on is equivalent diameter and specified nominal area. This behavior by the Aspen correlation is explained more in-depth in Section 4.2 and compares the other model's effective area predictions. As a result, Aspen's MAPD for M752Y was 28.0%, considerably higher than the 9.84% and 6.16%, seen in M252Y and M452Y, respectively. Delft

model is also very sensitive to geometric changes but unlike Aspen, the impact is not on the effective area term but rather the mass transfer coefficient terms. It is the only model dependent on multiple packing corrugation dimensions which are corrugation side length, corrugation base length, and corrugation height. Most of the other models only have corrugation side length as a parameter or exclude all three of those parameters like in Song.

Compared to M452Y, which generally saw an improvement of model prediction capabilities from M252Y, M752Y resulted in an overall decrease in performance. Almost 30% of predicted HETP points across the preloading regime were underpredicted by the models with M752Y. The correlation by Song is the only instance where MAPD was lower at M752Y versus M252Y. Still, a bulk of Song's predicted HETP values were underpredicted for M752Y. It is important to note that the HETP predicted by Song is also dependent on bed height, as there is a bed height parameter in the liquid mass transfer coefficient equation. For all the other models, sensitivity of predicted HETP across the examined systems and packings is a result of changes to packing geometry and slight fluctuations to physical property inputs. Song is quite sensitive to bed height changes and these experiments do fluctuate in bed height for the experiments. As discussed earlier, FRI adjusts packing bed height based on the efficiency of the packing being tested. For this data that means quite a variability in packing bed height, at the upper end, packing bed height was 3.67 m (M252Y experiments) and 1.99 m (M752Y experiments), at the lower end. In some instances, a change from the upper end to the lower end of FRI's packed bed heights can singlehandedly account to a ~20% change in predicted HETP by Song. Despite its sensitivity, it still performs relatively well in terms of MAPD at each packing and bed height.

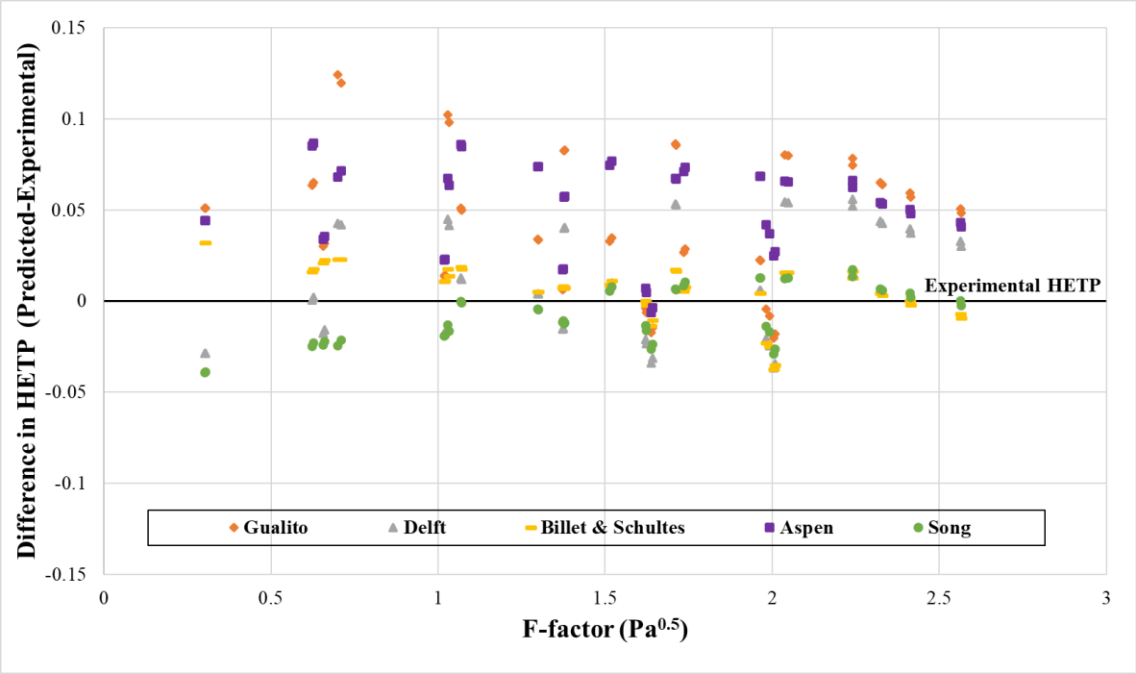

Figure 4.6. Bias plot across the preloading regime (Predicted Model HETP-Experimental HETP) for all systems with MellapakPlus 752Y.

Table 4.1. Summary of Model HETP Performance.

Packing Type	Test System	Pressure (bara)	Gualito MAPD	Delft MAPD	B&S MAPD	Aspen MAPD	Song MAPD
MellapakPlus 252Y	C6/C7	0.33	15.8%	11.2%	2.46%	3.56%	11.8%
	C6/C7	1.65	8.14%	6.21%	8.18%	18.2%	12.1%
	O/P-Xylene	0.13	33.9%	28.2%	2.90%	7.77%	17.5%
M252Y Average	n/a	n/a	19.3%	15.2%	4.51%	9.84%	13.8%
MellapakPlus 452Y	C6/C7	0.33	5.64%	4.52%	4.04%	10.5%	8.35%
	C6/C7	1.65	10.6%	3.96%	13.6%	2.23%	8.83%
	O/P-Xylene	0.13	29.2%	19.4%	2.84%	5.75%	5.91%
M452Y Average	n/a	n/a	15.1%	9.29%	6.83%	6.16%	7.70%
MellapakPlus 752Y	C6/C7	0.33	16.9%	5.73%	7.33%	34.1%	6.13%
	C6/C7	1.65	12.4%	12.5%	8.54%	13.0%	12.8%
	O/P-Xylene	0.13	50.1%	27.7%	7.46%	37.0%	6.71%
M752Y Average	n/a	n/a	26.5%	15.3%	7.78%	28.0%	8.55%

The results from Table 4.1 have been previously discussed to highlight strengths and weaknesses of models in different scenarios. In general, all models studied have certain scenarios where their selection to estimate an HETP would be an adequate choice. The exceptions to this would be the o/p-xylene system for Gualito and Delft, which the models predicted poorly with for all packings studied. Also, the Aspen correlation at M752Y had trouble predicting for both systems in vacuum despite how well it performed with the same systems with the other two packings. Despite much of the validation and development work for these models, especially the older ones, being at packings of nominal areas around 250 m^2/m^3, many of them still performed well or even better at larger nominal areas and at different geometric dimensions.

4.5.2 COMPARISON OF EFFECTIVE AREA PREDICTIONS

Multiple observations can be made about the wide range of results of the model's effective area predictions, seen in Figure 4.7 and Figure 4.8. For one, it is apparent that the definition of effective area is not agreed upon for all models. In Figure 4.7, the fractional area of C6/C7 at 0.33 bara with MellapakPlus 252Y is reported. Aspen correlation has a much higher predicted effective area than the other models, in fact, the effective area is greater than the specified nominal area of the packing. Hanley and Chen state that effective area, where mass transfer occurs, should not be limited to just the packing area where wetting may occur. The model considers additional ways of mass transfer, such as waves, liquid filaments and droplets that do not occur directly on the wetted surface of the packing. Therefore, the predicted fractional area of the Aspen model was larger than unity for all the systems analyzed in this study.

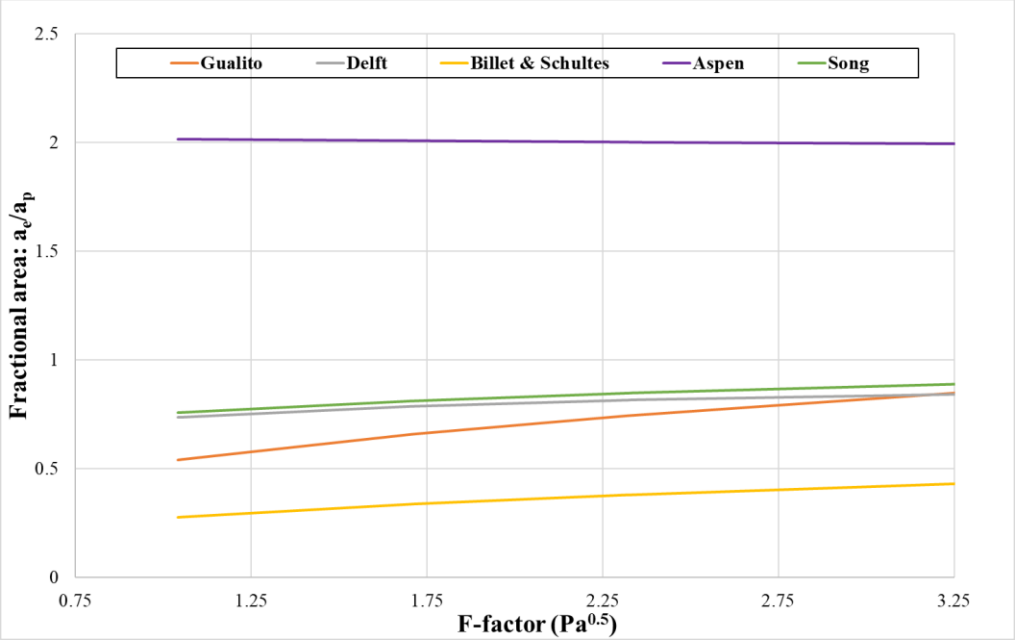

Figure 4.7. Fractional area of C6/C7 at 0.33 bara with MellapakPlus 252Y.

The other correlations tend to have a fractional area below unity and associate effective area with the wetting of the packing. There are some instances at higher liquid loads where the effective area does increase greater than the specified nominal area, but only by a small margin. Another observation is the general agreement of fractional area increasing with F-factor between Gualito, Delft, Billet & Schultes and Song. This relates back to the interpreted definition of effective area, because as F-factor increases and a system approaches flooding, there would be more wetting of the packing.

As stated earlier, the Delft model utilizes an effective area that was first developed by Onda et al.[15] and is modified slightly with the addition of a parameter for fraction of packing surface area occupied by holes. Onda et al.[15] developed the effective area term from CO_2 absorption experiments. The packing type utilized for this experiment were all random packings. Similarly, the effective area term in the Song correlation was developed from CO_2 absorption experiments but with a larger focus on structured packings. Despite the difference in packings, which

ultimately influenced the regressed correction factors in both terms, the effective area predictions of both models were still quite similar for the system presented in Figure 4.7 and Figure 4.8.

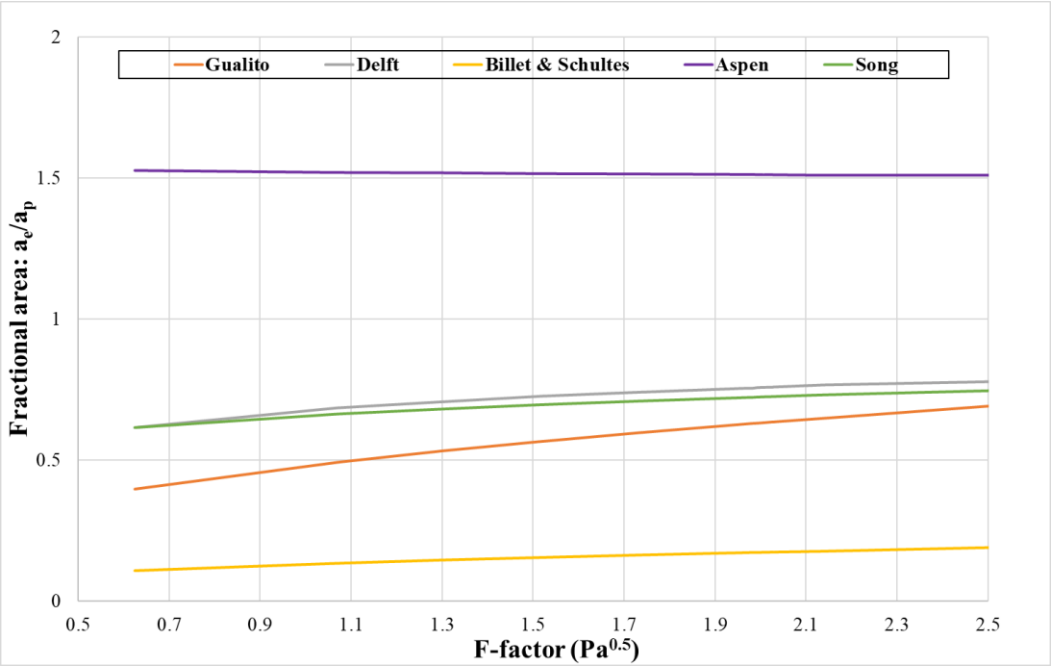

Figure 4.8. Fractional area of C6/C7 at 0.33 bara with MellapakPlus 752Y.

In Figure 4.8, the fractional areas are essentially shifted downward with the higher nominal area packing for the same system presented in Figure 4.7. The major declines in predicted fractional area, compared to Figure 4.7, are seen in Aspen and Billet & Schultes, where declines were ~25% and ~50%, respectively. That type of decrease, with the other mass transfer coefficients held constant, would result in a large increase of HETP prediction. For Aspen, the only geometrical parameters in the model are equivalent diameter and specified nominal area. Equivalent diameter via the Reynolds, Weber and Froude number and the specified nominal area are present in the effective area term. Equivalent diameter is reported in the liquid and gas mass transfer coefficient terms but cancels out, therefore the only changes to the k_L and k_G are due to small fluctuations in physical properties between the two experiments. So, the effective area term, due to geometrical changes of the packing being analyzed, is the main reason for changes in

HETP prediction discussed in Section 4.1. Although Billet & Schultes has an even larger decline in predicted fractional area than Aspen, its adverse effect on predicted HETP is not seen at M752Y. This is due to the packing-specific constants that were regressed to minimize overall prediction error, for each packing. The other remaining models have much smaller fractional area declines, around 5-10%, which have a smaller overall impact on predicted HETP than the previous discussed cases.

4.6 CONCLUSIONS

Five HETP correlations – Gualito, Billet & Schultes, Delft, Aspen and Song, were evaluated with Fractionation Research Inc., experimental data. The tests were conducted with high-capacity structured packing, MellapakPlus 252Y, MellapakPlus 452Y and MellapakPlus 752Y, with multiple hydrocarbon systems above and below atmospheric pressure. Billet & Schultes provided the best performance in terms of MAPD across all packings, benefitting from regressed packing-specific constants. Surprisingly, the Song correlation performed very well despite it being developed from non-distillation data. Aspen performed strong at M252Y and M452Y before overpredicting significantly with the same systems at M752Y. Gualito and Delft provided predicted HETP values that were safe estimates across the preloading regime except for the o/p-xylene test system, where errors were very large.

CHAPTER V

THE INFLUENCE OF PHYSICAL PROPERTIES ON STRUCTURED PACKING HETP CORRELATIONS

The contents of this chapter will be published in the proceedings of Distillation & Absorption 2022.

5.1 ABSTRACT

This study focused on the impact of physical properties on structured packing HETP correlations in the literature. A model derived from inadequate HETP data will not only affect where it may perform poorly but will also impact the relationship between specific physical properties and the model's predicted HETP. The correlations included in this study were Gualito (1997), Billet & Schultes (1999), Aspen (2012), Delft (2014), and Song (2018). A sensitivity analysis was conducted to determine the effect of physical properties on the predicted HETP from the above models. A Monte Carlo analysis was performed to quantify uncertainty in the HETP model predictions due to expected variability in physical property data. Experimental HETP data utilized for this study represented pressures ranging from 0.13 – 27.6 bara. Analysis indicated that the observed relationship between liquid viscosity and predicted HETP did not show expected trends in the Gualito and Billet & Schultes correlations.

5.2 INTRODUCTION

The correlations analyzed in this study were Gualito, Billet & Schultes (1999 version), Delft Model, Aspen, and Song. A full description of the models is provided in Chapter 2 and a brief recap is also in Chapter 4. For this study, only the preloading regime working equations of Billet & Schultes (1999) were considered. This was done so that a similar comparison can be made to other models. Billet & Schultes do not provide the packing-specific constants (C_L and C_V) in the mass transfer coefficient terms, for the packing type analyzed in this study. Therefore, the C_L was determined to be 1.490 and C_V equals 0.517, which were regressed with the FRI Mellapak 250Y hydrocarbon HETP data also used in this study. The Delft model utilized in this study features the revised effective area term, and the later modifications to the φ and k_L terms. The Aspen model, developed by Hanley and Chen, utilizes the sheet metal structured packing k_L, k_G, and effective area terms in this study.

5.3 RESULTS AND DISCUSSION

The experimental data used in the sensitivity analysis and the test systems in Monte Carlo analysis are outlined in figures published by FRI.[32] This data is from Fractionation Research Inc. (FRI) Mellapak 250Y experiments, which tested multiple binary hydrocarbon mixtures (C6/C7, O/P-Xylene and IC4/NC4) across a pressure range of 0.13-27.6 bara. In addition to these systems, an aqueous mixture (MeOH/Water) was included from Sulzer's published Mellapak 250Y data.[66] The column diameter for the FRI and Sulzer experiments are 1.2 m and 1.0 m, respectively.

5.3.1 SENSITIVITY ANALYSIS

In this paper, the results of the liquid viscosity and surface tension sensitivity tests were selected due to their potential impact on HETP. The aim of this work was to outline differences between the models that the physical properties may influence on predicted HETP. For all the test systems, except MeOH/Water at 1 bar, the physical properties corresponded to experimental HETP data at their respective F-factors. This is considered the "baseline" physical property set.

The HETP was then calculated across a range of F-factors with this set. Using this baseline set, a specific physical property was varied systematically while keeping all other physical properties fixed at their baseline values. The HETP percent change was then calculated between the modified sets and the original HETP with the "baseline" physical properties. It is important to note that the data seen in the figures below are an average percent change across all the preloading regime points in that specific system. The sensitivity analysis results presented in the tornado plots below include the respective physical property when the property was varied by 20%, with the rest of the physical properties being held constant. The selection of ±20% for sensitivity testing is meant to be representative of possible error caused by physical property prediction, experimental measurement, assumptions, or a combination of them all.

The liquid viscosity sensitivity results are seen in Figures 5.1-5.5. The expected relationship between HETP and liquid viscosity is that an increase in liquid viscosity results in an increase in HETP. This expectation is also supported by experimental liquid viscosity studies on structured packing[61] and sieve trays.[70] The effect of liquid viscosity on HETP with the Gualito model can be seen in Figure 5.1. In most of the systems, HETP decreased with increasing liquid viscosity. In Figure 5.2, the Billet & Schultes model sensitivity results can be seen, as it displayed a closely uniform response in HETP, across all the analyzed test systems. For all the test systems in Figure 5.2, HETP decreased with increasing liquid viscosity. This counter-intuitive result in Figure 5.1 and Figure 5.2 is mostly a result of each model's a_e term dependence on liquid viscosity. The similarity in results should not be surprising as both correlations use some of the same HETP experiments and have similar liquid viscosity placement in the a_e and k_L terms, as well as with similar exponents.

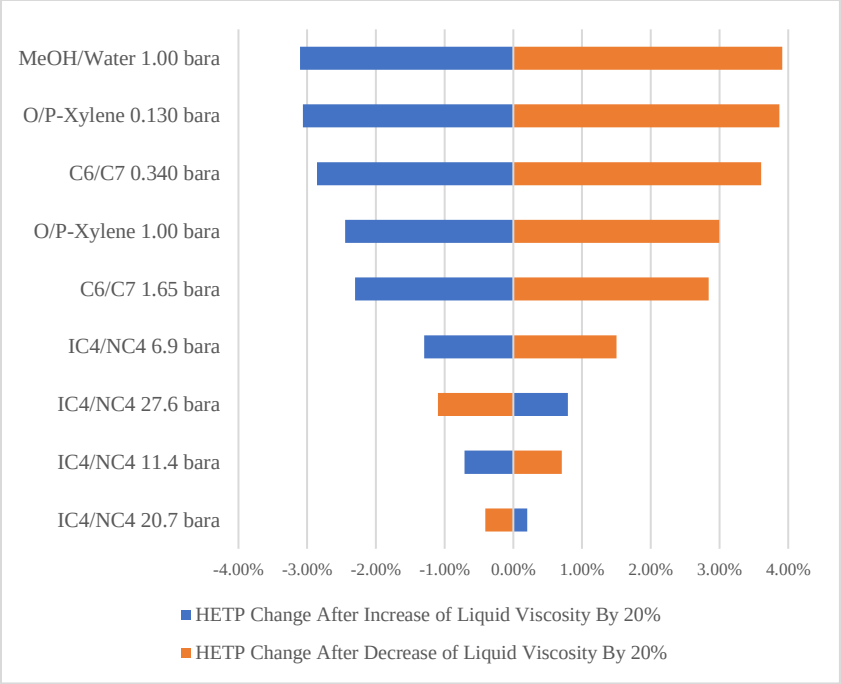

Figure 5.1. Effect of liquid viscosity on Gualito Model with Mellapak 250Y.

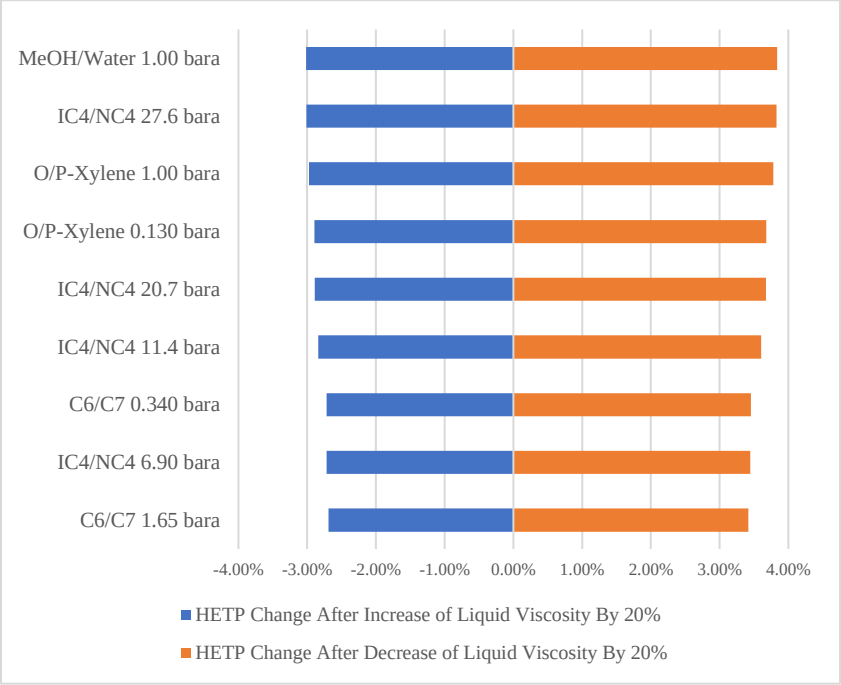

Figure 5.2. Effect of liquid viscosity on Billet and Schultes with Mellapak 250Y.

In Figures 5.3-5.5, the overall trend is as expected, HETP increased with increasing liquid viscosity. The major discrepancy between these figures is the systems display a differing range in sensitivity. Delft model results, seen in Figure 5.3, have negligible change in HETP for the lower pressure systems, but are much more sensitive for the higher-pressure hydrocarbon systems. The opposite is true in Figure 5.4 and Figure 5.5 with the impact of liquid viscosity on Song and Aspen, respectively. With Song, the liquid viscosity only appears in the k_L term, where it is divided by liquid density and raised by the power of -0.4. For the higher-pressure systems analyzed, liquid viscosity decreases significantly but its impact is held in-check by liquid density that is also decreasing for those systems, unlike the Delft model where smaller liquid viscosities will have larger impacts on HETP. The Delft model has a similar placement of liquid viscosity in the k_L term as Billet & Schultes but due to the a_e term, the HETP and liquid viscosity trend seen in these models is the opposite.

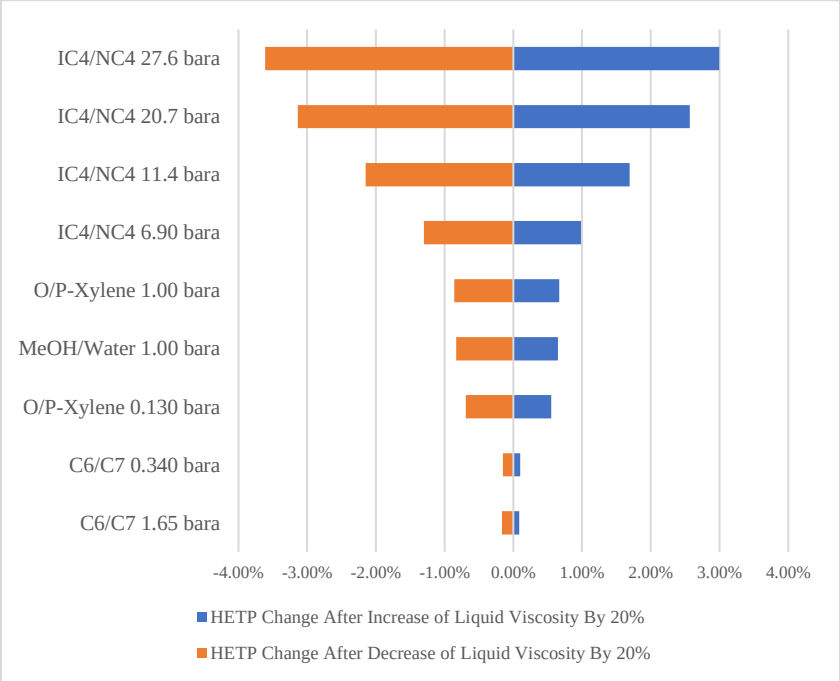

Figure 5.3. Effect of liquid viscosity on Delft Model with Mellapak 250Y.

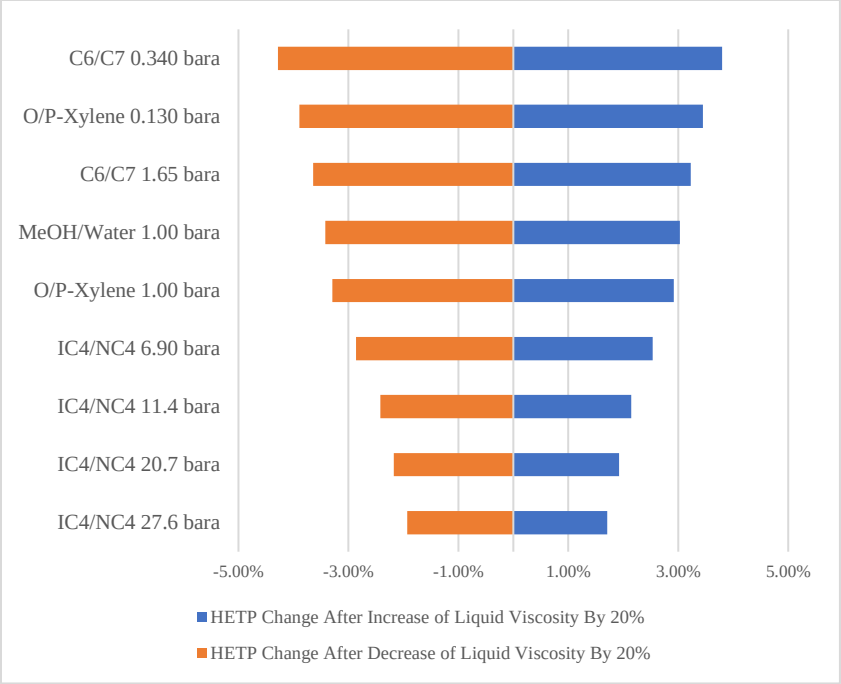

Figure 5.4. Effect of liquid viscosity on Song with Mellapak 250Y.

The Aspen model has similar behavior to Song model with liquid viscosity, seen in Figure 5.5. As HETP change is more sensitive with the lower pressure systems but unlike Song, HETP change is negligible for higher pressure changes. The relationship of liquid viscosity in the k_L terms is similar for Aspen and Song, but Aspen has a liquid viscosity term present in the a_e term unlike Song.

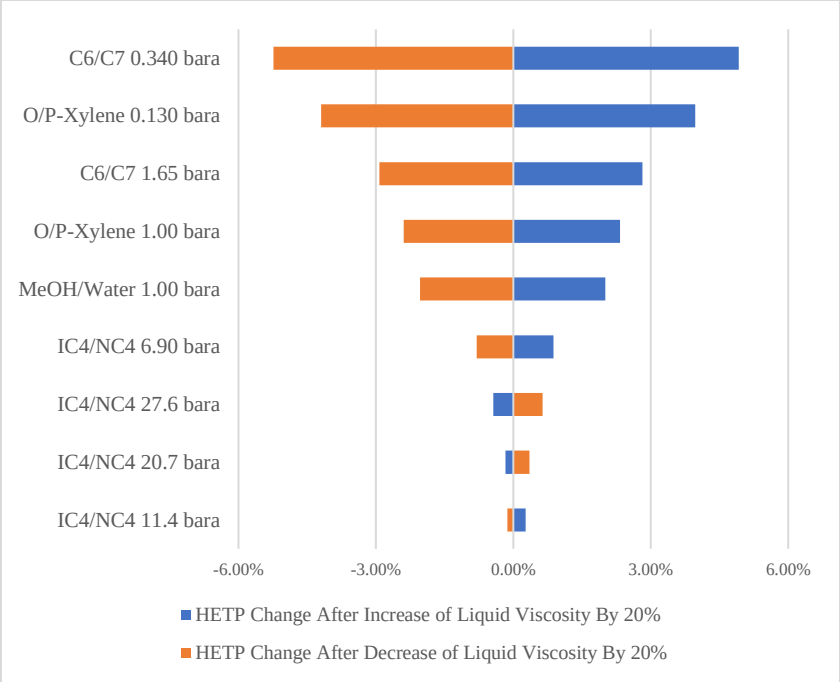

Figure 5.5. Effect of liquid viscosity on Aspen with Mellapak 250Y.

Outside of Gualito and Billet & Schultes, the models generally showed increasing HETP with increasing liquid viscosity. The sensitivity analysis was replicated with structured packings at different nominal areas (up to 500 m^2/m^3). The overall trends seen in Figures 5.1-5.5 with Mellapak 250Y are very similar to the results seen with different types of common structured packings. The surface tension sensitivity results are seen in Figures 5.6-5.9. The expected trend should be a decrease of HETP with a decrease of surface tension, as wetting would be enhanced and thus mass transfer improved. The surface tension impact on the HETP models is sometimes not as straightforward as other regressed physical property relationships because it can rely on model rules that seem arbitrary. For example, Gualito has a term called reference surface tension that is equal to 0.045 N/m. The liquid hold-up correction factor (F_t) changes based on being above or below this value. As seen in Figure 5.6, Gualito model's HETP change for the hydrocarbon systems were $\pm$3%, but as the system's surface tension increased past 0.045 N/m, the model's behavior became very sensitive in the MeOH/Water system. For Billet & Schultes correlation, HETP does not change with the modification of surface tension for the hydrocarbon

systems present. This is due to rules in the model's paper, where if a system's surface tension is below 0.030 N/m, the surface tension is ultimately set to 0.030 N/m. For the MeOH/Water system, Billet & Schultes predicted HETP had increased by 15% after an increase of surface tension by 20% and HETP decreased by 15% after surface tension was decreased by 20%. The Delft model does not have any rules like this, so the surface tension is more responsive at low pressures but has negligible impacts on HETP for the high-pressure systems, as seen in Figure 5.7.

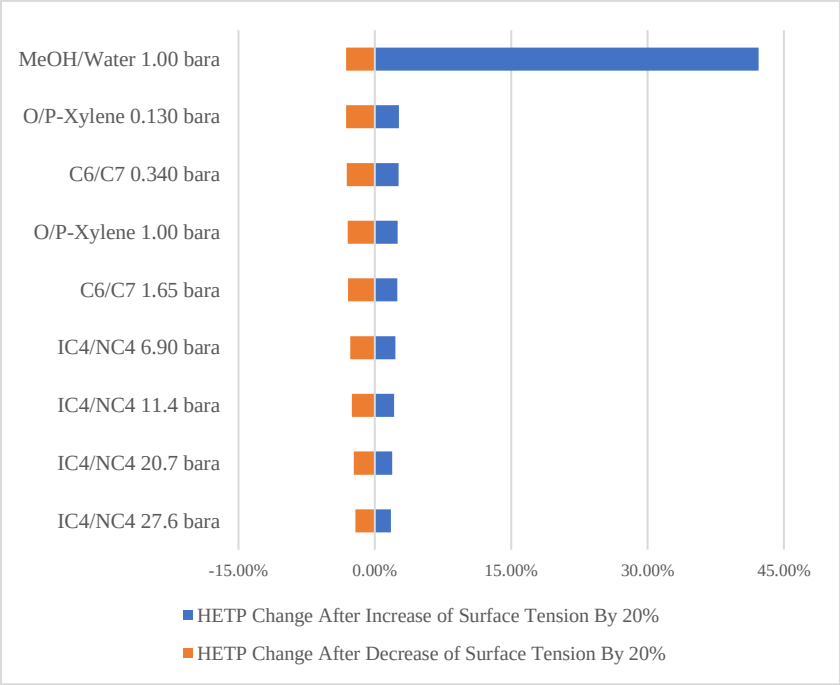

Figure 5.6. Effect of surface tension on Gualito Model with Mellapak 250Y.

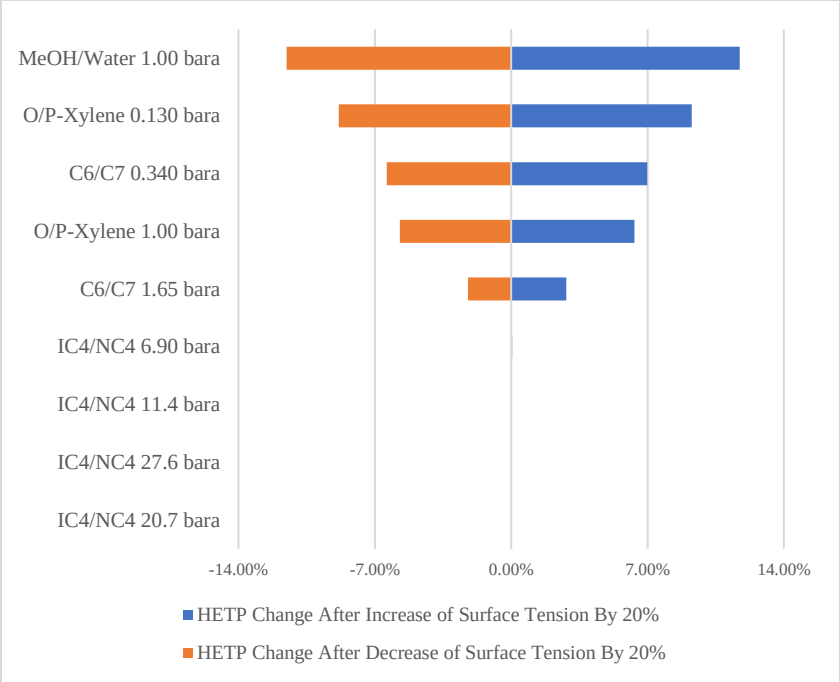

Figure 5.7. Effect of surface tension on Delft with Mellapak 250Y.

Both Song and Aspen behave similarly in that the HETP change seems to be independent of the test system being calculated, seen in Figure 5.8 and 5.9, respectively. The only occurrence of surface tension in either of the models is found in the denominator of the a_e term, where Aspen is more sensitive due to having a larger exponent on the surface tension term.

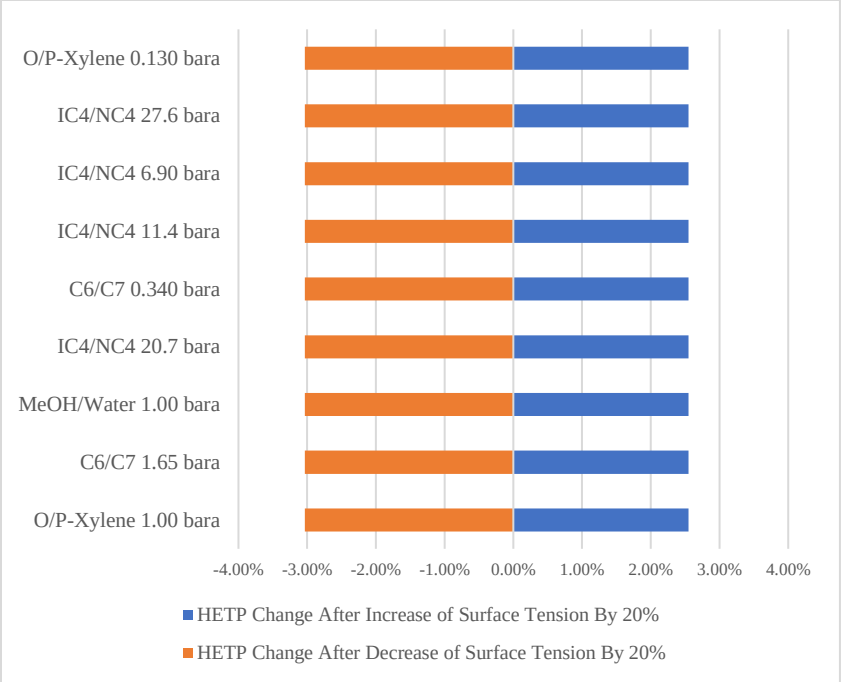

Figure 5.8. Effect of surface tension on Song with Mellapak 250Y.

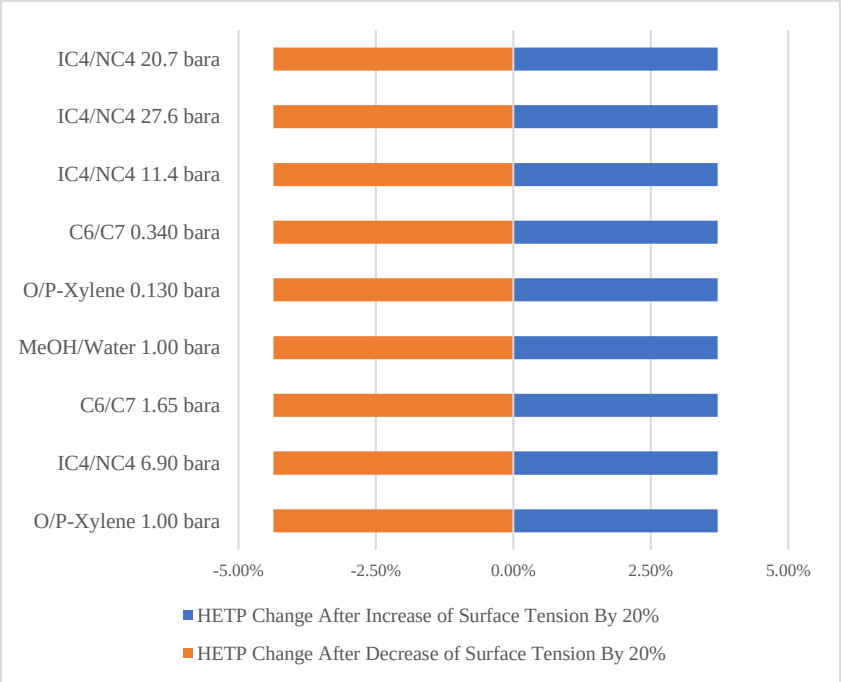

Figure 5.9. Effect of surface tension on Aspen with Mellapak 250Y.

If Billet & Schultes models are used without the surface tension rules, the results would be similar to Aspen and Song, but more sensitive as surface tension's exponent is much larger.

Delft model is not sensitive at high pressures because the a_e equation has an exponential term that subtracts from one and is then multiplied by a_p and another geometric term. As the surface tension gets smaller, the exponential term gets closer to one but at a low enough surface tension, changes to that physical property result in a negligible change to effective area and HETP. Although most of the models investigated showed an increase in HETP with an increase in surface tension, the models did not agree upon the degree of sensitivity surface tension should have on HETP. As stated earlier for liquid viscosity, the study was replicated at different nominal areas with similar sensitivity results. For both studies, it is worth noting that since Billet & Schultes model requires regressed packing-specific constants, its sensitivity results are dependent on utilized regression database and packing type.

5.3.2 MONTE CARLO SIMULATION

Monte Carlo technique is useful for understanding model uncertainty that is caused by a model's inputs. In this case, the inputs were liquid/vapor density, liquid/vapor viscosity, liquid/vapor diffusivity, surface tension, stripping factor, and for only Aspen's model, molecular weight. A normal distribution of 10,000 random values was generated for each input parameter. The lower and upper bounds for the truncated, normal distribution are constructed based on a lighter component composition of 99.9% and 0.1%, which provides the range of the input parameter. The physical property range inputs were generated with Aspen Plus for each system. Aspen Plus relies on prediction models to generate physical properties, which will have some inaccuracy but the lower/upper input bounds for each model are consistent and can still provide a fair comparison of uncertainty for each system. The Monte Carlo simulations are run across a range of preloading regime F-factors, in which the mean and standard deviation are calculated, to further analyze uncertainty with Equation 5.1. Equation 5.1 is a ratio of standard deviation to mean, otherwise known as the coefficient of variation.

$$\text{Coefficient of Variation (CV)} = \frac{\text{Standard Deviation}}{\text{Mean}} \quad (5.1)$$

In addition to comparing uncertainty, HETP model performance was also evaluated for these systems. Predicted HETP values from models corresponded to actual physical property inputs, at each F-factor, that were taken from FRI and Sulzer experiments. The FRI experiments used a composition at the middle of the bed and the Sulzer experiment was an average of top and bottom compositions. The average of predicted model and experimental HETP values (m) across the pre-loading regime are reported in Table 5.1. Obviously, average prediction values from each model do not capture the complete picture but it does provide for a summary of how each model over/under predicted each dataset. The experimental pre-loading HETP column in Table 1 are the average values except for the reported ranges in the high-pressure systems, which varies due to a "hump" only seen in these systems. The coefficient of variation results from the Monte Carlo simulations can also be seen below in Table 5.1.

Table 5.1. Comparison of Uncertainty and Performance Evaluation

			Gualito		B&S		Delft		Aspen		Song	
Test System	P (bara)	Exp. HETP (m)	HETP (m)	CV	HETP (m)	CV	HETP (m)	CV	HETP (m)	CV	HETP (m)	CV
C6/C7	0.340	0.47	0.53	0.055	0.37	0.051	0.50	0.057	0.45	0.089	0.46	0.069
C6/C7	1.65	0.39	0.42	0.044	0.35	0.046	0.39	0.043	0.32	0.058	0.39	0.051
O/P-Xylene	0.130	0.37	0.53	0.022	0.33	0.014	0.44	0.023	0.33	0.0090	0.33	0.0069
O/P-Xylene	1.00	0.34	0.45	0.018	0.32	0.013	0.33	0.019	0.28	0.012	0.27	0.0071
IC4/NC4	6.90	0.35	0.33	0.016	0.35	0.015	0.29	0.018	0.26	0.025	0.33	0.015
IC4/NC4	11.4	0.23-0.37	0.31	0.015	0.31	0.017	0.25	0.017	0.25	0.024	0.31	0.017
IC4/NC4	20.7	0.32-0.56	0.38	0.023	0.40	0.024	0.18	0.027	0.23	0.021	0.26	0.023
IC4/NC4	27.6	0.51-0.73	0.72	0.044	0.61	0.030	0.12	0.038	0.21	0.020	0.20	0.028
MeOH/ Water	1.00	0.31	0.47	0.26	0.32	0.13	0.49	0.16	0.31	0.097	0.32	0.060

It was found that Song had the lowest average CV, with the systems analyzed above, with a value of 0.031. This can be explained by its low number of working equations and having the least physical property terms in its a_e term. It also had the least recurrences of the same physical

properties throughout the k_L and k_G terms. The highest average CV was in the Gualito model, with an approximate value of 0.055. The Gualito model to predict HETP must solve a pressure drop model first, which increases the number of inputs and thus uncertainty. For the performance evaluation, including every individual HETP pre-loading point, Billet & Schultes performed the best with a weighted mean absolute error of 18%, helped by the necessary regressed packing constants. It also had the second least uncertainty across the systems, after Song. When averaging just the low-pressure hydrocarbon systems, Aspen had the lowest with 13%.

5.4 CONCLUSIONS

This work presented the results of sensitivity tests and Monte Carlo simulations on commonly used HETP correlations in the literature. The sensitivity tests were conducted to highlight differences between HETP model sensitivities and how a model may perform with an uncertain physical property input. Predicted HETP by the models varied widely with changes in liquid viscosity and surface tension. The Monte Carlo simulations outlined differences in uncertainty and the effect of variations in physical properties on the HETP predicted by the models. The uncertainty results were coupled with a performance evaluation for a practitioner to select an HETP correlation for a specific test system.

CHAPTER VI

FUTURE WORK AND CONCLUSIONS

A physical property and HETP performance study was conducted with five structured packing HETP correlations – Billet & Schultes, Delft, Gualito, Aspen and Song. The physical property portion of the study included physical property sensitivity testing and Monte Carlo simulation of nine unique systems. The sensitivity testing was meant to highlight the differences in models caused by assumptions, different physical property ranges used for development, etc. As a result of the testing, the counter-intuitive relationships between HETP and liquid viscosity were observed with the Billet & Schultes and Gualito correlations. Even when models agreed in the overall relationship between liquid viscosity and HETP, there was less agreement in the degree of sensitivity between higher and lower pressure systems. In addition to liquid viscosity, the differences in dependency on surface tension were highlighted between all the models. Some correlations demonstrated changes in 15% or more with predicted HETP because of a surface tension input change of 20%, while other correlations were impacted by less than 3% in HETP change. Overall, the physical property sensitivity results hoped to not only quantify the sensitivity of models with surface tension and liquid viscosity but prove to be a warning for practitioners who utilize these correlations outside of their validated physical property ranges. The final aspect of the physical property study included Monte Carlo simulation, to determine which correlation would have the highest uncertainty due to their input parameters.

Gualito had the highest uncertainty of the analyzed correlations, due to the large number of equations required to solve the pressure drop and efficiency aspects of the model.

In addition to the physical property study, a performance evaluation of the correlations was included. The first was an analysis of all the same systems from the physical property study with Mellapak 250Y, to couple performance data with uncertainty calculations from Monte Carlo simulation. There were also other systems analyzed and packings, as presented in Chapter 4, ranging from nominal areas of 250 to 500 m^2/m^3. Billet & Schultes correlation consistently predicted HETP accurately, due to the packing-specific constants, which were regressed for each set of data and corresponding packing. Gualito performed well overall but had consistent weakness with o/p-xylene systems. No model could predict the efficiency hump seen in high pressure structured packing. The newer models of Aspen and Song performed well, with Song being quite the surprise due to its development from an air/water column databank. Effective area predictions were also a focal point of study, including each model's interpretation of its definition. Overall, the goal was to quantify HETP performance and provide observations and points of emphasis, if possible, of why the models were performing poorly with specific data.

In terms of future work, there is multiple routes that this research can be further pursued. The simplest is to recreate the same study with more correlations that have fallen by the wayside, there is a jungle of structured packed HETP correlations and not all have been given a fair shot. Another route is for a future graduate student to take observations and conclusions from this study to produce an updated or new efficiency correlation. The physical property study or performance data could guide a researcher in terms of selected test systems for experiments. Also, many small observations made in this study, for example, Song's performance could be improved with distillation data if it were a weaker function of liquid load, could be taken to design a model with improved performance. The ultimate goal for this research area of structured packing efficiency correlations would be to definitively measure terms like effective area and other parameters, so as to not contribute another correlation where those important terms are uncertain.

REFERENCES

1. Kiss, A.A., Distillation technology – still young and full of breakthrough opportunities. Journal of Chemical Technology & Biotechnology, **2014**. 89(4): p. 479-498.
2. Fenske, M., Fenske-Underwood Equation. Ind. Eng. Chem **1932**, p. 32.
3. Winn, F., New relative volatility method for distillation calculations. Petrol. Refin, **1958**. 37(5): p. 216-218.
4. Kister, Henry Z. Distillation Design. New York: McGraw-Hill, **1992**.
5. Lewis, W.; Whitman, W. Principle of Gas Absorption. Ind. Eng. Chem. **1924**, 16, p. 1215–1220.
6. Górak, A.; Sorensen, E., Distillation: fundamentals and principles. Academic Press, **2014**.
7. Wang, G.Q., X.G. Yuan, and K.T. Yu, Review of Mass-Transfer Correlations for Packed Columns. Industrial & Engineering Chemistry Research, **2005**. 44(23): p. 8715-8729.
8. Morsi, B.I. and O.M. Basha. Mass Transfer in Multiphase Systems. **2015**.
9. Bunch, D.W., A study of turbulent mass transfer in a wetted-wall column. Ph.D. Dissertation, Missouri University of Science and Technology, **1964**.
10. Gilliland, E.R. and T.K. Sherwood, Diffusion of Vapors into Air Streams. Industrial & Engineering Chemistry, **1934**. 26(5): p. 516-523.
11. Lopez-Toledo, J., Heat and Mass Transfer Characteristics of a Wiped Film Evaporator. Ph.D. Dissertation, University of Texas at Austin, **2006**.
12. McCarter, R.J. and L.F. Stutzman: A.I.Ch.E Journal 502. **(1959).**
13. Schwarz, W.H. and H.E. Hoelscher: A.I.Ch.E. Journal 2. p. 101 **(1956)**.

14. Johnstone, H. and R. Pigford, Distillation in a wetted-wall column. Trans. Am. Inst. Chem. Eng, **1942**. 38(1): p. 25-51.
15. Onda, K., H. Takeuchi, and Y. Okumoto, MASS TRANSFER COEFFICIENTS BETWEEN GAS AND LIQUID PHASES IN PACKED COLUMNS. Journal of Chemical Engineering of Japan, **1968**. 1(1): p. 56-62.
16. Hanley, B. and C.-C. Chen, New mass-transfer correlations for packed towers. AIChE Journal, **2012**. 58(1): p. 132-152.
17. Billet, R. and M. Schultes, Predicting mass transfer in packed columns. Chemical Engineering & Technology, **1993**. 16(1): p. 1-9.
18. Billet, R. and M. Schultes, Prediction of Mass Transfer Columns with Dumped and Arranged Packings: Updated Summary of the Calculation Method of Billet and Schultes. Chemical Engineering Research and Design, **1999**. 77(6): p. 498-504.
19. Bravo, J., J.A. Rocha, and J. Fair, Mass transfer in gauze packings. Hydrocarbon Processing, **1985**. 64: p. 91-95.
20. Yanagi, T. and M. Sakata, Performance of a commercial scale 14% hole area sieve tray. Industrial & Engineering Chemistry Process Design and Development, **1982**. 21(4): p. 712-717.
21. Billet, R., Optimization and Comparison of Mass Transfer Columns. Inst. Chem. Eng. Symp. Ser., **1969**. 32: p. 4-42.
22. Higbie, R. The Rate of Absorption of a Pure Gas into a Still Liquid during Short Periods of Exposure. **1935**.
23. Rocha, J.A., J.L. Bravo, and J.R. Fair, Distillation columns containing structured packings: a comprehensive model for their performance. 1. Hydraulic models. Industrial & Engineering Chemistry Research, **1993**. 32(4): p. 641-651.

24. Rocha, J.A., J.L. Bravo, and J.R. Fair, Distillation Columns Containing Structured Packings: A Comprehensive Model for Their Performance. 2. Mass-Transfer Model. Industrial & Engineering Chemistry Research, **1996**. 35(5): p. 1660-1667.
25. McNulty, K.; Hsieh, C. L. Hydraulic Performance and Efficiency of Koch Flexipac Structured Packing. Paper presented at the Fall AIChE National Meeting, Los Angeles, CA, November **1982**.
26. Chen, G. K.; Kitterman, L.; Shieh, J. H. Development of a New Generation of High Efficiency Packing for Mass Transfer Operations. Chem. Eng. Prog. **1982**, p. 79 (9), 48.
27. Chen, G. K.; Kitterman, L.; Shieh, J. H. "Glitsch High Efficiency Packings—Preliminary Design Information"; Addendum to Glitsch Publication No. 40283, Glitsch, Inc.: Dallas, TX, **1983**.
28. Murrieta, C. Liquid Phase Mass Transfer in Structured Packing. Separations Research Program report, The University of Texas at Austin, Austin, TX, October **1991.**
29. Shi, M. and Mersmann, A., Effective interfacial area in packed columns. Ger. Chem. Eng, **1985**. 8: p. 87-96.
30. McGlamery, G. G. Liquid Film Transport Characteristics of Textured Metal Surfaces. Ph.D. Dissertation, The University of Texas at Austin, Austin, TX, **1988.**
31. Gualito, J.J., et al., Design Method for Distillation Columns Filled with Metallic, Ceramic, or Plastic Structured Packings. Industrial & Engineering Chemistry Research, **1997**. 36(5): p. 1747-1757.
32. Fitz, C.W., Kunesh, J.G., and Shariat, A., Performance of Structured Packing in a Commercial-Scale Column at Pressures of 0.02−27.6 bar. Industrial & Engineering Chemistry Research, **1999**. 38(2): p. 512-518.
33. Olujic, Z., Development of a complete simulation model for predicting the hydraulic and separation performance of distillation columns equipped with structured packings. Chemical and Biochemical Engineering Quarterly, **1997**. 11: p. 31-46.

34. Petukhov, B.S., Heat Transfer and Friction in Turbulent Pipe Flow with Variable Physical Properties, in Advances in Heat Transfer, J.P. Hartnett and T.F. Irvine, Editors, **1970**. Elsevier. p. 503-564.
35. Millsaps, K. and Pohlhausen, K., Heat Transfer by Laminar Flow from a Rotating Plate. Journal of the Aeronautical Sciences, **1952**. 19(2): p. 120-126.
36. Karman, T.V., Uber laminare und turbulente, Z. angew. Math. Mech., **1921**. 1: p. 244-247.
37. Fair, J.R., et al., Structured Packing Performance-Experimental Evaluation of Two Predictive Models. Industrial & Engineering Chemistry Research, **2000**. 39(6): p. 1788-1796.
38. Olujić, Ž., et al., Predicting the Efficiency of Corrugated Sheet Structured Packings with Large Specific Surface Area. Chemical and Biochemical Engineering Quarterly, **2004**. 18: p. 89-96.
39. Olujić, Ž., et al., Experimental Characterization and Modeling of High Performance Structured Packings. Industrial & Engineering Chemistry Research, **2012**. 51(11): p. 4414-4423.
40. Olujić, Ž. and Seibert, A.F., Predicting the Liquid Phase Mass Transfer Resistance of Structured Packings. Chem. Biochem. Eng. Q., **2014**. 28: p. 409-424.
41. Song, D. Effect of Liquid Viscosity on Liquid Film Mass Transfer for Packings. Doctoral Dissertation, University of Texas, Austin, Texas, **2017**.
42. Tsai, R.E., et al., Influence of viscosity and surface tension on the effective mass transfer area of structured packing. Energy Procedia, **2009**. 1(1): p. 1197-1204.
43. Wang, C., et al., Dimensionless Models for Predicting the Effective Area, Liquid-Film, and Gas-Film Mass-Transfer Coefficients of Packing. Industrial & Engineering Chemistry Research, **2016**. 55(18): p. 5373-5384.

44. Seibert, A.F., Application of Air/Water Derived Mass Transfer Models to Distillation [Powerpoint slides]. AIChE Galveston Spring Meeting, **2017**. p. 1-32.
45. Nawrocki, P.A., Z.P. Xu, and K.T. Chuang, Mass transfer in structured corrugated packing. The Canadian Journal of Chemical Engineering, **1991**. 69(6): p. 1336-1343.
46. Henriques de Brito, M., U. von Stockar, and P. Bomio, Predicting the liquid phase mass transfer coefficient kL for the Sulzer structured packing Mellapak, **1992**. 128: p. 137-144.
47. Hanley, B., B. Dunbobbin, and D. Bennett, A Unified Model for Countercurrent Vapor/Liquid Packed Columns. 1. Pressure Drop. Industrial & Engineering Chemistry Research, **1994**. 33(5): p. 1208-1221.
48. Hanley, B., B. Dunbobbin, and D. Bennett, A Unified Model for Countercurrent Vapor/Liquid Packed Columns. 2. Equations for the Mass-Transfer Coefficients, Mass-Transfer Area, the HETP, and the Dynamic Liquid Holdup. Industrial & Engineering Chemistry Research, **1994**. 33(5): p. 1222-1230.
49. Brunazzi, E. and A. Paglianti, Liquid-Film Mass-Transfer Coefficient in a Column Equipped with Structured Packings. Industrial & Engineering Chemistry Research, **1997**. 36(9): p. 3792-3799.
50. Shetty, S. and R.L. Cerro, Fundamental Liquid Flow Correlations for the Computation of Design Parameters for Ordered Packings. Industrial & Engineering Chemistry Research, **1997**. 36(3): p. 771-783.
51. Xu, Z.P., A. Afacan, and K.T. Chuang, Predicting Mass Transfer in Packed Columns Containing Structured Packings. Chemical Engineering Research and Design, **2000**. 78(1): p. 91-98.
52. Del Carlo, L., Ž. Olujić, and A. Paglianti, Comprehensive Mass Transfer Model for Distillation Columns Equipped with Structured Packings. Industrial & Engineering Chemistry Research, **2006**. 45(23): p. 7967-7976.

53. Olujić, Ž., et al., Fractionation Research Inc. Test Data and Modeling of a High-Performance Structured Packing. Industrial & Engineering Chemistry Research, **2013**. 52(13): p. 4888-4894.
54. Olujić, Ž., et al., Performance characteristics of an intermediate area high performance structured packing. Chemical Engineering Research and Design, **2015**. 99: p. 14-19.
55. Jammula, A.K., Whiteley, R., Cai, T., Resetarits, M., Performance of Structured Packing HETP Correlations [Powerpoint slides]. AIChE Houston Spring Conference, **2012**. p. 1-34.
56. Wolf-Zöllner, V., F. Seibert, and M. Lehner, Performance comparison of different pressure drop, hold-up and flooding point correlations for packed columns. Chemical Engineering Research and Design, **2019**. 141: p. 388-401.
57. Mangers, R.J. and A.B. Ponter, Effect of Viscosity on Liquid Film Resistance to Mass Transfer in a Packed Column. Industrial & Engineering Chemistry Process Design and Development, **1980**. 19(4): p. 530-537.
58. Tsai, R.E., et al., Influence of viscosity and surface tension on the effective mass transfer area of structured packing. Energy Procedia, **2009**. 1(1): p. 1197-1204.
59. Song, D., A.F. Seibert, and G.T. Rochelle, Effect of Liquid Viscosity on the Liquid Phase Mass Transfer Coefficient of Packing. Energy Procedia, **2014**. 63: p. 1268-1286.
60. Bader, A.J., et al., Effect of liquid-phase properties on separation efficiency in a randomly packed distillation column. The Canadian Journal of Chemical Engineering, **2015**. 93(6): p. 1119-1125.
61. Bradtmöller, C. and S. Scholl, Geometry and viscosity effects on separation efficiency in distillation. Chemical Engineering Research and Design, **2015**. 99: p. 75-86.
62. Patberg, W.B., et al., Effectiveness of mass transfer in a packed distillation column in relation to surface tension gradients. Chemical Engineering Science, **1983**. 38(6): p. 917-923.

63. Stemmet, C.P., et al., Influence of liquid viscosity and surface tension on the gas–liquid mass transfer coefficient for solid foam packings in co-current two-phase flow. Chemical Engineering Research and Design, **2008**. 86(10): p. 1094-1106.
64. Olujić, Ž., Effect of Column Diameter on Pressure Drop of a Corrugated Sheet Structured Packing. Chemical Engineering Research and Design, **1999**. 77(6): p. 505-510.
65. Ottenbacher, M., et al., Structured packing efficiency—Vital information for the chemical industry. Chemical Engineering Research and Design, **2011**. 89(8): p. 1427-1433.
66. Meier, W., R. Hunkelar, and D. Stoecker, Performance of the new Regular Tower Packing "Mellapak". IChemE Symp. Series, **1979**. 56: p. 3.3/1-3.3/17.
67. Zuiderweg, F.J., Olujic, Z., Kunesh, J.G., Liquid backmixing in structured packing in high pressure distillation. IChemE Symp. Ser., **1997**. 142: p. 865-872.
68. Cai, T.J., et al., Effect of Bed Length and Vapour Maldistribution on Structured Packing Performance. Chemical Engineering Research and Design, **2003**. 81(1): p. 85-93.
69. Pilling, M.W., Kehrer, F., Speigel, L., Testing of Mellapakplus M452.Y at Fractionation Research, Inc. [Powerpoint slides]. AIChE Orlando Spring Conference, **2006.**
70. Manivannan, R.G., Cai, T., McCarley, K., Vennavelli, A., Mohammad, S., Aichele, C.P.., Point efficiency of sieve trays at elevated liquid viscosities. Chemical Engineering Research and Design, **2020**. 159, 138-145.

APPENDICES

APPENDIX A

A.1. MATLAB Function M File – Billet & Schultes correlation

```
function
[HETP,h_t,U_Lbar,k_L,k_G,a_ph,Re_L]=billetschultesfun(F_v,p_L,p_G,sigma
,vis_L,vis_G,D_L,D_G,lambda,a_p,E,s)

%% Inputs required

% Billet & Schultes (Preloading equations only) 1993/1999
% The 1993 paper or the 1999 paper with just the preloading equations
for
% Billet & Schultes correlation.

n=length(F_v);

% Superficial velocity calculations
U_Gs = F_v./((p_G).^0.5); % m/s
U_Ls = U_Gs.*(p_G./p_L);

% Surface Tension Rule
sigma=sigma';
count = 0;
for ii=sigma;
    count = 1+count;
    if ii < 0.030;
        sigma(1,count)=0.030;
    else
        sigma(1,count)= ii;
    end
end
sigma=sigma';

p = pi;
g_c = ones(n,1)*1; % gravity conversion factor
g = ones(n,1)*9.80665; % gravitational constant (m/s^2)

% Billet & Schultes packing specific parameters
C_L = ones(n,1)*1.490; % Packing specific constant regressed for
respective packing (liquid), must be changed for respective packing
C_V = ones(n,1)*0.5167; % Packing specific constant for respective
packing (vapor), must be changed for respective packing/data
```

```
d_h = 4.*(E./a_p); % Hydraulic diameter (m)

%% Liquid hold-up calculation for preloading regime
h_t = (12.*(vis_L.*a_p.^2.*U_Ls)./(p_L.*g)).^(1/3);

%% Mass transfer coefficient calculations
Re_G_new = (p_G.*U_Gs)./(vis_G.*a_p);
Sc_G_new = (vis_G)./(p_G.*D_G);

% Preloading equations of effective area, velocity, etc.
apha = 1.5.*((a_p.*d_h).^(-0.5)).*(((U_Ls.*d_h.*p_L)./vis_L).^(-
0.2)).*(((U_Ls.^2.*p_L.*d_h)./sigma).^0.75).*((U_Ls.^2)./(g.*d_h)).^-
0.45;
a_ph = apha.*a_p;
U_Lbar = U_Ls./h_t;

% Liquid/gas mass transfer coefficients for preloading regime
k_L = C_L.*12.^(1/6).*U_Lbar.^(1/2).*(D_L./d_h).^(1/2);
k_G = C_V.*(1./((E-
h_t).^(1/2))).*((a_p./d_h).^(1/2)).*D_G.*(Re_G_new).^(3/4).*(Sc_G_new).
^(1/3);

%% Calculation of HETP
HETP =
((U_Gs./(k_G.*a_ph))+lambda.*(U_Ls./(k_L.*a_ph))).*(log(lambda)./(lambd
a-1));


 end
```

A.2. MATLAB Function M File – Delft Model

```
function
[HETP,a_e,k_L,k_G]=delftfun(F_v,p_L,p_G,sigma,vis_L,vis_G,D_L,D_G,lambd
a,a_p,E,theta,s,h_pe,b,h)

%% Inputs required
% Delft Model 2004,2014
n=length(F_v);

U_Gs = F_v./((p_G).^0.5); % m/s
U_Ls = U_Gs.*(p_G./p_L);
omega = ones(n,1)*0.1; % Constant for Mellapak, Montz and other
packings similar with perforations
% Check 2004 paper for more information on constants
p = pi; % saves p as pi (3.14...)
g_c = ones(n,1)*1; % gravity conversion factor
g = ones(n,1)*9.80665; % gravitational constant (m/s^2)
alpha_L=atand((cosd(90-theta))./(sind(90-
theta).*cos(atan(b./(2.*h))))); % Effective corrugation angle

%% Geometric Calculations
del = ((3.*vis_L.*U_Ls)./(p_L.*g.*a_p.*sind(alpha_L))).^(1/3); % Liquid
film thickness (m)
```

```
l_gpe = h_pe./sind(theta); % Length of the gas flow channel in a
packing element (m)
d_hG = (((b.*h-2.*del.*s).^2)./(b.*h))./((((b.*h-
2.*del.*s)./(2.*h)).^2+((b.*h-2.*del.*s)./(b)).^2).^0.5+((b.*h-
2.*del.*s)./(2.*h))); % Hydraulic diameter of a triangular gas flow
channel (m)
phi = 1; % Reversion back to old Sherwood gas number from original
Delft Model publication
h_L = del.*a_p; % Liquid hold-up (m)

%% Effective Velocity Calculations
U_Ge = U_Gs./((E-h_L).*sind(theta));
U_Le = U_Ls./(E.*h_L.*sind(alpha_L));

%% Dimensionless Number Calculations
Sc_G = vis_G./(p_G.*D_G); % Schmidt number in gas phase
Re_Grv = (p_G.*(U_Ge+U_Le).*d_hG)./vis_G; % Reynolds number in gas
phase based on relative velocity
Re_Ge = (p_G.*U_Ge.*d_hG)./vis_G; % Effective Reynolds number in gas
phase
xi_GL = (-2.*log10(((del./d_hG)./3.7)-
(5.02./Re_Grv).*log10(((del./d_hG)./3.7)+(14.5./Re_Grv)))).^-2; % Gas-
liquid friction factor
Sh_Glam = 0.664.*Sc_G.^(1/3).*(Re_Grv.*(d_hG./l_gpe)).^(1/2); %
Sherwood number for laminar flow
Sh_Gturb =
((Re_Grv.*Sc_G.*((xi_GL.*phi)./8))./(1+12.7.*((xi_GL.*phi)./8).^(1/2).*
(Sc_G.^(2/3)-1))).*(1+(d_hG./l_gpe).^(2/3));

%% Mass Transfer Coefficient Calculations
k_Glam = (Sh_Glam.*(D_G))./(d_hG);
k_Gturb = (Sh_Gturb.*(D_G))./(d_hG);
k_G = (k_Glam.^2+k_Gturb.^2).^(1/2);
k_L = 2.*((D_L.*U_Ls)./(p.*E.*h_L.*s)).^(1/2); % 2014 Olujic and
Seibert new kL term

%% Effective Area Calculation
Re_L = (p_L.*U_Ls)./(a_p.*vis_L);
We_L = (p_L.*U_Ls.^2)./(a_p.*sigma);
Fr_L = ((U_Ls.^2).*a_p)./g;
a_e = (1-omega).*a_p.*(1-exp(-
1.45.*((0.075./sigma).^0.75).*(Re_L.^0.1).*(Fr_L.^-
0.05).*(We_L.^0.2))); % updated effective area term from 2004 DM paper

%% Calculation of HETP
HETP =
((U_Gs./(k_G.*a_e))+lambda.*(U_Ls./(k_L.*a_e))).*(log(lambda)./(lambda-
1));


end
```

A.3. MATLAB Function M File – Aspen Model

```
function
[HETP,a_e,k_L,k_G]=Aspenfun(LMW,GMW,F_v,p_L,p_G,sigma,vis_L,vis_G,D_L,D
_G,lambda,a_p,E,theta)
n=length(F_v);

% Superficial velocity calculations
U_Gs = F_v./((p_G).^0.5); % m/s
U_Ls = U_Gs.*(p_G./p_L); % m/s

p = pi; % saves p as pi (3.14...)
g_c = 1; % gravity conversion factor
g = ones(n,1)*9.80665; % gravitational constant (m/s^2)

% Liquid/Gas Concentration and Flux calculations
LMW2 = LMW.*(1./1000); % (kg/mol)
GMW2 = GMW.*(1./1000); % (kg/mol)
c_L = p_L./LMW2; % Liquid concentration (mol/m^3)
c_G = p_G./GMW2; % Gas concentration (mol/m^3)
L = U_Ls.*c_L; % Liquid molar flux (mol/m^2 sec)
G = U_Gs.*c_G; % Gas molar flux (mol/m^2 sec)

% Dimensionless calculations
d_e = 4.*E./a_p; % equivalent diameter
Re_L = (d_e.*U_Ls.*p_L)./(vis_L);
Re_G = (d_e.*U_Gs.*p_G)./(vis_G);
We_L = (d_e.*p_L.*U_Ls.^2)./(sigma);
Fr_L = (U_Ls.^2)./(g.*d_e);
Sc_L = vis_L./(p_L.*D_L);
Sc_G = vis_G./(p_G.*D_G);

% Mass transfer coefficients
k_L = 0.33.*Re_L.*Sc_L.^(1./3).*((c_L.*D_L)./d_e);
k_G =
0.0084.*Re_G.*Sc_G.^(1/3).*((c_G.*D_G)./d_e).*(cosd(theta)./(cos(p./4))
).^-7.15;
a_e = a_p.*(0.539.*Re_G.^0.145.*Re_L.^-0.153.*We_L.^0.2.*Fr_L.^-
0.2.*(p_G./p_L).^-
0.033.*(vis_G./vis_L).^0.090.*(cosd(theta)./cos(p./4)).^4.078);

C_y = log(lambda)./(lambda-1);
C_x = (lambda.*log(lambda))./(lambda-1);

% HETP Calculation
HETP = (G./a_e).*((C_y./k_G)+(C_x./k_L));

end
```

A.4. MATLAB Function M File – Gualito correlation

```
function
[HETP,F_t,c,a_e,k_L,k_G,h_L,Fr_L,We_L,dpdz,U_Le,U_Ge]=gualitofun(F_v,p_
L,p_G,sigma,vis_L,vis_G,D_L,D_G,lambda,a_p,E,theta,s)
```

```
n=length(F_v);

% Superficial velocity calculation
U_Gs = F_v./((p_G).^0.5); % Gas superficial velocity (m/s)
U_Ls = U_Gs.*(p_G./p_L); % Liquid superficial velocity (m/s)

p = pi; % saves p as pi (3.14...)
g_c = ones(n,1)*1; % Gravitational constant
g = ones(n,1)*9.80665; % Gravitational acceleration (m/s^2)

% Gualito specific constants for metal packings
A_1 = ones(n,1)*29.12;
A_2 = ones(n,1)*0.36;
B_1 = 5.21;
B_2 = -16.83;
C_1 = ones(n,1)*0.177;
C_2 = ones(n,1)*88.774;
D_1 = ones(n,1)*0.614;
D_2 = ones(n,1)*71.35;
sigma_ref = 0.045; % (metal) surface tension reference based on
material of packing
F_SE = ones(n,1)*0.35; % Packing specific constant, see Gualito
p_air = ones(n,1)*1.2; % air density at 1 bar, unclear of what temp ?
(kg/m^3)


%% Pressure drop calculation
We_L = ((U_Ls.^2).*p_L.*s)./(sigma.*g_c); % Weber number for liquid
Re_L = (U_Ls.*s.*p_L)./(vis_L); % Reynolds number for liquid
Fr_L = (U_Ls.^2)./(s.*g); % Froude number for liquid

c = ones(length(sigma),1)*1;
count = 0;
sigma=sigma';
for ii=sigma;
    count = 1+count;
    if ii < sigma_ref;
        c(count,1)=0.90;
    else
        c(count,1)= B_1.*10.^(B_2.*ii);
    end
end
sigma=sigma';


% using eqn 14 for ae/ap or Correction Factor for total hold-up
F_t =
((((We_L.*Fr_L).^0.15).*A_1.*(s.^A_2))./((Re_L.^0.2).*(E.^0.6).*(1-
0.93.*c).*(sind(theta)).^0.3)).*(1.2./(1+0.2.*exp(30.*(U_Ls./(2.*U_Gs))
)));
a_e = F_t.*a_p.*F_SE;
F_t =
((((We_L.*Fr_L).^0.15).*A_1.*(s.^A_2))./((Re_L.^0.2).*(E.^0.6).*(1-
0.93.*c).*(sind(theta)).^0.3));
% Flood Pressure Drop Calculation
dpdz_flood = 1500+65000.*U_Ls; % flood pressure drop in Pa/m
% Dry Pressure Drop Calculation
```

```
dpdz_dry =
((p_G./p_air).^(0.4)).*(((C_1.*p_G.*U_Gs.^2)./(s.*(E.^2).*(sind(theta))
.^2))+((C_2.*vis_G.*U_Gs)./(s.^2.*E.*(sind(theta)))));

dpdz_new = dpdz_dry;
% Iteration Process
h_L =
((4.*F_t)./s).^(2/3).*((3.*vis_L.*U_Ls)./(p_L.*E.*(sind(theta)).*g.*(((
p_L-p_G)./p_L).*(1-(dpdz_new./dpdz_flood))))).^(1/3); % Liquid hold-up
(dimensionless)
dpdz = dpdz_dry./((1-(D_1+D_2.*s).*h_L).^5);
while abs(dpdz_new-dpdz) > 10^-3;
dpdz_new = dpdz;
h_L =
((4.*F_t)./s).^(2/3).*((3.*vis_L.*U_Ls)./(p_L.*E.*(sind(theta)).*g.*(((
p_L-p_G)./p_L).*(1-(dpdz_new./dpdz_flood))))).^(1/3); % Liquid hold-up
(dimensionless)
dpdz = (dpdz_dry)./((1-(D_1+D_2.*s).*h_L).^5);
end
h_L =
((4.*F_t)./s).^(2/3).*((3.*vis_L.*U_Ls)./(p_L.*E.*(sind(theta)).*g.*(((
p_L-p_G)./p_L).*(1-(dpdz./dpdz_flood))))).^(1/3);

% With convergence here, dpdz is accurate & final h_L can be used for
rest
% of model

%% Mass transfer coefficient calculations
U_Ge = U_Gs./(E.*(1-h_L).*sind(theta)); % Effective gas velocity (m/s)
U_Le = U_Ls./(E.*h_L.*(sind(theta))); % Effective liquid velocity (m/s)
k_L = 2.*(((D_L.*U_Le)./(p.*s)).^(1/2));
k_G =
0.054.*(D_G./s).*(((U_Ge+U_Le).*p_G.*s)./vis_G).^0.8.*(vis_G./(D_G.*p_G
)).^0.33;

%% Calculation of HETP
HETP =
((U_Gs./(k_G.*a_e))+lambda.*(U_Ls./(k_L.*a_e))).*(log(lambda)./(lambda-
1));

end
```

A.5. MATLAB Function M File – Song correlation

```
function
[HETP,a_e,k_L,k_G]=Songfun(F_v,p_L,p_G,sigma,vis_L,vis_G,D_L,D_G,lambda
,a_p,E,theta,Z)
n=length(F_v);

% Superficial velocity calculations
U_Gs = F_v./((p_G).^0.5); % m/s
U_Ls = U_Gs.*(p_G./p_L); % m/s

p = pi; % saves p as pi (3.14...)
g_c = ones(n,1)*1; % gravity conversion factor
```

```
g = ones(n,1)*9.80665; % gravitational constant (m/s^2)

n=ones(n,1)*1; % correction term for type of packing (=1 for structured
packing)

% kL & kG (mass transfer coefficient) calculations
k_L = 0.12.*U_Ls.^0.565.*(vis_L./p_L).^-
0.4.*(D_L.^0.5).*g.^(1/6).*a_p.^-0.065.*((Z./1.8).^-0.54);
k_G = 0.28.*U_Gs.^0.62.*(vis_G./p_G).^-
0.12.*(D_G.^0.5).*a_p.^0.38.*((sind(2.*theta)).^0.65)

% Effective Area calculation
a_e = a_p.*(1.16.*n.*((p_L./sigma).*g.^(1./2).*U_Ls.*a_p.^(-
3./2)).^0.138);

% HETP calculation
HETP =
((U_Gs./(k_G.*a_e))+lambda.*(U_Ls./(k_L.*a_e))).*(log(lambda)./(lambda-
1));

end
```

A.5. MATLAB Parent M File – Example for calling one of the functions

```
% This is the main file, which runs every correlation (the correlations
are
% functions that get called to this file and take physical
property/packing
% information inputs below. Lines 49-54 have all the correlations,
delete
% or add % in order to have a certain correlation run/not run.

clear,clc

% Physical property inputs

% Input physical properties (SI units)
% Example of some preloading points of an o/p-xylene system at 0.130
bara physical properties and their arrangement inorder to
% calculate HETP for each F-factor.
F_v = [0.687244038 1.05561849 1.57186725]; % F-factor (Pa^0.5)
p_L = [815.3404622 813.7386145 816.9423099]; % Liquid density (kg/m^3)
p_G = [0.560646683 0.560646683 0.496572777]; % Gas density (kg/m^3)
vis_L = [0.000358 0.000358 0.000367]; % Liquid viscosity (Pa*s)
vis_G = [0.0000075 0.0000074 0.0000074]; % Gas viscosity (Pa*s)
D_L = [3.9875E-09 3.9922E-09 3.8475E-09]; % Liquid diffusivity
(m^2/sec)
D_G = [0.000017522 0.00001767 0.000019892]; % Gas diffusivity (m^2/sec)
sigma = [0.02252 0.02251 0.02282]; % Surface tension (N/m)
lambda = [0.943033695 0.930602316 0.912197792]; % Stripping factor
LMW = [106.167 106.167 106.167]; % Liquid molecular weight (kg/kmol)
GMW = [106.167 106.167 106.167]; % Gas molecular weight (kg/kmol)
```

```
% Geometric Characteristics, input your packing information below
n=length(F_v);
theta = ones(n,1)*45; % (Corrugation angle (deg)),Example if
corrugation angle was 45 degrees, rest of geometric parameters should
follow this format
E = ones(n,1)*(insert value); % Void fraction
s = ones(n,1)*(insert value); % Corrugation side (m)
b = ones(n,1)*(insert value); % Corrugation base (m)
h = ones(n,1)*(insert value); % Corrugation height (m)
h_pe = ones(n,1)*(insert value); % Height of packing element (m)
Z = ones(n,1)*(insert value); % Packed bed height (m)
a_p = ones(n,1).*(4.*s)./(b.*h); % Should use this equation but below
you can specify an already calculated a_p
%a_p = ones(n,1)*(insert a_p value here) % Use Nominal packing area
equation to determine a_p and input in place. (m^2/m^3)

% Re-arranging

F_v=F_v';
p_L=p_L';
p_G=p_G';
vis_L=vis_L';
vis_G=vis_G';
D_L=D_L';
D_G=D_G';
sigma=sigma';
lambda=lambda';
LMW=LMW';
GMW=GMW';

% file name of each function must be the same, for ex “gualitofun” must
be the name of the m file of that function in order for the parent file
to work and properly call any of the HETP correlation functions

[HETP,F_t,c,a_e,k_L,k_G,h_L,Fr_L,We_L,dpdz,U_Le,U_Ge]=gualitofun(F_v,p_
L,p_G,sigma,vis_L,vis_G,D_L,D_G,lambda,a_p,E,theta,s);


clc
fprintf('HETP values: \n')
fprintf('%f \n', HETP)
```

VITA

Andrew Peter Starrantino

Candidate for the Degree of

Master of Science

Thesis: PERFORMANCE EVALUATION AND PHYSICAL PROPERTY STUDY OF STRUCTURED PACKING HETP CORRELATIONS

Major Field: Chemical Engineering

Biographical:

Education:

Completed the requirements for the Master of Science in Chemical Engineering at Oklahoma State University, Stillwater, Oklahoma in July, 2022.

Completed the requirements for the Bachelor of Science in Chemical Engineering at Clarkson University, Potsdam, New York in May, 2020.

Experience:

Graduate Research Assistant/Graduate Teaching Assistant, School of Chemical Engineering, Oklahoma State University, Stillwater, Oklahoma, August 2020 – June 2022